NOTICE

AVIS

The quality of this microform is heavily dependent upon the quality of the original thesis submitted for microfilming. Every effort has been made to ensure the highest quality of reproduction possible.

La qualité de cette microforme dépend grandement de la qualité de la thèse soumise au microfilmage. Nous avons tout fait pour assurer une qualité supérieure de reproduction.

If pages are missing, contact the university which granted the degree.

S'il manque des pages, veuillez communiquer avec l'université qui a conféré le grade.

Some pages may have indistinct print especially if the original pages were typed with a poor typewriter ribbon or if the university sent us an inferior photocopy.

La qualité d'impression de certaines pages peut laisser à désirer, surtout si les pages originales ont été dactylographiées à l'aide d'un ruban usé ou si l'université nous a fait parvenir une photocopie de qualité inférieure.

Reproduction in full or in part of this microform is governed by the Canadian Copyright Act, R.S.C. 1970, c. C-30, and subsequent amendments.

La reproduction, même partielle, de cette microforme est soumise à la Loi canadienne sur le droit d'auteur, SRC 1970, c. C-30, et ses amendements subséquents.

Canada

UNIVERSITY OF ALBERTA

PERFORMANCE OF FILTERED OD-QPSK FOR PERSONAL WIRELESS COMMUNICATIONS

By

Ⓒ

Jun He

A thesis submitted to the Faculty of Graduate Studies and Research in partial fulfillment of the requirements for the degree of **MASTER OF SCIENCE.**

DEPARTMENT OF ELECTRICAL ENGINEERING

EDMONTON, ALBERTA

SPRING 1993

Canada

UNIVERSITY OF ALBERTA

RELEASE FORM

NAME OF AUTHOR: **Jun He**

TITLE OF THESIS: **Performance of Filtered OD-QPSK for Personal Wireless Communications**

DEGREE: **Master of Science**

YEAR THIS DEGREE GRANTED: **Spring 1993**

Permission is hereby granted to the University of Alberta Library to reproduce single copies of this thesis and to lend or sell such copies for private, scholarly or scientific research purposes only.

The author reserves all other publication and other rights in association with the copyright in the thesis, and except as hereinbefore provided neither the thesis nor any substantial portion thereof may be printed or otherwise reproduced in any material form whatever without the author's prior written permission.

Jun He

10116 87Ave
Edmonton, Alberta T6E 2P2

DATE: _Mar 5, 1993_

UNIVERSITY OF ALBERTA

FACULTY OF GRADUATE STUDIES AND RESEARCH

The undersigned certify that they have read, and recommend to the Faculty of Graduate Studies and Research for acceptance, a thesis entitled **PERFORMANCE OF FILTERED OD-QPSK FOR PERSONAL WIRELESS COMMUNICATIONS** submitted by **Jun He** in partial fulfillment of the requirements for the degree of **Master of Science**.

©

_____
Dr. Paul A. Goud, Co-Supervisor
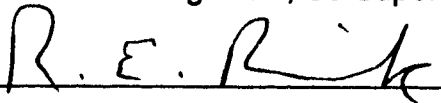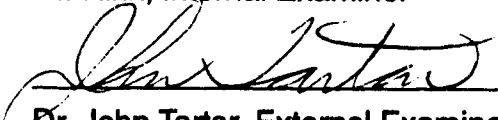
_____
Dr. Colin G. Englefield, Co-Supervisor

_____
Dr. Rink, Internal Examiner

_____
Dr. John Tartar, External Examiner

DATE: 93. 03. 01

Dedicated to my parents and brother,

For their nourishment, support and encouragement.

ABSTRACT

This thesis proposes and studies several ODQPSK systems to achieve power and spectrally efficient operation in personal wireless communications. Over the past decade, the increased demand for mobile radio services has made efficient utilization of the limited spectrum resource more important than ever. Due to the inherent high modulation efficiency of linear modulation schemes, these modulation methods have attracted much attention for future enhanced-performance mobile communication systems. On the other hand, in order to achieve cost-effective implementation of the mobile portable units, transmitter power amplifiers are always made to operate near the saturation region, which creates both amplitude-to-amplitude(AM-AM) and amplitude-to-phase(AM-PM) nonlinearities in the amplifier characteristics. These forms of distortion will result in spectral spreading for signals with a large envelope variation, thus eliminating any spectral advantage of the linear modulation scheme used. For example, $\pi/4$-DQPSK, the current standard linear modulation used in the second generation digital cellular systems, has a 20dB envelope variation. For this case, to reduce spectral spreading, significant amplifier linearization would be needed. However, this could cause extra power consumption and increase the complexity of implementation in mobile portables.

Another way of resolving the problem is to use linear modulation schemes with as low an envelope fluctuation as possible so that transmitter linearization can be made more easily. It is also preferred that the chosen modulation will allow the use of differential detection at the receiver since, in a typical mobile radio channel, coherent detection usually results in an unacceptably high bit error rate floor. In this regard, some modulation methods with largely reduced envelope variation such as conventional Nyquist filtered OQPSK and staggered QAM are excluded as they necessitate coherent reception at the receiver.

With these considerations in mind, three ODQPSK systems using different transmitter and receiver filtering schemes have been proposed and investigated. These are: Square-Root-Raised-Cosine ODQPSK(SRC-ODQPSK) and Smooth Transition ODQPSK(ST-ODQPSK). There are also two versions of SRC-ODQPSK; one uses a pair of identical 4-th root raised cosine(4RRC) filters as the transmitter and receiver filters, while the other uses a square-root raised cosine(SRRC) filter as the transmitter filter and a 4-th order Butterworth filter as the receiver filter. Nonredundant error correction techniques have also been studied to apply to ODQPSK modulation. Computer simulations have been conducted to investigate various characteristics of these systems including power spectral density, envelope fluctuation and error-rate performance in different mobile radio channel scenarios. These results are compared with those of $\pi/4$-DQPSK and GMSK, as these modulation methods have been adopted for use in the new digital cellular systems in North America and Europe, respectively. The results show that the three proposed schemes have a much better envelope property than $\pi/4$-DQPSK. The achievable spectral efficiency lies in between that of $\pi/4$-DQPSK and GMSK. Of the three systems, SRC-ODQPSK with 4RRC filter can achieve the best error performance. In a nonlinear AWGN channel, it has a 3dB E_b/N_o gain over $\pi/4$-DQPSK for a BER of 10^{-4}. In a linear AWGN channel, it is inferior to $\pi/4$-DQPSK by 1dB. In a fast Rayleigh fading channel, however, the irreducible error floor is lower than that of $\pi/4$-DQPSK. It is observed that the excellent error performance, compact spectrum and good envelope characteristic, as well as very simple receiver configurations make these ODQPSK schemes, especially SRC-ODQPSK with 4RRC filtering, very attractive for use in power- and bandwidth-limited mobile radio applications.

ACKNOWLEDGMENTS

TABLE OF CONTENTS

LIST OF FIGURES

LIST OF TABLES

LIST OF ABBREVIATIONS

AMPS	Advanced Mobile Phone Service
AM-AM	Amplitude to Amplitude
AM-PM	Amplitude to Phase
AWGN	Additive White Gaussian Noise
BER	Bit Error Rate
BOSS	Block Oriented System Simulator
CDMA	Code Division Multiple Access
CPM	Continuous Phase Modulation
C/D	Direct-Path-to-Delay-Path Power Ratio
DECT	Digital European Cordless Telecommunications
DMSK	Differential Minimum Shift Keying
FDMA	Frequency Division Multiple Access
FM	Frequency Modulation
GMSK	Gaussian Minimum Phase Shift Keying
GSM	Group Speciale Mobile
IF	Intermediate Frequency
ISI	Intersymbol Interference
MSK	Minimum Shift Keying
NEC	Nonredundant Error Correction
NRZ	Non-Return-to-Zero
OQPSK	Offset Keying QPSK
PSD	Power Spectral Density
QAM	Quadrature Amplitude Modulation
QPRS	Quadrature Partial Response Signalling
QPSK	Quadrature Phase Shift Keying
SNR	Signal to Noise Ratio
SRC-ODQPSK	Square Root Raised Cosine Offset Differential QPSK
SRRC	Square Root Raised Cosine

ST-ODQPSK	Smooth Transition Offset Differential QPSK
TCM	Trellis-Coded Modulation
TDMA	Time Division Multiple Access
VSELP	Vector-sum Excited Linear Predictive Coding
$\pi/4$-DQPSK	$\pi/4$ Shifted Differential QPSK
4RRC	4-th Root Raised Cosine

LIST OF SYMBOLS

a_i Transmitted i-th symbol

d_{ki} Output symbol of the k-th order detector at the i-th time slot

D_{ki} same as r_{ki}

e_{ki} Symbol error present at the k-th order detector at the i-th time slot

E_b Energy per bit

N Number of syndrome patterns

N_o Single-sided power spectral density of white Gaussian noise

p_i Stationary probability of state i

$p_{ik}^{(n)}$ n-step state transition probability from state i to k

Q State transition probability matrix

r_{ki} Received noisy symbol by the k-th order detector at the i-th time slot

S_{ki} Syndrome obtained from the k-th order detector at the i-th time slot

T Symbol duration

T_b Bit duration

α Rolloff factor for the raised cosine filter

θ_{ki} Phase difference detected by the k-th order detector at the i-th time slot

θ_j Absolute carrier phase at the j-th time slot

ε_j Phase error present in θ_j

CHAPTER 1   INTRODUCTION

The past decade has witnessed a rapid growth of mobile radio services, particularly of mobile cellular telephony. This has created a series of technological challenges which require the exploration of advanced techniques to obtain higher capacity while maintaining good performance. The most important of these are spectrally and power efficient modulation and demodulation methods, powerful channel encoding/decoding and equalization strategies to combat severe fading conditions encountered in the mobile radio environment, low bit-rate source speech encoding, cell site frequency re-use plans, and cell splitting. In this thesis, investigations are conducted on advanced digital modulation/demodulation schemes and error protection techniques for achieving more efficient and reliable communications over mobile radio channels.

1.1 Evolution and development of mobile radio

The history of mobile radio communication can be traced back to the last century. In 1880, Hertz first demonstrated radio communication, marking the beginning of the wireless era[1]. However, the first practical demonstration of radio communication did not occur until 1897, when Marconi successfully transmitted a radio signal between a land-based station and a tugboat over an 18-mi path. In 1921, experiments with police car radio dispatch were initiated by the Detroit police department. In the early 1930's, the first two-way mobile communications were put in use by the Bayonne police department in New Jersey, USA[2].

The dream of portable communication for the general public, especially that of the car telephone was, however, not realized until the advent of cellular radio systems. Following field trials at Bell Laboratories, the first Advanced Mobile

Phone Service(AMPS) system, which uses analog FM and the concept of spectrum reuse, began commercial operation in 1983[3].

Due to the rapidly increasing number of AMPS subscribers, the increased but still limited capacity of the new system soon became a problem in some metropolitan areas. To overcome the limitations of this first generation analog cellular technology, extensive and in-depth research work was initiated in the field of digital technologies to increase spectral efficiency, enhance system performance and improve the quality of services. Currently, three major standards have been established for second generation digital cellular systems, namely, the Group Speciale Mobile(GSM) system, the Digital European Cordless Telecommunications(DECT) system and the North American IS-54 system [4][5] [6]. A fourth system, using code division multiple access(CDMA), is also creating great interest[6]. Both GSM and DECT adopt time division multiple access(TDMA) as the channel access technique and Gaussian minimum phase shift keying(GMSK) as the digital modulation scheme. Using the same access protocol, the North American IS-54 system employs π/4-DQPSK as the modulation scheme. All three systems use digital speech transmission and advanced encoding techniques to improve system performance in the mobile radio channels. Apart from the specified frame structure and transmission rate, there are two distinct differences arising from the chosen modulation schemes. GSM and DECT systems do not need linear power amplifiers, due to the constant envelope property of GMSK modulation. In contrast, π/4-DQPSK has a power variation of about 20dB, which requires extensive transmitter linearization. On the other hand, the North American IS-54 system offers a higher bandwidth efficiency than the GSM and DECT systems. The transmission rate is 48.6kb/s with a channel spacing of 30kHz, yielding a spectral efficiency of 1.62 b/s/Hz; this is a 20% improvement over the 1.35 b/s/Hz efficiency obtained by the GSM system.

2

Generally speaking, the most noticeable improvement of all second generation digital cellular systems over the first generation analog FM system is the considerably increased information transmission rate.

1.2 The mobile radio communication channel

A typical land mobile radio communication channel can be characterized statistically by a random fading process. As a mobile unit moves along a fading path in an urban environment, variations in signal amplitude may amount to 40dB. This phenomenon is attributable to the effects of multiple-path reflections from surrounding buildings and also to the frequent absence of line-of-sight transmission. Amplitude fading can be further divided into two fading processes, long-term fading and short-term fading. Usually, long-term fading is caused by slow variations in topography, leading to a Log-normal distribution, while short-term fading is due to the reflectivity of various types of scatterers, either stationary or moving, giving rise to a Rayleigh distribution. The two fading effects are also known as shadowing and multipath fading, respectively. Fig.1.1 illustrates the generation of multipath fading in a mobile radio environment.
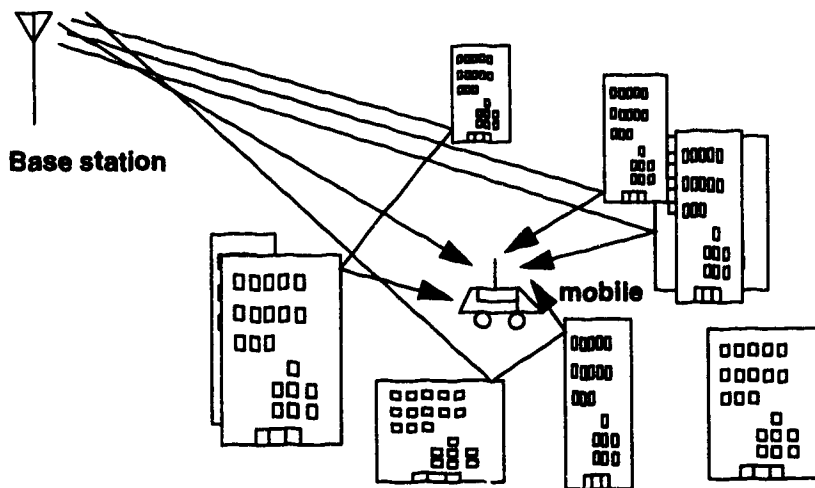
Fig.1.1 A land multipath fading environment

Since short-term fading has the dominant effect on the degradation of system performance, this type of fading is most c   studied and used to characterize the fading effects found in a typical mobile radio channel[1]. Fig.1.2 shows a portion of a computer simulated Rayleigh fading process used in this project. During a deep fade, the signal may suffer a dramatic degradation. Hence, it is reasonable to expect that the fading present in a mobile radio channel is the major factor causing burst errors and poor system performance.
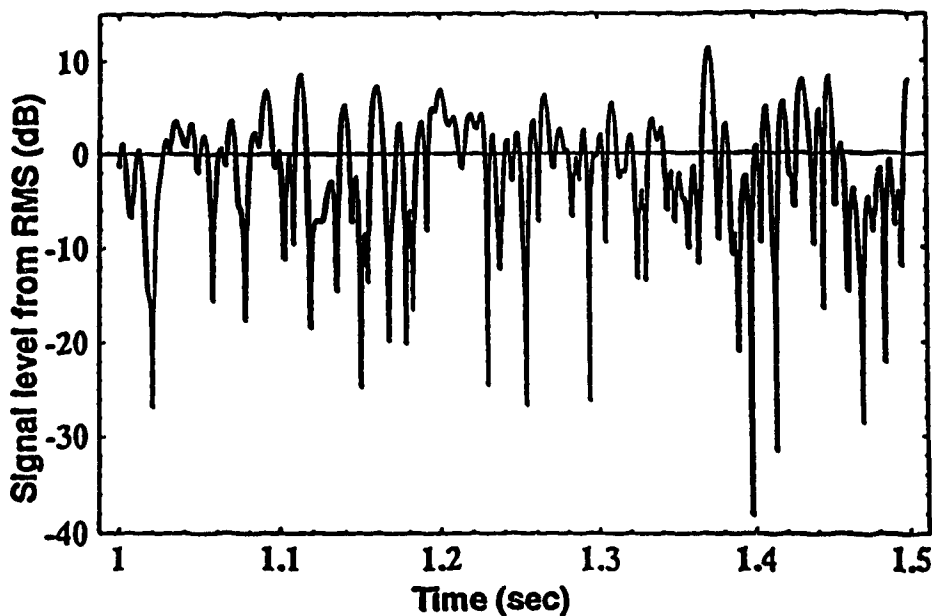
Fig.1.2 A typical fading signal received at a mobile unit.
Carrier frequency: 850MHz. Doppler frequency: 90Hz.
Vehicle speed: 114km/h.

Mathematically, the various types of fading encountered in practical scenarios can be generalized as Nakagami fading, described by the following probability density function:

$$p(R) = \frac{2}{\Gamma(m)} \left(\frac{m}{\psi}\right)^m R^{2m-1} exp\left(-\frac{mR^2}{\psi}\right)$$

$$m \geq \frac{1}{2}, R \geq 0 \qquad (1.1)$$

where R is the signal magnitude, and m and ψ are parameters determining the probabilistic density function[8]. For example, this distribution includes Rayleigh fading for m=1, and the one-sided Gaussian distribution for m=0.5. It also approximates the Log-normal distribution for large m when $\sqrt{\frac{\psi}{e}} \le R \le \sqrt{\psi e}$, where "e" is Euler's constant. The Rician distribution, found in a mobile satellite channel, may also be approximated by the Nakagami distribution. The four distribution functions, Rayleigh, Rician, Log-normal and Nakagami distributions, are sufficient for describing any fading phenomenon in almost all practical situations[9].

In addition to the above-mentioned amplitude fading, the transmitted signal is affected by other factors. These are:

1) Doppler shift due to the relative movement between the base-station and the portable unit. The maximum Doppler shift, f_m, can be expressed as f_m=V/λ Hz, where V is the vehicle speed and λ is the carrier wavelength.

2) The delay spread caused by surrounding buildings and objects. A large delay spread could cause a dramatic degradation in the system error performance, especially for high bit rate systems such as GSM. A delay-spread channel is also called a time-dispersive or frequency-selective channel. When the delay spread is very small compared to the channel signalling interval, the channel is termed a flat fading channel.

3) Fast random phase and frequency modulation caused by the Doppler shift. This usually results in an **irreducible error floor** for systems operating in a flat fading channel. A typical random phase modulation waveform generated from the computer simulation is shown in Fig.1.3.

4) Additive White Gaussian Noise(AWGN) present in a wireless channel.
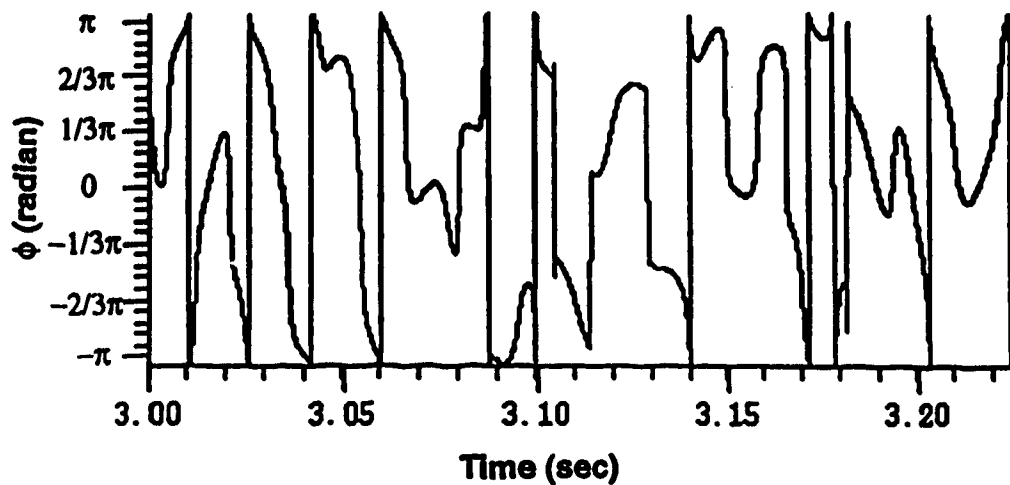
Fig.1.3 Random phase modulation corresponding to the Rayleigh fading in Fig.1.2.

1.3 Technological challenges for future mobile communication systems

In order to meet the increasing demand for mobile radio services, future mobile digital systems are expected not only to exploit the allotted frequency spectrum more efficiently, but also to provide enhanced system performance and cost-effective new services. Hence, innovative technologies and strategies become crucial for the practical realization of these future systems. The most important technologies may be categorized as follows:

1) spectrally and power efficient modulation methods

2) several multiple access techniques, such as time division multiple access (TDMA), code division multiple access (CDMA) and frequency division multiple access (FDMA)

3) new low-rate speech coding techniques, such as vector-sum excited linear predictive coding (VSELP)

6

4) powerful combined coding and modulation schemes, such as trellis-coded modulation(TCM)

5) improved anti-fading transmission and receiving techniques, such as equalization and forward error correction

6) co-channel/adjacent channel interference reduction techniques

Among these technologies, modulation methods are especially important as they directly influence the best achievable system performance. The criteria for an efficient modulation scheme are threefold: spectral efficiency, power efficiency and good performance in the fading environment.

To obtain power efficient operation, the requirements are:

1) To obtain good dc to ac conversion efficiency, transmitter rf power amplifiers should operate in a nonlinear mode, such as class B or class C.

2) The required signal-to-noise ratio(SNR) should be minimized for a specified bit error rate(BER) or symbol error rate(SER) performance. In other words, the selected modulation scheme should have as small an intersymbol interference level as possible at the transmitter output, and be robust against multipath fading, random phase modulation, and delay spread.

Since nonlinear power amplifiers would cause significant spectral spreading and generate numerous intermodulation products for signals with a non-constant envelope, the first condition implies that constant envelope modulation schemes such as continuous phase modulation(CPM) be used. Modulation schemes that give rise to amplitude variations may also be employed, provided that the transmitter is linearized. However, the greater the envelope fluctuation, the greater the degree of linearization that will be required, since the severity of spectral spreading is usually proportional to the amount of envelope

variation. In this regard, a linear modulation scheme with an envelope fluctuation that is as small as possible is preferred.

To obtain spectrally efficient operation, the modulated signals should:

1) have a small main lobe bandwidth

2) have a fast spectral rolloff

3) be insensitive to nonlinear amplification (considering the difficulty of transmitter linearization)

For these purposes, quadrature phase shift keying(QPSK), multi-level quadrature amplitude modulation(M-ary QAM) and quadrature partial response signalling(QPRS) should be considered, as they can provide a higher spectral efficiency than CPM. It is also noted that these criteria are conflicting in nature, because linear modulation schemes usually have a large envelope fluctuation, thus eliminating any spectral advantages over CPM after nonlinear amplification. Taking both spectral and power efficiencies into consideration, the study of linear modulation schemes with small envelope variation becomes very important.

In mobile radio communications, apart from power and spectral considerations, reliable performance in the fairly hostile fading environment is also necessary. The channel is characterized by Rayleigh fading or Rician fading, Doppler spread, delay dispersion and random phase modulation.

1.4 Motivations for conducting this project

Recent advances in power amplifier linearization techniques[10][11][12] have made possible the use of conventional linear modulation schemes such as QPSK, M-ary QAM and, more recently, $\pi/4$-DQPSK. However, conventional QPSK and M-ary QAM have very large carrier envelope variations since the signal phasors pass through the origin of the vector space(I and Q), and $\pi/4$-

8

DQPSK has a 20dB peak-to-peak power variation[13]. This imposes stringent technical requirements on the transmitter linearization, thus increasing circuit complexity and cost in both the portable units and the base-stations.

Although differential detection suffers from a 3dB SNR loss as compared to coherent detection in a static AWGN channel, it exhibits superior error performance to coherent detection due to its inherent robustness against fast random phase and frequency modulation in the mobile fading channel. An additional advantage of differential detection is that it allows the use of a simple receiver configuration, which is advantageous from the viewpoint of cost-effective circuit implementation in the portable units.

One way of alleviating the problem of transmitter linearization is to employ Offset Keying QPSK(OQPSK) modulation, since it has an inherent significantly reduced envelope variation, compared to $\pi/4$-DQPSK. However, it is widely believed[14][15] that the conventional Nyquist filtered OQPSK system does not allow the use of a noncoherent detection method, such as differential detection, without incurring a significant performance penalty. Recently, a noncoherent correlation detection technique has been proposed for ODQPSK, using a different filtering strategy[16]. However, this detection method requires complex receiver structure and detection algorithms. To the author's knowledge, little work has been done so far with respect to differentially detected OQPSK modulation schemes. Therefore, it is worthwhile to investigate and develop an effective method to achieve the differential detection of OQPSK, while maintaining good bit error rate performance in linear AWGN, nonlinear AWGN and fast Rayleigh fading scenarios. This new modulation method should be able to operate satisfactorily in power and bandwidth limited land or satellite mobile communication systems, and would have the advantage of cost-effective implementation.

Another means of improving system performance is achievable by using powerful error correction encoding techniques, such as the widely-used convolutional codes and Reed-Solomon(RS) codes. Punctured convolutional and RS codes have also been used to cater to the non-stationary property of the mobile radio channel[17]. Powerful as they are, their encoding gains can be obtained only by increasing the gross data rate, thus reducing the efficiency of spectrum utilization.

With the aim of overcoming the drawbacks of redundant coding schemes, nonredundant error correction(NEC) schemes have been proposed[18]. NEC techniques take advantage of the inherent property of a differential detection system. That is, a redundant code can be obtained at the receiver by using the outputs of multi-differential detectors. This unique code has been proved to be a rate $1/L$ convolutional code, where L represents the number of differential detectors used[19]. Various versions of NEC methods have been applied to MSK, BPSK and QPSK transmision systems[20][21][22], but not yet to OQPSK. In this project, a differentially detected OQPSK receiver structure is developed to accommodate the NEC method. Three kinds of error correction algorithm, which realize single, double and triple error correction, have been evaluated by means of computer simulation. The performance of these schemes for OQPSK modulation is also analyzed for different differential encoding methods .

1.5 Thesis organization

This thesis deals mainly with digital modulation/demodulation techniques suitable for use in mobile radio communications. Some error protection and differential encoding techniques are also investigated. Error performance in static AWGN and typical mobile radio fading channels is studied by means of computer simulation. The resulting performance is compared with that of two major

systems, the IS-54 North American standard and the GSM European standard, under various channel conditions.

Chapter 1 provides an introduction to the salient aspects of mobile radio communications and to the motivation and organization of this thesis.

Chapter 2 briefly introduces two classes of modulation, i.e., quadrature linear modulation and continuous phase modulation, and gives a detailed description of the proposed differential OQPSK systems using different filtering strategies. They are Square Root Raised Cosine ODQPSK(SRC-ODQPSK) and Smooth Transition ODQPSK(ST-ODQPSK). For SRC-ODQPSK, both the matched filter receiver and Butterworth filter receiver are discussed. The principles of some powerful anti-fading redundant codes and nonredundant error correction are also explained in this chapter. Algorithms relating to different nonredundant error correction schemes are given.

Chapter 3 describes the computer simulation of the above modulation systems. A system simulation software package, Block Oriented System Simulator(BOSS), is introduced in this chapter. The BOSS implementations of different transceivers and of various nonredundant error correction schemes are explained.

In Chapter 4, the performance of several digital modulation systems currently recommended for digital cellular communications is compared with the proposed modulation systems, under various channel conditions. The power spectral density and envelope variation characteristics are studied for linearly and nonlinearly amplified channels. Also, the improvement of bit error rate performance due to the use of single, double and triple error correction schemes is discussed.

Chapter 5 summarizes and presents conclusions on this project. Some suggestions for continuing this research in the area of modulation and channel error protection are also presented.

The theoretical derivation of the power spectral density function of ST-ODQPSK signals is given in Appendix A. The FORTRAN programs used for simulating single, double and triple error correction schemes are listed in Appendix B. Syndrome patterns used for triple error correction are listed in Appendix C. Other FORTRAN support subroutines, used to create BOSS primitive modules, are listed in Appendix D.

CHAPTER 2 MODULATION/DEMODULATION AND
ERROR PROTECTION TECHNIQUES

2.1 Spectrally efficient linear modulation methods

Spectrally efficient linear modulation schemes such as M-ary PSK, QPRS and M-ary QAM are usually employed in those highly bandwidth-limited communication systems for which the channel characteristics do not introduce severe performance degradation. The disadvantages of these techniques lie in the considerable power variation of the modulated signals. For instance, QPRS and M-ary QAM signals exhibit envelope variation even without any filtering. In MPSK, the signals have a non-constant envelope after transmitter filtering. $\pi/4$-DQPSK, the second generation digital modulation scheme for land mobile communications, has a large envelope variation of up to 20dB after transmitter raised cosine filtering(α=0.35). RF Power amplifiers used in radio transmitters usually introduce nonlinear amplitude(AM-AM) and nonlinear phase(AM-PM) distortion when operated near or at saturation to obtain high efficiency. In other words, these power amplifiers are rf envelope-sensitive devices. Hence, large rapid variations in signal power could result in much distortion in the amplified signals, usually in the form of spectral spreading, which is proportional to the envelope fluctuation of the input signal. In the worst case, all the major sidelobes of the original signal could be completely restored, independent of the filtering operation used. Considering that analytical studies of nonlinear amplification are extremely complex and do not provide sufficient insight into the performance degradation of the investigated linear modulation, computer simulation is performed. As well, an ideal hard-limiter can be used to approximate a practical saturated Class C high power amplifier, as described in [23]. The input/output

13

power characteristic of an ideal hard-limiter with infinite bandwidth is given in Fig.2.1.
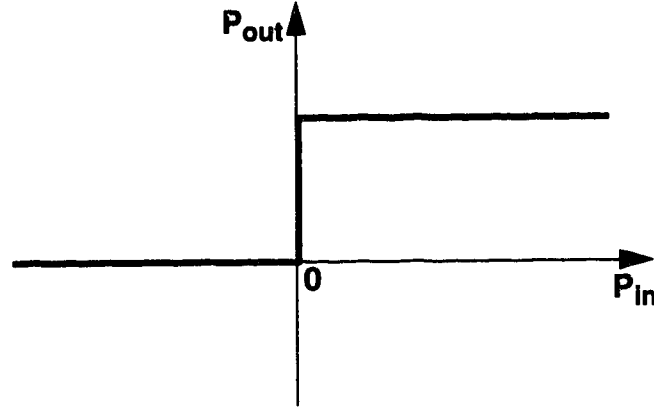
Fig.2.1 Input-output characteristic of an ideal hard limiter

As has been derived in [23], the input/output relationship of an ideal hard-limiter can be expressed in terms of the quadrature components of the input signal as follows:

$$I_2(t) = \frac{\sqrt{C}I_1(t)}{\left(I_1(t)^2 + Q_1(t)^2\right)^{1/2}} \qquad (2\text{-}1)$$

$$Q_2(t) = \frac{\sqrt{C}Q_1(t)}{\left(I_1(t)^2 + Q_1(t)^2\right)^{1/2}} \qquad (2\text{-}2)$$

where $I_1(t)$ and $Q_1(t)$ are the in-phase and quadrature baseband components of the modulated signal at the input to the hard-limiter. $I_2(t)$ and $Q_2(t)$ represent the corresponding output quadrature signals. C is a constant dependent upon the output saturation power. As a result of the infinite bandwidth, the phase of the input signal is passed undistorted. It is noted that the envelope of the input signal should always be larger than zero for these equations to hold true.

14

The following sub-section presents a description of the North American digital cellular modulation scheme, π/4-DQPSK, and its envelope characteristic.

2.1.1 π/4-DQPSK

As an improvement over the conventional QPSK scheme, π/4-QPSK was initially proposed by P. Baker to reduce the envelope variation from infinity to 20dB[13]. It allows the use of various detection methods, i.e., coherent, differential or limiter/discriminator detection, and is now accepted for use in second generation digital cellular systems in North America. The block diagram of the π/4-DQPSK transmitter is shown in Fig.2.2.
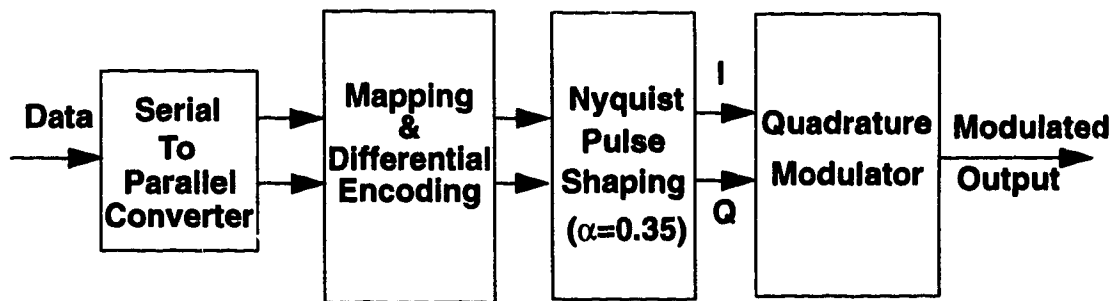
Fig.2.2 Block diagram of π/4-DQPSK transmitter

The mapping processor transforms the four-state constellation of QPSK into an eight-state constellation, as shown in Fig. 2.3. As a result, the output signal from the mapping block may take on 8 different values, namely (±1,0), (0,±1), (±0.707,±0.707). Also, the phase transitions between any two successive symbols are limited to ±45 and ±135 degrees, thereby preventing the signal envelope trajectories from crossing the origin. Fig.2.4 shows the envelope fluctuation of π/4-DQPSK modulated signals after the transmitter Nyquist filtering. Conventional QPSK is also shown for comparison.

15
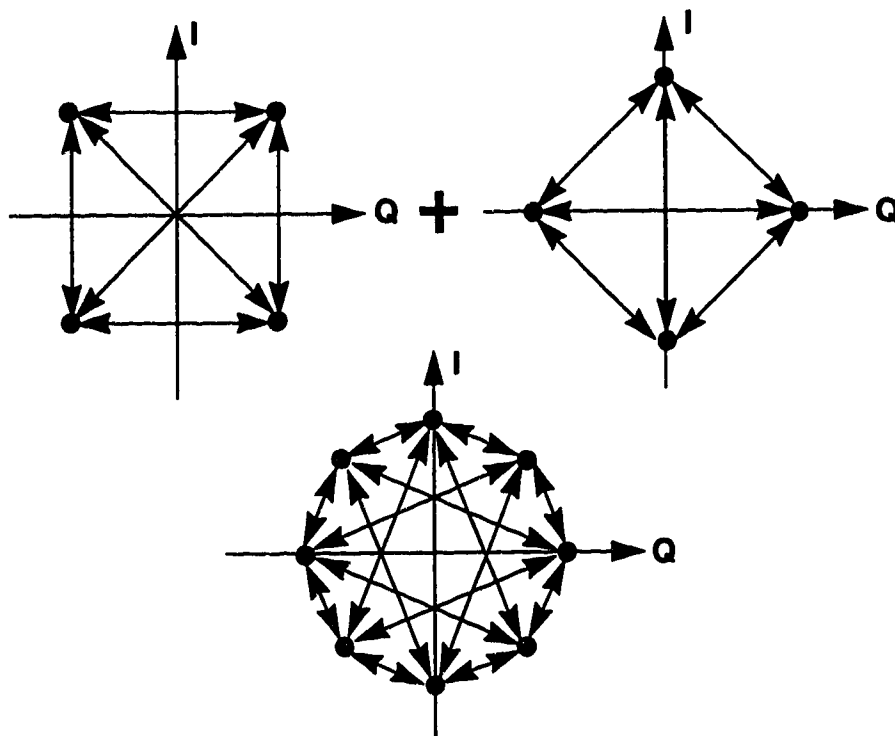
Fig.2.3 Constellation of π/4-DQPSK signals

(a)

(b)
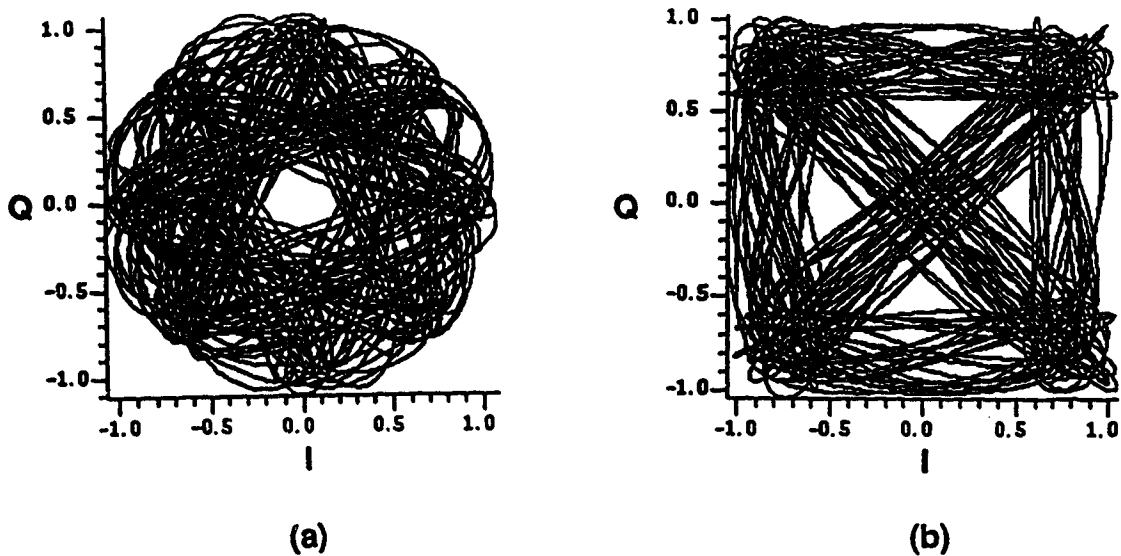
Fig.2.4 Envelope trajectories of (a) π/4-DQPSK (b) QPSK

16

2.2 Gaussian Minimum Phase Shift Keying

Gaussian Minimum Phase Shift Keying(GMSK) is the modulation scheme chosen by Europe and Australia for use in their second generation digital cellular systems. Basically, GMSK is a modification to the well-known Minimum Phase Shift Keying(MSK) modulation, in which a Gaussian-shaped low pass filter is added in front of the frequency modulator. Therefore, it is a type of continuous phase modulation(CPM), which is characterized by the constant envelope property. The modulation index is chosen as 0.5, to achieve minimum bandwidth occupancy. The block diagram of a GMSK transmitter is given in Fig.2.5.

```
┌─────────┐      ┌─────────┐      ┌──────────┐  Output
│  Data   │ ───▶ │Gaussian │ ───▶ │    FM    │ ───────▶
│ Source  │      │   LPF   │      │Modulator │
└─────────┘      └─────────┘      └──────────┘
                                   Mod. Index: 0.5
```
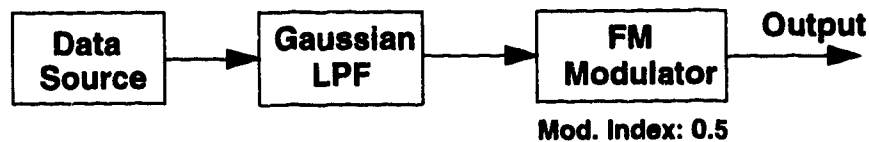
Fig.2.5 Block diagram of GMSK transmitter

By changing the 3dB cutoff frequency of the pre-modulation Gaussian low pass filter, the output spectrum width can be reduced significantly, without disrupting the constant envelope characteristic. However, the insertion of a Gaussian low pass filter will dramatically reduce the eye opening due to the intersymbol interference caused by filtering. As will be discussed in Chapter 4, this will result in a significant performance penalty in a linear AWGN channel, when compared with the previously described π/4-DQPSK modulation. Hence, for the GMSK modulation format, there exists a trade-off between its error performance and spectral efficiency. The major advantage of GMSK is that its performance is not affected by amplifier nonlinearities, thereby avoiding transmitter linearization

problems. Like π/4-DQPSK, GMSK also allows differential detection, coherent detection and limiter/discriminator detection.

2.3 Offset Keying QPSK

Offset Keying QPSK(OQPSK) modulation is quite similar to conventional QPSK except that the quadrature bit stream is delayed by one-bit duration,T_b, with respect to the in-phase bit stream. The serial-to-parallel converter is taken to operate on the principle of reading in two data bits at a time, and reading them out at half the bit rate, two at a time. Nyquist pulse shaping is applied to both streams. The filtered signals are then quadrature modulated and transmitted over the channel. A schematic diagram of OQPSK transmitter is shown in Fig.2.6.

Data → Serial To Parallel Converter → T_b → Nyquist Pulse Shaping → I, Q → Quadrature Modulator → Output
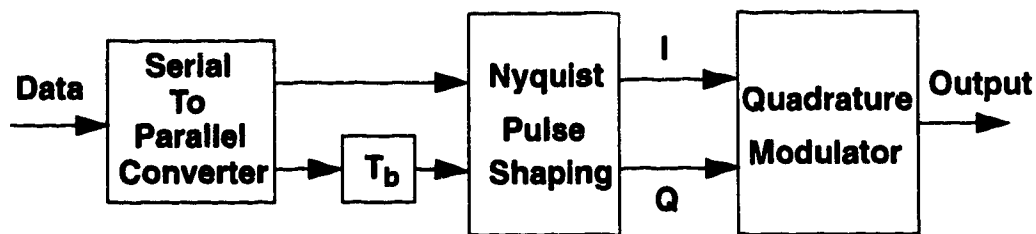
Fig.2.6 Block diagram of OQPSK transmitter

As a result of the one-bit offset, simultaneous transitions in the I and Q data streams are prohibited. Between two successive signalling intervals, the maximum phase rotation of the signal vector is limited to 90 degrees. Consequently, the amount of envelope variation in the modulated signals is effectively reduced to just several decibels. Fig.2.7 shows the envelope characteristic of Nyquist filtered OQPSK signals. It is generally believed that OQPSK signals have the smallest power variation of all four-level quadrature modulation schemes. The drawback of conventional(or Nyquist filtered) OQPSK is that this type of signal cannot be satisfactorily demodulated by a non-coherent detection method such as standard differential detection. The maximum phase

18

differential required by differential detection between two successive signalling intervals cannot be well preserved in conventional OQPSK. This excludes OQPSK from being used in general mobile radio applications, since differential detection is an effective means to combat fast random phase and frequency modulation incurred in the mobile radio channel, and also allows a simple receiver configuration.
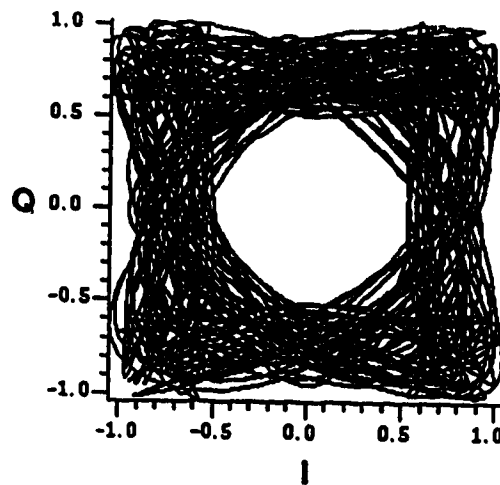
Fig.2.7 Envelope trajectories of filtered OQPSK

2.4. Proposed offset differential QPSK schemes

As described in the previous section, differential detection is preferred in order to achieve good performance in a fast fading channel. With the aim of accommodating differential reception for OQPSK modulation, several modified versions of the conventional OQPSK system have been developed and investigated in this project. Generally speaking, these systems have the advantages of a largely reduced envelope variation compared to other linear modulation schemes, a more compact spectrum than that of constant envelope modulation schemes such as GMSK , and good error performance in mobile radio channels. This section first describes different differential encoding/decoding

19

techniques that can be used for these systems. Next, each of these systems is explained in detail.

2.4.1 Differential encoding strategies

Although it is possible in principle to achieve ISI-free transmission for OQPSK signals, the detection method employed at the receiver usually directly affects the error performance of the whole system. Therefore, selecting the right detection techniques becomes critical to the performance of the system. For OQPSK modulation, three types of detection can be employed, namely, coherent detection, differential detection and discriminator detection. However, only differential detection methods are dealt with in this thesis, as they appear attractive for mobile radio applications.

In this work, two kinds of differential encoding/decoding schemes have been developed for OQPSK signals: two-bit differential encoding and three-bit differential encoding. The block diagram of a two-bit differential encoding/decoding circuit is given in Fig.2.8. A three-bit differential encoding/decoding circuit is shown in Fig.2.9. It is interesting to note that the three-bit encoder is also equivalent to the cascade of three one-bit differential enocders, as shown in Fig.2.10.
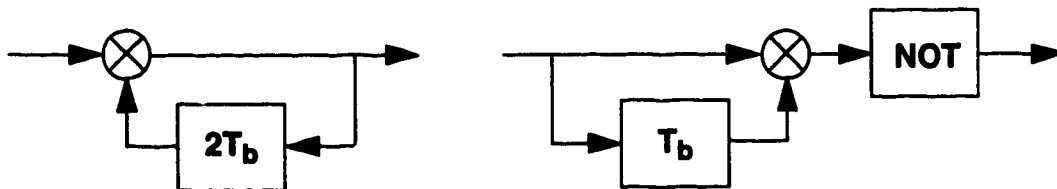
Fig.2.8 Block diagram of two-bit differential encoder & decoder
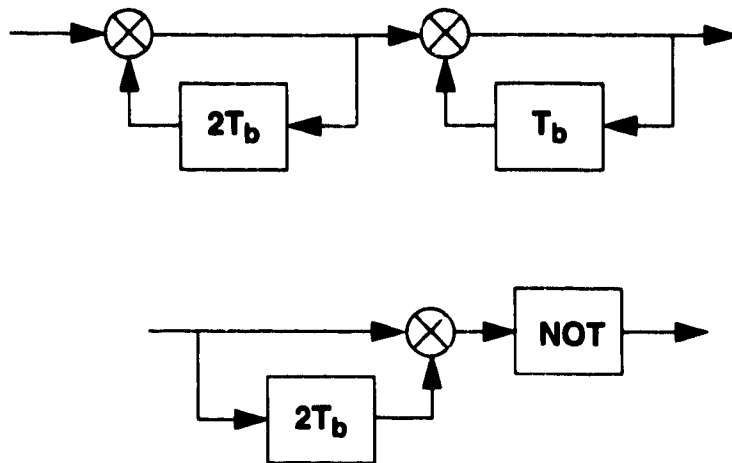
Fig.2.9 Block diagram of three-bit differential encoder & decoder
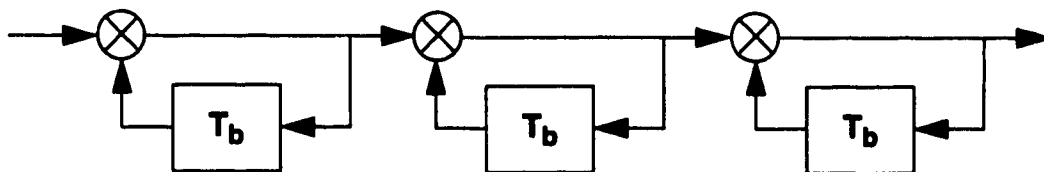
Fig.2.10 Equivalent three-bit differential encoder

In the two-bit encoding scheme, the transmitted data stream is delayed by $2T_b$, and multiplied by (or EX-ORed with) the source data stream to obtain the differentially encoded data. The receiver takes the received signal and multiplies it with its one-bit delayed version. A NOT gate is then used to obtain the original signal. If rf signals are present, a low pass filter and decision circuit need to be inserted between the multiplier and the NOT gate(note that the NOT gate may also be absorbed into the decision circuit). The three-bit encoder is a combination of a one-bit and a two-bit differential encoder; for decoding, the three-bit encoder requires a decoder with two-bit delay. The operation of the three-bit encoding/decoding circuit is similar to that of two-bit encoding/decoding circuit. As will be

21

discussed in Chapter 4, the two differential encoding techniques yield a different error performance in linear, nonlinear and Rayleigh fading channels. The mechanism can be explained as follows.

Fig.2.11 shows the the decision planes for two-bit and three-bit differentially encoded OQPSK signals. Since this is a phase modulated system, the detection of the data signal only involves phase-related operations. Consequently, the decision area can be characterized by a circular plane. As can be seen, in the two-bit scheme, the decision region for bit "1" corresponds to an angular area of 270 degrees, while bit "0" has a decision sector of 90 degrees. For the three-bit encoded case, bit "1" and bit "0" each occupy a decision region of 90 degrees, which is quite similar to that of QPSK detection. The two-bit encoded system has a larger phase margin than its three-bit counterpart. As well, the amount of delay involved in the differential detection process is one-symbol duration for three-bit differential encoding, and one-bit duration for two-bit differential encoding. Therefore, one can expect that the two-bit encoding scheme will have a better performance than the three-bit encoding scheme. The exception is that, when nonredundant error correction is used along with encoding, three-bit encoded system turns out to be better than two-bit encoded system. This will be discussed in Chapter 4.

(a)   (b)
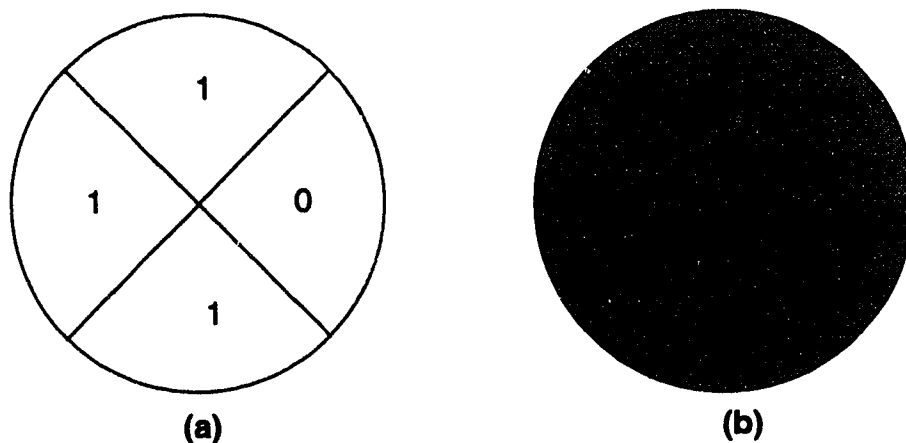
Fig.2.11 Decision planes for (a) two-bit encoding scheme
(b) three-bit encoding scheme

2.4.2 Square Root Raised Cosine ODQPSK transceiver

In this section, the Square Root Raised Cosine ODQPSK(SRC-ODQPSK) system is presented and discussed. Two different versions of the SRC-ODQPSK system are possible, which employ different transmitter baseband pulse shaping and receiver filtering techniques. They are:

❏ A 4th Root Raised Cosine(4RRC) filter receiver with the same type of pulse shaping at the transmitter.

❏ A Butterworth filter receiver with Square Root Raised Cosine(SRRC) transmitter pulse shaping.

2.4.2.1 SRC-ODQPSK system with 4RRC filter receiver

The system block diagram is shown in Fig.2.12. The transmitter includes a data source, a differential encoder, a serial/parallel converter, a delay element, two baseband pulse shapers and a quadrature modulator. First, the random data stream is differentially encoded so that the actual information is carried in the differential phase changes between successive bit intervals. As long as these phase properties are well preserved during transmitter pulse shaping, the receiver can reliably decode such information and convert it back to the original data signal, using a corresponding differential decoding circuit. In a practical radio channel, the transmitted signal is usually subject to the corruption of Additive White Gaussian Noise(AWGN) and fading effects such as Rayleigh or Rician fading. Random phase and frequency modulation may also be imposed upon the phase of the modulated signals in a fast fading scenario, due to the effect of large Doppler spread. After the differential encoding, the encoded data signal is then serial-to-parallel converted and fed to the I and Q baseband channels. The signal on the Q channel is offset with respect to the I channel by one bit duration or one-

half the symbol duration. To efficiently utilize the spectrum resources, 4RRC pulse shaping is performed on both the inphase and quadrature channels. Another advantage of using 4RRC pulse shaping lies in that this can guarantee ISI free transmission in a linear AWGN channel. In a quasi-static channel, this type of filtering can still yield sub-optimal results. The filtered signal is shown in Fig.2.13. It is observed that this signal is corrupted by ISI due to the transmitter filtering. As will be shown later, however, this ISI can be effectively eliminated after receiver filtering(see page 28). Fig.2.14 shows the envelope property of the filtered signal. Clearly, the envelope trajectory of this signal exhibits an even smaller variation than that of a conventional OQPSK signal.

(a)

(b)
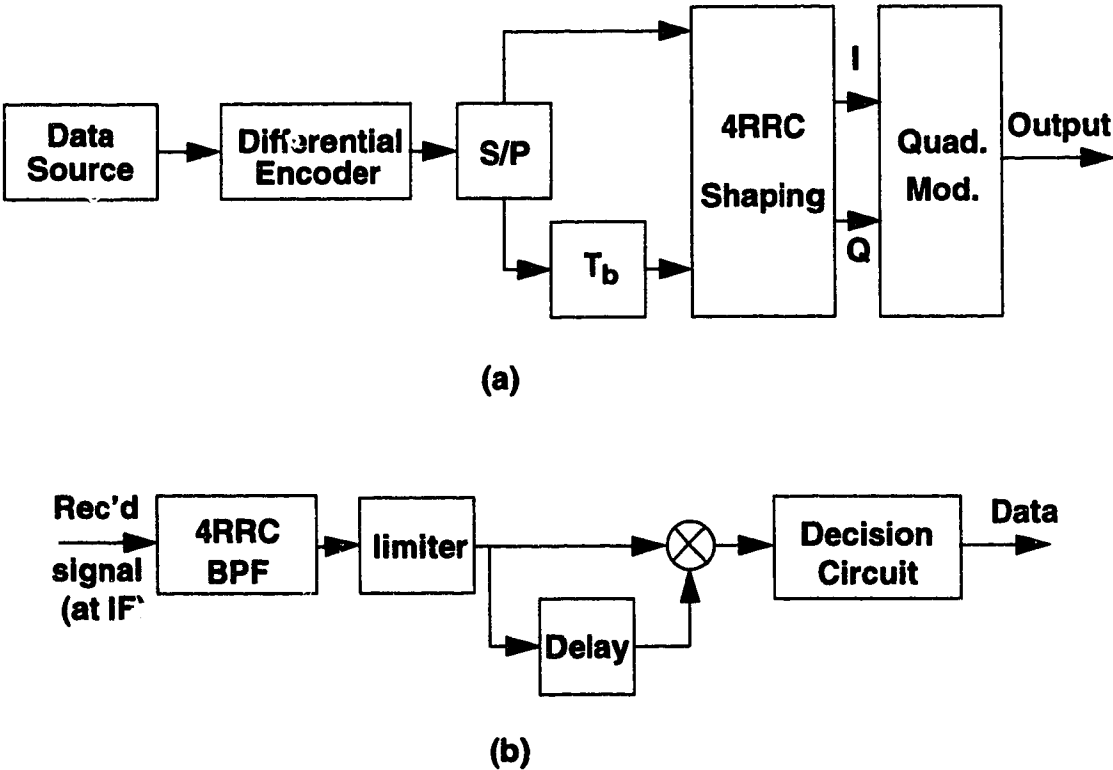
Fig.2.12 Block diagram of (a) SRC-ODQPSK transmitter (4RRC shaping)
(b) receiver structure

24
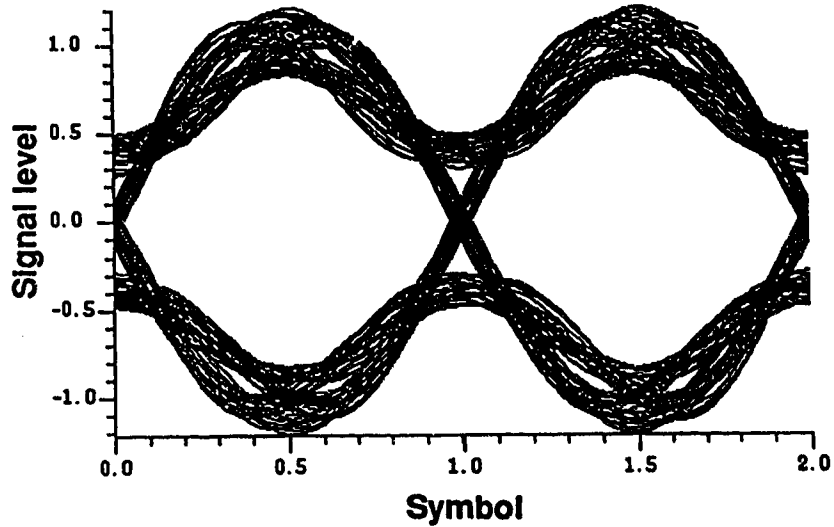
Fig.2.13 Eye diagram of 4RRC-filtered in-phase signal
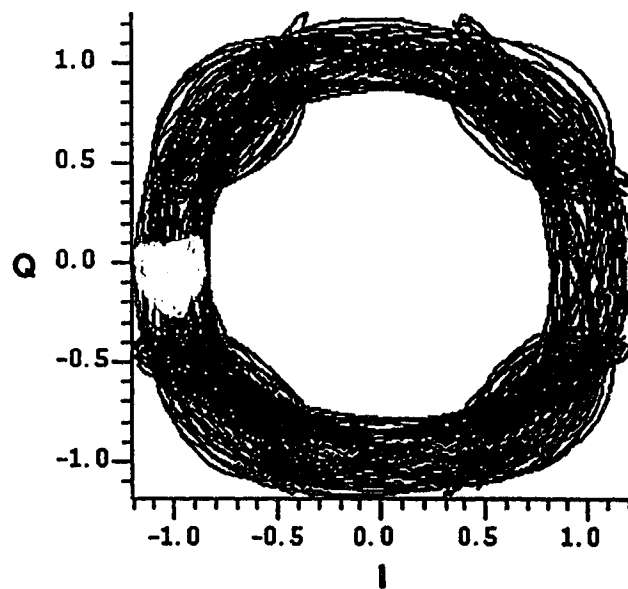
Fig.2.14 Envelope trajectory of 4RRC-filtered ODQPSK signal

The filtered signals are fed to the quadrature modulator and transmitted. The receiver structure is actually the same as that of a conventional binary DPSK receiver. Another 4RRC filter of the same type is used as the IF bandpass filter to give the best signal-to-noise ratio at the output of the receiver filter. A conventional binary differential detection circuit can be used to recover the data stream. As

discussed in the previous section, the amount of delay required in the differential detection process depends upon the differential encoding scheme used at the transmitter. Correspondingly, the decision circuit could have one or two decision thresholds. From Fig.2.11, it is not difficult to determine that, for two-bit differential encoding, the threshold should be $\cos(\pi/4)=0.707$, while for the case of three-bit encoding, the optimal thresholds are 0.707 and -0.707. Specifically, for two-bit differential encoding, a "0" should be decided if the level of the sampled signal is larger than 0.707, and a "1" is decided otherwise. For three-bit differential encoding, a "0" is decided if the absolute value of the sampled signal is larger than 0.707, and a "1" is decided if the value is in between 0 and 0.707. These threshold values are selected so as to maximize the phase tolerance of the system, regardless of magnitude information. In the decision circuit, the recovered lowpass analog signal is sampled once for every one bit. The resulting sampling rate is thus double that of the other QPSK schemes, assuming that all systems have the same bit rate. This property may be an additional advantage from the point of view of increasing the robustness against random phase interference in a mobile radio channel.

In this scheme, the pulse shaping filter used is a 4th Root Raised Cosine (4RRC) filter. At the receiver, another 4RRC filter is employed, which exactly matches the transmitter pulse shaper. It should be noted that this combination is not equivalent to a matched filter pair. The reason for this can be easily found out by referring to the eye diagram of the signals at the output of the receiver filter(Fig.2.15).
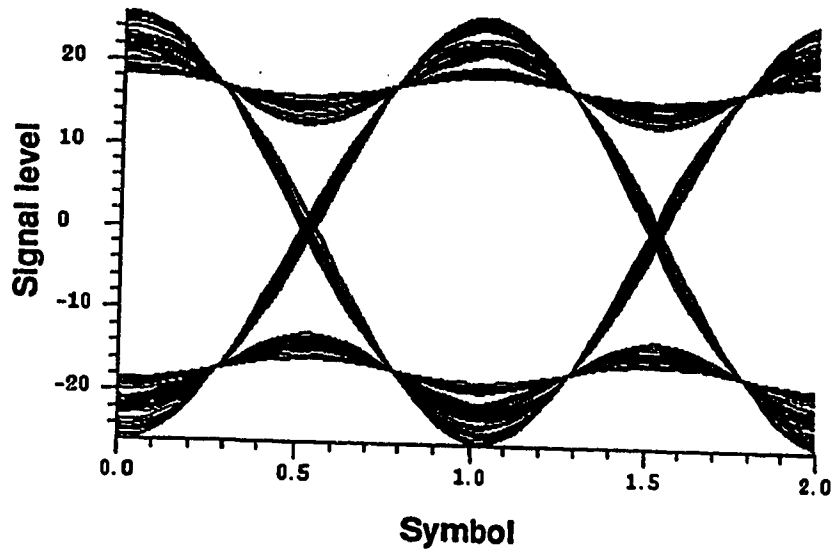
Fig.2.15 Eye diagram of the in-phase signal at receiver filter output

As can be seen, although the received signal is ISI-free at each sampling instant, the sampled signal level does not correspond to the maximum level within each pulse. It is well known that, for the case of using a matched filter pair, the output signal from the receiver filter should reach its maximum magnitude at each sampling point, so that the best error performance can be obtained for a given signal-to-noise ratio. Consequently, it is expected that this 4RRC-filtered system will suffer a certain degree of performance penalty in this respect, as compared to some other Nyquist filtered QPSK schemes. Later on, it will be shown that this penalty can be largely compensated for by using two-bit differential encoding and bit-by-bit detection techniques at the receiver. As a matter of fact, SRC-ODQPSK can achieve a better error performance than a Gray encoded DQPSK scheme, provided that optimal sampling is achievable.

The magnitude response of a 4th Root Raised Cosine(4RRC) filter is defined as follows:

27

$$H(f) = \begin{cases} 1 & 0 < |f| < \dfrac{1-\alpha}{2T} \\[2ex] \left[\dfrac{1}{2}\left(1 - \sin\left[\dfrac{\pi T}{\alpha}\left(|f| - \dfrac{1}{2T}\right)\right]\right)\right]^{\frac{1}{4}} & \dfrac{1-\alpha}{2T} < |f| < \dfrac{1+\alpha}{2T} \\[2ex] 0 & |f| > \dfrac{1+\alpha}{2T} \end{cases}$$

$$(2.5)$$

where T is the symbol period ($T=2T_b$), and α is the rolloff factor. For the discussed OQPSK modulation schemes, α is unity.

The impulse response of this filter is difficult to obtain analytically. Therefore, numerical integration is used to obtain the time domain impulse response of the 4RRC filter. Fig.2.16 shows the resulting impulse response generated from computer simulation. The corresponding frequency-domain magnitude response is shown in Fig.2.17.
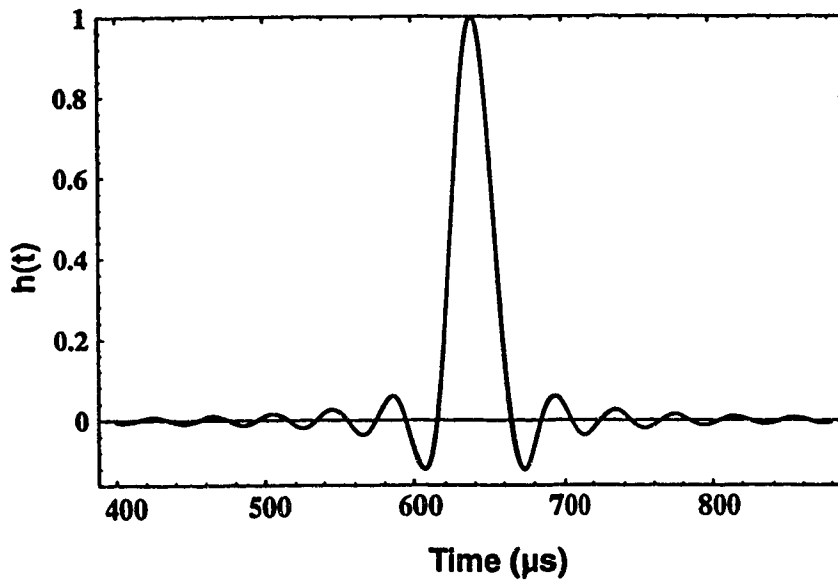
Fig.2.16 Impulse response of a 4RRC filter
for $\alpha=1$ & $T=40\mu s$

28
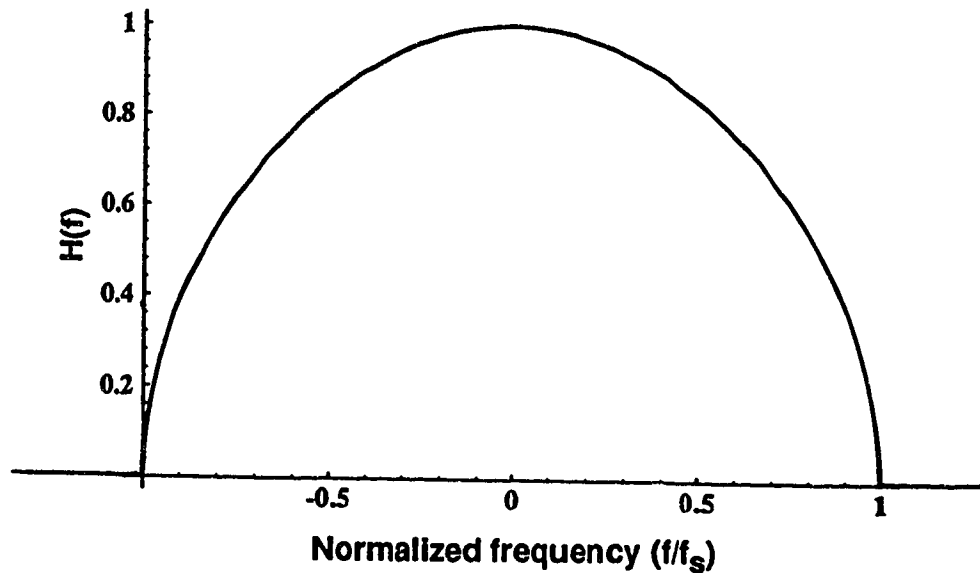
Fig.2.17 Magnitude response of a 4RRC filter

2.4.2.2 SRC-ODQPSK system with Butterworth filter receiver

The block diagrams for the above transmitter and receiver are shown in Fig.2.18. As can be observed, the system configuration is quite similar to the previously described 4RRC system. The only difference is that the baseband pulse shaping filters now used are changed to square root raised cosine filters, and that the receiver filter is now a Butterworth filter.

The definition of a SRRC filter is given as follows.

$$H(f) = \begin{cases} 1 & 0 < |f| < \dfrac{1-\alpha}{2T} \\[2mm] \sqrt{\dfrac{1}{2}\left(1 - \sin\left[\dfrac{\pi T}{\alpha}\left(|f| - \dfrac{1}{2T}\right)\right]\right)} & \dfrac{1-\alpha}{2T} < |f| < \dfrac{1+\alpha}{2T} \\[2mm] 0 & |f| > \dfrac{1+\alpha}{2T} \end{cases}$$

$$(2.6)$$

The magnitude response of this filter, and the corresponding impulse response are shown in Fig.2.19 and Fig.2.20, respectively.

29
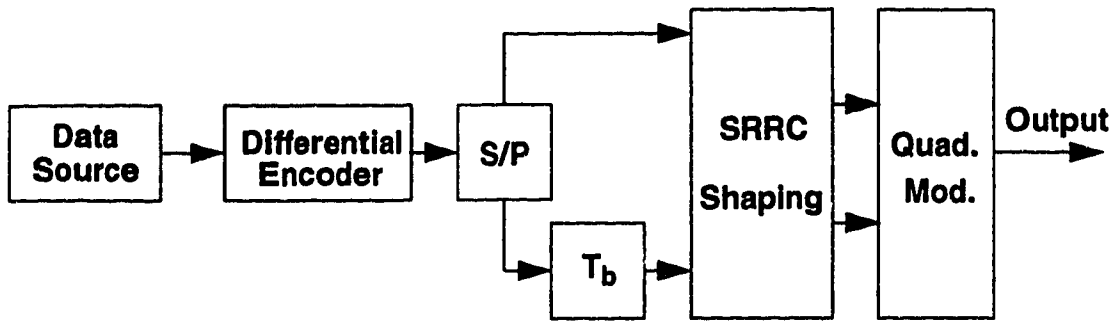
(a)
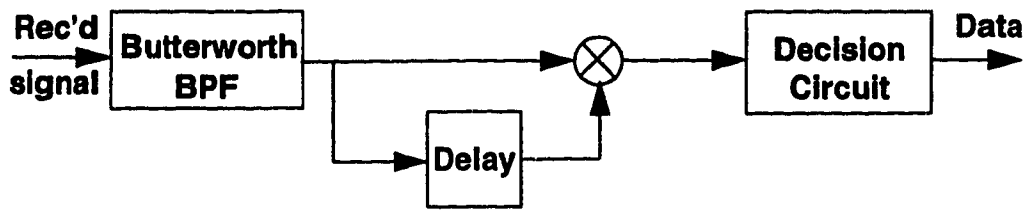
(b)

Fig.2.18 Block diagram of SRC-ODQPSK system with Butterworth filter receiver, (a) transmitter (b) receiver

Normalized frequency (f/f$_s$)
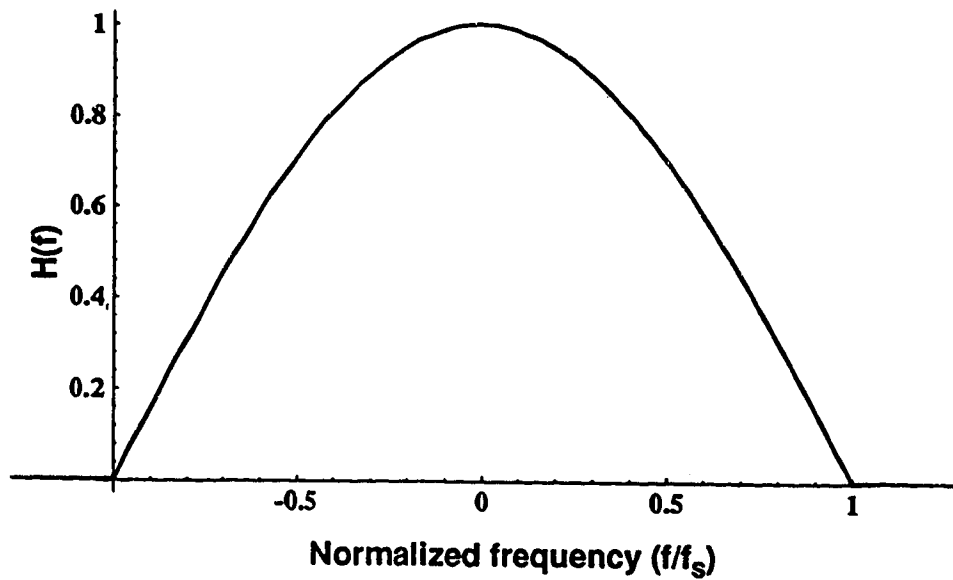
Fig.2.19 Magnitude response of a SRRC filter
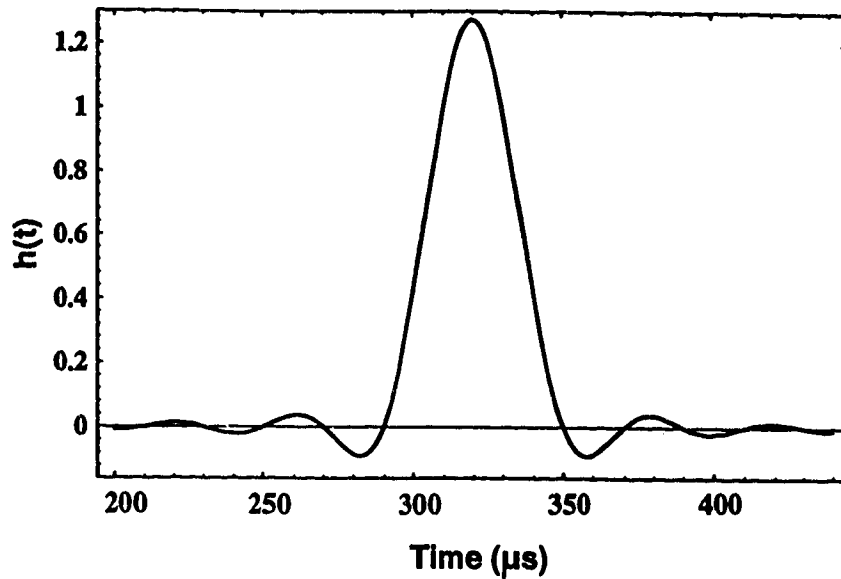
**Fig.2.20 Impulse response of a SRRC filter
for α=1 & T=40μs**

The 3dB cutoff frequency of the 4th order Butterworth filter is chosen to be 0.9f_s, where f_s is the symbol rate. This value is chosen as a tradeoff to maximally suppress the noise power, while not degrading the information signal itself significantly. The eye diagram of SRRC-filtered signal at the transmitter output is shown in Fig.2.21. As expected with SRRC filtering, the transmitter output signal has no intersymbol interference at every sampling instant, thus the differential phase changes are preserved perfectly. This approach is different from what is used in the 4RRC system, where transmitter filtering does not guarantee the ISI-free transmission characteristic. The receiver Butterworth filter will introduce some intersymbol interference, as shown in Fig.2.22. However, it can be proved in computer simulation that this only results in a small degradation in system error performance. The envelope characteristic of a SRRC-filtered ODQPSK signal is illustrated in Fig.2.23. It can be easily observed from this graph that its envelope variation is even smaller than 4RRC-filtered ODQPSK, conventional OQPSK, QPSK or π/4-DQPSK.

31
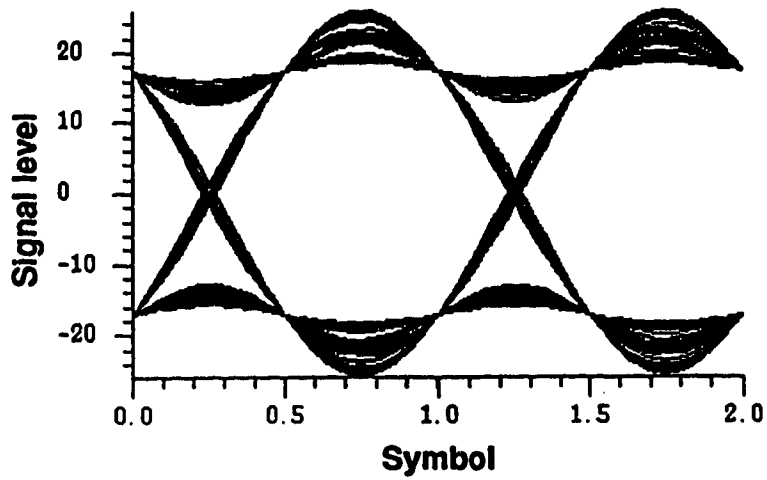
Fig.2.21 Eye diagram of the filtered in-phase signal
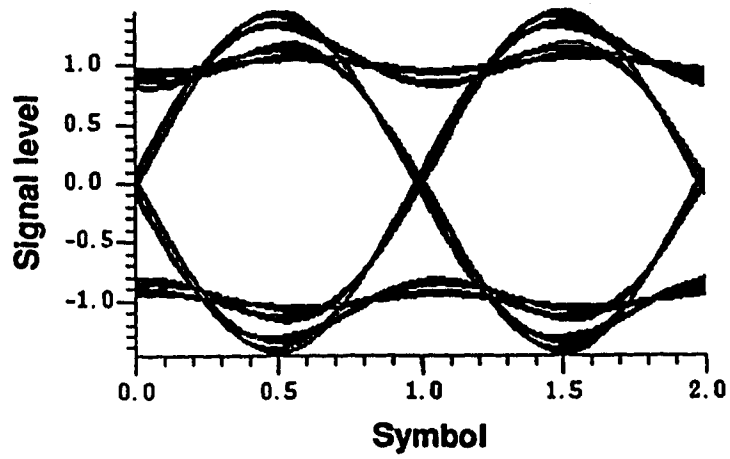
Fig.2.22 Eye diagram of the received filtered signal
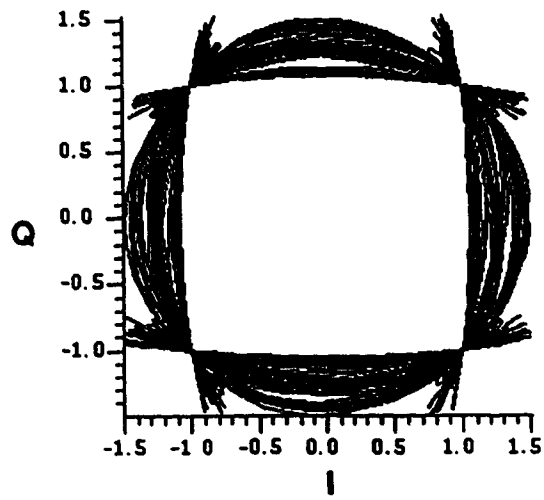
Fig.2.23 Envelope trajectory of SRRC-filtered signal

2.4.3 Smooth Transition ODQPSK system

In a Smooth Transition ODQPSK(ST-ODQPSK) system, sinusoidal pulse shaping is used to replace the familiar raised cosine shaping operation. The transceiver structure is basically the same as that of the SRC-ODQPSK system with a Butterworth filter receiver, except that the two baseband raised cosine-type pulse shapers are now replaced by two specific waveform shapers, followed by two 4th order Butterworth filters. The cutoff frequency of these lowpass filters is chosen as $0.95f_s$. The receiver Butterworth filter has a cutoff frequency of f_s. These frequencies are selected in such a manner that the noise power is reduced as much as possible without causing much distortion to the signal.

The sinusoidal waveshaping is performed according to the relationship of the adjacent two symbols. If they are of the same polarity, the output symbol from the waveform shaper simply equals the input. If they are of opposite polarity, a half-sinusoidal waveform is transmitted in the first half of one symbol period. Mathematically, this processing can be formulated as follows:

- if $a_n = -a_{n-1}$, then

$$b_n = a_{n-1} \cdot \cos(2\pi/Tt) \quad \text{for} \quad (n-1)T < t < (n-1)T + T/2$$

$$= a_n \quad \text{for} \quad T/2 + (n-1)T < t < nT$$

- if $a_n = +a_{n-1}$, then

$$b_n = a_n \quad \text{for} \quad (n-1)T < t < nT$$

where a_n denotes the incoming bit to the processor in the nth interval, and b_n denotes the outgoing bit from the processor in the nth interval. T is one symbol duration.

This waveform manipulation is quite similar to that described in [23]. There are several advantages to using such waveshaping. Firstly, differential detection

33

can be achieved with the processed signals. Secondly, it helps to greatly reduce the sidelobes in the signal spectrum, while maintaining the 3dB envelope fluctuation characteristic of the original signal. Thirdly, the jitter-free property is retained even though the signal is passed through an analog filter, which is important for the extraction of timing information from the detected baseband signal. Fig.2.24 shows the eye diagram of the processed in-phase signal. Clearly, this signal has no intersymbol interference, and is also jitter free.
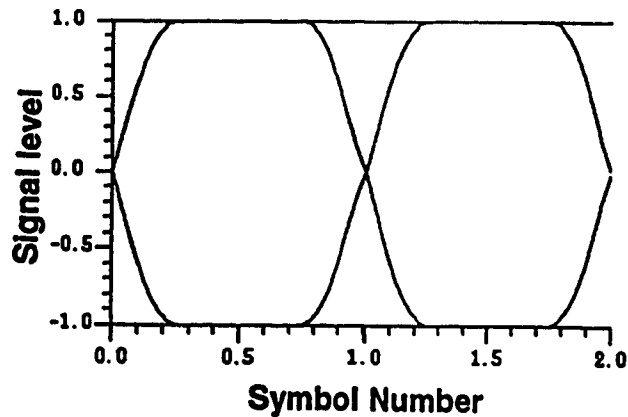
Fig.2.24 Eye diagram of the processed in-phase signal

A ST-ODQPSK transmitter circuit has been built up. The measured signal constellation after filtering is shown in Fig.2.25. It can be observed that ST-ODQPSK signal has the smallest envelope fluctuation.
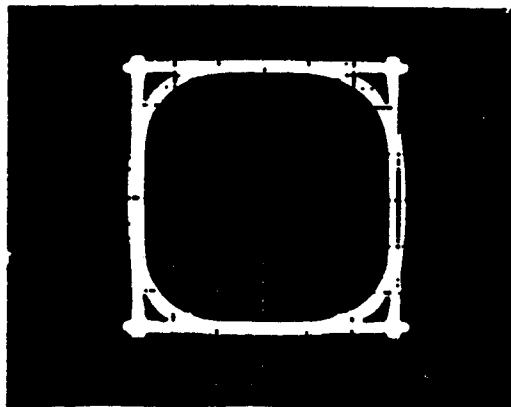
Fig.2.25 Envelope fluctuation of ST-ODQPSK signal

34

The required waveform shaping can be realized in several ways. Judging from the eye diagram shown in Fig.2.24, it is observed that, in principle, a linear filter(e.g. a FIR filter) can be designed to achieve the needed waveform shaping operation. However, such a filter will be difficult to design, and may need a very high order to approximate the required shape. Based on these considerations, another approach using operational amplifiers and a digital logic circuit is adopted. Fig.2.26 shows schematic diagram of the circuit to perform the waveform shaping operation.
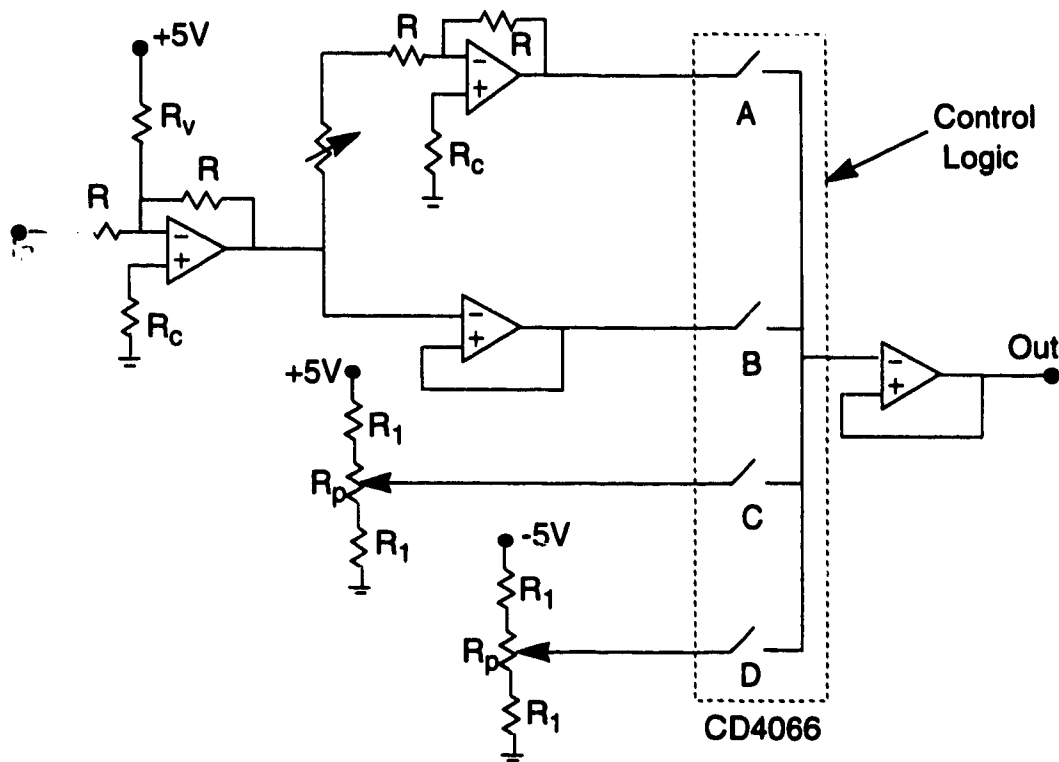
Fig.2.26 Sinusoidal waveshaping circuit

The input to this circuit is a sinusoidal wave, which is synchronized with the rising edge of the data stream. A CMOS analog switch CD4066, controlled by a digital logic circuit, is used to multiplex the four inputs, A-D, into the output. The schematic diagram of the control logic is shown in Fig.2.27.
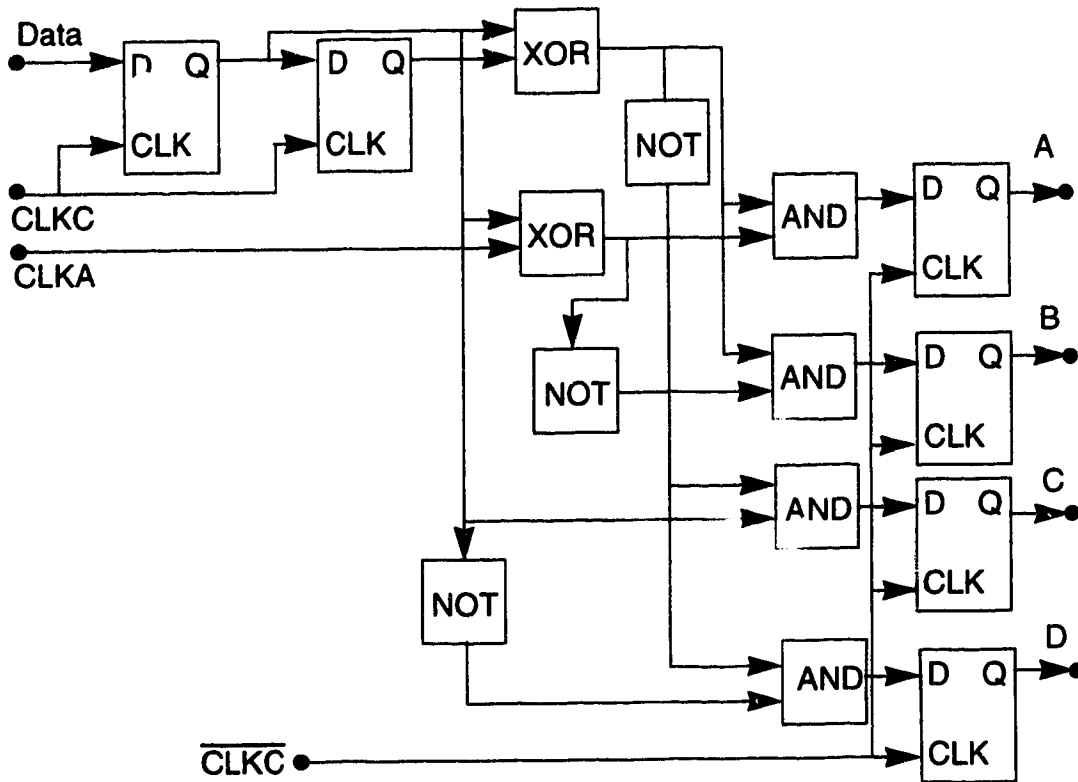
Fig.2.27 Schematic diagram of the switch control logic

The inputs to the control logic circuit are the data stream and several clock signals. The relationship between the data signal and clock signals are illustrated in Fig.2.28. As seen from this graph, the four clock signals, CLKA, CLKB, CLKC and $\overline{CLKC}$ can be easily generated from the input data stream, using some simple logic operations.

Computer simulation of these circuits will be discussed in the next chapter. By using a Markov chain model, the power spectral density(PSD) function of the ST-ODQPSK signal can be derived analytically. The detailed derivation of the PSD function can be found in Appendix A. The final result is given in (2-7).

Data

CLKA

CLKB

CLKC

$\overline{CLKC}$
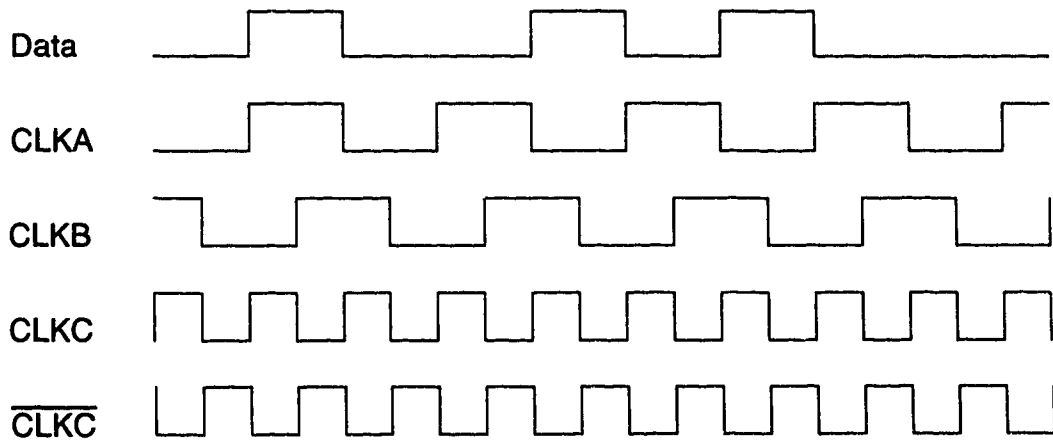
Fig.2.28 Clock signals for the control logic circuit

$$P(x) = \left[\frac{\sin(\pi x)}{2\pi x}(1 + \cos(\pi x)) - \frac{\sin(\pi x)}{\pi}\cos^2\left(\frac{1}{2}\pi x\right)\frac{x}{x^2 - 1} \right]^2$$

$$- \frac{\sin^4(\pi x)}{4x^2\pi^2(x^2 - 1)^2(-1)}$$

(2-7)

where x is the normalized frequency f/f_s. The power spectral density functions of ST-ODQPSK, MSK and unfiltered QPSK are shown in Fig.2.29. Of the three schemes, ST-ODQPSK exhibits the fastest spectral rolloff. Its spectral sidelobes are also lower than unfiltered QPSK and MSK. It can be noted, however, that ST-ODQPSK requires slightly more bandwidth than the previously described SRC-ODQPSK. Therefore, SRC-ODQPSK is more suitable than ST-ODQPSK for use in applications with stringent bandwidth restrictions.

Up to this point, several ODQPSK systems using different baseband pulse shaping techniques have been described in detail. The advantages and disadvantages of these schemes have also been discussed. The error performance of these systems in a typical mobile radio channel will be presented in Chapter 4.

37
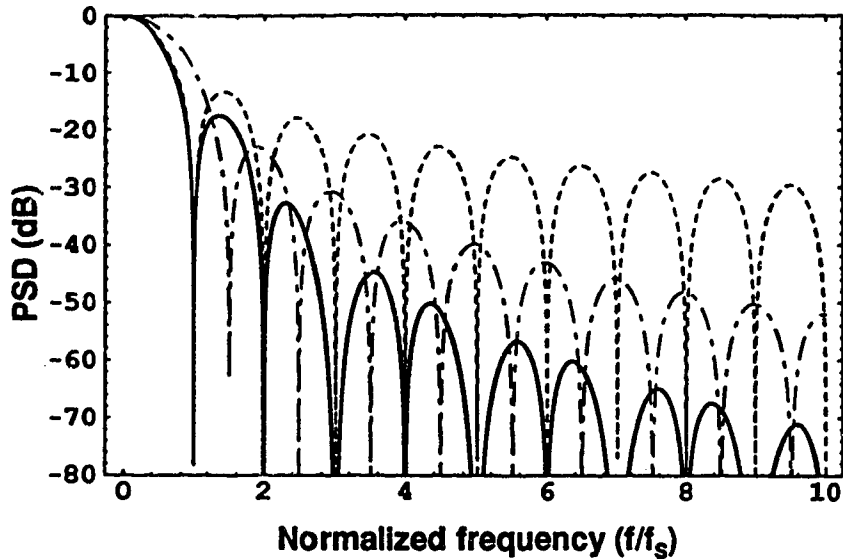
Fig.2.29 Power spectral density of ST-ODQPSK, QPSK and MSK.
Solid: ST-ODQPSK , dashed: QPSK, dotted & dashed: MSK

2.5 Error control coding techniques

Basically, there are two methods used for error protection, differing in their inherent error correction mechanisms. One is redundant error correction. These are the most widely researched and used techniques in practice since they have powerful error correction capability in any kind of transmission environment. Another is nonredundant error correction(NEC). Since NEC can achieve error correction without introducing any redundancy into the data signal, these techniques appear very useful in applications where the data rate is limited and good error performance is also required. Recently, NEC techniques have received much attention, and several different versions of NEC have been applied to $\pi/4$-DQPSK, M-ary PSK and MSK modulation schemes. Considerable performance improvement has been reported in the hardlimited Rician fading channel encountered in mobile satellite communications[21].

This thesis studies NEC techniques which can be adapted for the previously described ODQPSK systems. In the following sections, the principles

of nonredundant error correction are first introduced, and then several error correction schemes developed for ODQPSK modulation and the associated error correction algorithms are described in detail.

2.5.1 Principles of nonredundant error correction

Nonredundant error correction(NEC) techniques were first introduced by P.Chow and D.Ko, for use in binary DPSK systems[18]. Later, several modified versions of NEC were developed for many other modulation schemes, including DMSK, M-ary DPSK and, more recently, π/4-DQPSK. Since these schemes are all based upon the same principles, M-ary DPSK is chosen as the modulation method in the following derivation, without loss of generality.

In an M-ary differential PSK system, the carrier phase in the i-th time slot can be expressed as:

$$\theta_i = \theta_{i-1} + \left(\frac{2\pi}{m}\right) \cdot a_i \qquad (2\text{-}8)$$

where a_i and θ_i are the transmitted data symbol and carrier phase in the i-th time slot, respectively. By iterations, it is easy to show that the following relationship also holds:

$$\theta_i = \theta_{i-k} + \sum_{j=0}^{k-1} \left(\frac{2\pi}{m}\right) \cdot a_{i-j} \qquad (2\text{-}9)$$

Under noise-free conditions, the phase difference of the received signal between the present i-th time slot and the k-th previous time slot is therefore:

$$\theta_{ki} = \theta_i - \theta_{i-k} = \left(\frac{2\pi}{m}\right) \sum_{j=0}^{k-1} a_{i-j} \qquad (2\text{-}10)$$

As the detected phase difference can only lie between 0 and 2π, (2-10) may be rewritten as:

$$\theta_{ki} = \left(\left[\sum_{j=0}^{k-1} a_{i-j}\right] mod(m)\right) \cdot \left(\frac{2\pi}{m}\right) \qquad (2\text{-}11)$$

Therefore, the output symbol d_{ki} of the phase detector with k time slot delay, i.e., the k-th order phase detector, is given as follows:

$$d_{ki} = \left[\sum_{j=0}^{k-1} a_{i-j}\right] mod(m) \qquad (2\text{-}12)$$

By using L phase detectors, L output symbols can be obtained in the i-th time slot. Based upon the fact that a k-th order differential detector output can be linearly generated from k previously output symbols from the first order detector, it is seen that the output symbols from the L differential detectors constitute a rate 1/ L convolutional code sequence with a constraint length of (L+1). It is known that the error correction capability of a convolutional code can be expressed by its minimum free distance, which is defined as the minimum Hamming distance among the encoded sequences generated by the transmitted data sequence having a nonzero starting symbol. Due to the unique property of the differential detection process, it is intuitively observed that the following data sequence can satisfy the above condition:

$$a_i = f$$

$$a_{i+1} = \bar{f}$$

$$a_{i+j} = 0 \quad for \quad (j < 0)\, and\, (j > 1) \qquad (2\text{-}13)$$

where $f = (1, 2, \ldots, m\text{-}1)$ and $\bar{f} = -f\, mod(m) = m\text{-}f$. The resulting output sequence is shown in Fig.2-30.

Time Slot	i	i+1	i+2	-	-	i+k	-	-	i+l	i+l+1
1st Order Detector	f	$\bar{f}$	0	-	-	0	-	-	0	0
2nd Order Detector	f	0	$\bar{f}$	-	-	0	-	-	0	0
-	-	-	-		-			-	-	
-	-	-	-		-			-	-	
K-th Order Detector	f	0	0	-	-	$\bar{f}$	-	-	0	0
-	-	-	-		-			-	-	
-	-	-	-		-			-	-	
L-th Order Detector	f	0	0	-	-	0	-	-	$\bar{f}$	0

Fig.2.30 Output sequence of L phase detectors

In the i-th time slot, the outputs of all L detectors are the same symbol f. In the (i+k)-th time slot, only the k-th order detector will have a non-zero output symbol. Consequently, on a corresponding trellis path emanating from and re-merging at the all-0 state, the minimum Hamming distance of the resulting sequence is 2L, which is the minimum distance of the convolutional code. Interestingly, in this case, the minimum distance is also equal to the minimum free distance of this convolutional code. If the observation interval is L, the minimum distance becomes (2L-1), which indicates that (L-1) errors can be corrected as long as the number of errors within the L^2 symbols in L time slots is less than (L-1).

When phase noise is present, the received carrier phase can be expressed as :

$$\theta_j^r = \theta_j + \varepsilon_j \qquad (2\text{-}14)$$

where ε_j is the phase error.

The difference between θ_i^r and θ_{i-k}^r is

41

$$\theta_i^r - \theta_{i-k}^r = \left[\left(\frac{2\pi}{m} \right) \cdot \sum_{j=0}^{k-1} a_{i-j} + (\varepsilon_i - \varepsilon_{i-k}) \right] mod(2\pi) \tag{2-15}$$

The received symbol r_{ki} at the k-th order detector output can be expressed as:

$$r_{ki} = d_{ki} + e_{ki} mod(m) = \sum_{j=0}^{k-1} a_{i-j} + e_{ki} mod(m) \tag{2-16}$$

where e_{ki} is the error. The Syndrome S_{ki} is obtained from the received symbol sequence r_{ki} as follows:

$$S_{ki} = \sum_{j=0}^{k} r_{1(i-j)} - r_{(k+1)i} mod(m)$$

$$= \sum_{j=0}^{k} e_{1(i-j)} - e_{(k+1)i} mod(m) \qquad k = 1 \sim L - 1$$

$$\tag{2-17}$$

As mentioned earlier, this convolutional code has an (L-1) error correction capability when the observation is limited to L time slots. Correspondingly, there will be L^2 different error symbols existing in the detection process. However, the combination pattern of the following (L-1)L syndromes differs for every error symbol if the total number of errors is less than (L-1):

$$\begin{bmatrix} S_{1i} & S_{1(i-1)} & S_{1(i-2)} & \cdots & S_{1(i-L+1)} \\ S_{2i} & S_{2(i-1)} & S_{2(i-2)} & \cdots & S_{2(i-L+1)} \\ \cdots & \cdots & \cdots & & \\ \cdots & \cdots & \cdots & & \\ S_{(L-} & S_{(L-1)(i-1)} & S_{(L-1)(i-2)} & \cdots & S_{(L-1)(i-L+1)} \end{bmatrix}$$

Therefore, the error symbol $e_{1(i-L+1)}$ can be detected from the syndrome pattern, and the correct symbol can be obtained by subtracting $e_{1(i-L+1)}$ from the received symbol $r_{1(i-L+1)}$.

If all the error symbols take on a value of either 1 or -1 mod(m), as in the case of binary transmission, it has been proved[16] that the number of syndrome patterns N can be limited to:

$$N = 2 \cdot \sum_{j=0}^{L-2} \binom{L^2-1}{j} \cdot 2^j \qquad (2\text{-}18)$$

Fig. 2.31 helps give a better perspective of the error correction mechanism of the NEC technique. For convenience, assume that a binary differential phase-modulated system is employed, and that a sequence of 101101110 is transmitted. Also, two errors, separated by more than two symbol intervals, are assumed to occur in the first-order differential detector. This system is required to correct a single error, thus two differential detectors are needed. According to (2-17), it is not difficult to obtain the output from the syndrome generating circuit and the correction pulse, as shown in Fig.2.31. As expected, both errors are successfully eliminated.
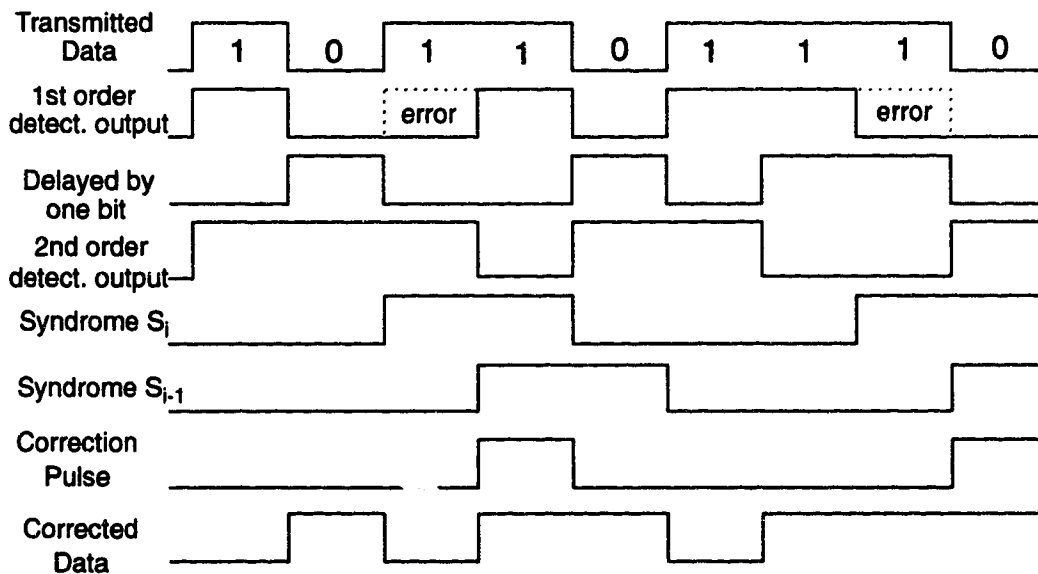
Fig.2.31 Illustration of error correction procedure

43

Based upon the above-mentioned principles, we can apply NEC techniques to ODQPSK modulation schemes. Single, double and triple error correction can be achieved by increasing the dimension of the syndrome matrix described earlier. In the following several sections, detailed implementation methods and the error correction algorithms of single, double and triple error correction schemes, which can be used for the proposed ODQPSK systems, are discussed.

2.5.2 Single error correction

Since there exist two kinds of differential encoding/decoding methods for ODQPSK systems, the derived NEC receivers are slightly different. In the following several sections, two-bit differential encoding is always assumed in developing the structure of the NEC receiver. For the case of three-bit differential encoding, only the final circuit implementations are given. However, the circuit design follows the same principles.

When applying (2-17) to ODQPSK systems, the specific detection method employed at the receiver should be taken into consideration. Although ODQPSK is a quadrature modulation scheme, bit-by-bit detection is taken at the receiver as in a binary PSK system. For this reason, the modulo constant m used in the previous section should be chosen as 2, instead of 4. Also, to achieve single error correction, L should be chosen as 2, i.e., two differential phase detectors are needed at the receiver.

With this in mind, the received signal at the output of the differential phase detector can be formulated as follows :

$$D_{1i} = d_i \oplus e_{D1i}$$
$$D_{2i} = d_i \oplus d_{i-1} \oplus e_{D2i} \qquad (2\text{-}19)$$

where D_{ki} is the k-th order detector output in the i-th time slot. d_i is the ideal noiseless data output in the i-th time slot. e_{Dki} indicates the error symbol at the k-th order detector output in the i-th time slot. The syndrome matrix now contains only two elements as given below:

$$S_i = D_{1i} \oplus D_{1(i-1)} \oplus D_{2i}$$

$$= d_i \oplus d_{i-1} \oplus e_{D1i} \oplus e_{D1(i-1)} \oplus d_i \oplus d_{i-1} \oplus e_{D2i}$$

$$= e_{D1i} \oplus e_{D1(i-1)} \oplus e_{D2i} \qquad (2\text{-}20)$$

The syndrome obtained in the previous interval is:

$$S_{i-1} = e_{D1(i-1)} \oplus e_{D2(i-1)} \oplus e_{D1(i-2)}$$

$$= e_{D1(i-1)} \oplus e_{D2(i-1)} \qquad (2\text{-}21)$$

In the above equation, the effect of $e_{D1(i-2)}$ is assumed to have been eliminated in the previous decoding interval. The error symbol $e_{D1(i-1)}$ can therefore be detected and corrected by the following operation:

$$e_{D1(i-1)} = S_i \cdot S_{i-1}$$

$$d_{i-1} = D_{1(i-1)} \oplus e_{D1(i-1)} \qquad (2\text{-}22)$$

The block diagram of single error correction circuit can be developed, based upon (2-19) - (2-22), and shown in Fig.2.32.
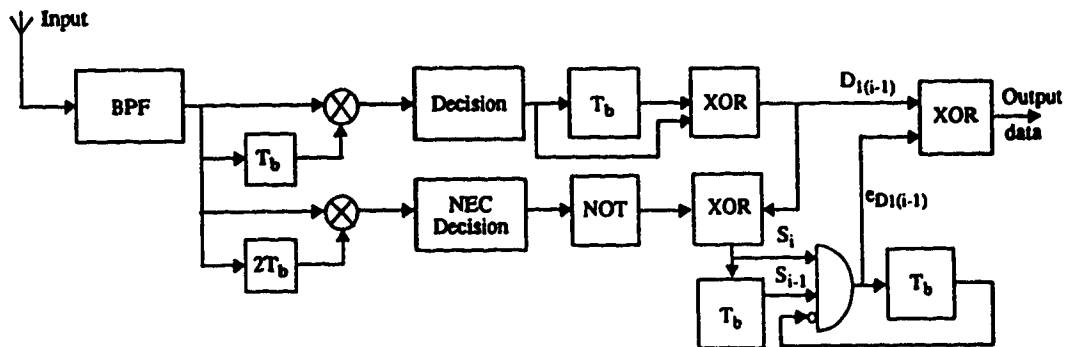
Fig.2.32 Single NEC circuit for two-bit encoded ODQPSK

45

The decision rules employed in the blocks "Decision" and "NEC Decision" correspond to those of one-bit and two-bit differential detection, respectively, as has been explained in Sec. 2.3.2.1. Similarly, the detection circuit for three-bit differentially encoded ODQPSK system can be derived, and shown in Fig.2.33.
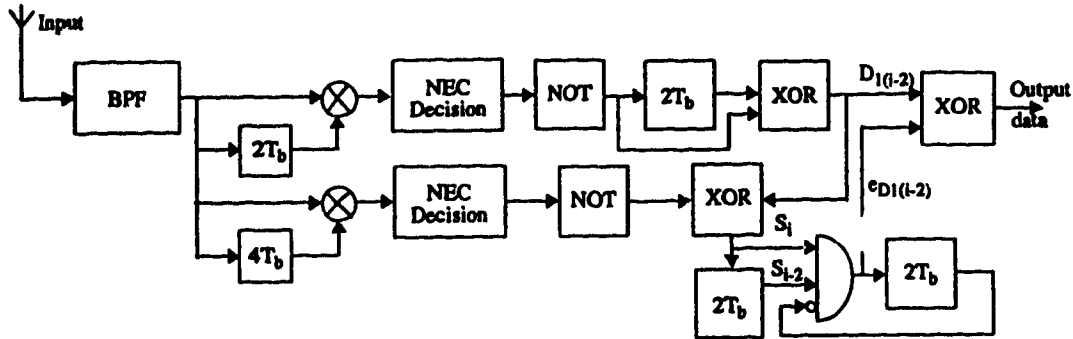
Fig.2.33 Single NEC circuit for three-bit encoded ODQPSK

2.5.3 Double error correction

For an NEC which can correct up to two errors, one first-order differential detector, one second-order differential detector, and one third-order differential detector are employed. Using the same method as in single error correction, the syndrome matrix is determined as follows:

$$\begin{bmatrix} S_{1i} & S_{1(i-1)} & S_{1(i-2)} \\ S_{2i} & S_{2(i-1)} & S_{2(i-2)} \end{bmatrix}$$

The six syndromes are constructed according to the relationships given in Equ.(2-23). When generating these equations, it is assumed that the effects of $e_{1(i-3)}$ and $e_{1(i-4)}$ have been eliminated in the previous decoding interval. These

$e_{1(I-2)}$ is "1" when they are detected and "0" otherwise, and thus error correction of the received data $r_{1(I-2)}$ can be performed at the I-th decision instant by adding $e_{1(I-2)}$ to $r_{1(I-2)}$.

The block diagram of the double error correction circuit is given in Fig.2.34.
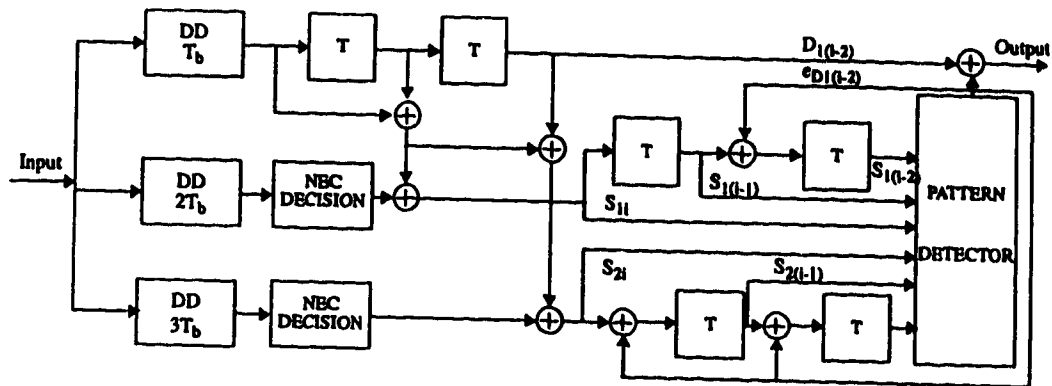
Fig.2.34 Block diagram of double error correction for two-bit encoded ODQPS'-

For three-bit encoded ODQPSK, the circuit diagram is given in Fig.2.35.
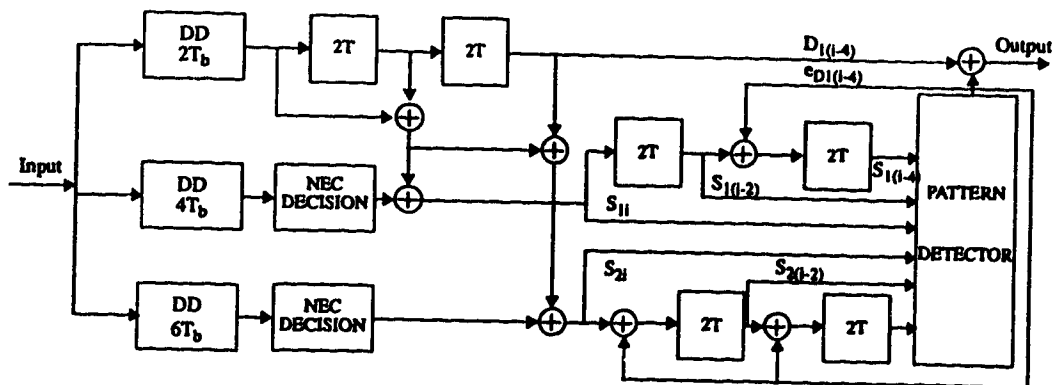
Fig.2.35 Block diagram of double error correction for three-bit encoded ODQPSK

48

$$S_{1i} = r_{1i} \oplus r_{1(i-1)} \oplus r_{2i}$$
$$= e_{1i} \oplus e_{1(i-1)} \oplus e_{2i}$$
$$S_{1(i-1)} = r_{1(i-1)} \oplus r_{1(i-2)} \oplus r_{2(i-1)}$$
$$= e_{1(i-1)} \oplus e_{1(i-2)} \oplus e_{2(i-1)}$$
$$S_{1(i-2)} = r_{1(i-2)} \oplus r_{1(i-3)} \oplus r_{2(i-2)}$$
$$= e_{1(i-2)} \oplus e_{2(i-2)}$$
$$S_{2i} = r_{1i} \oplus r_{1(i-1)} \oplus r_{1(i-2)} \oplus r_{3i}$$
$$= e_{1i} \oplus e_{1(i-1)} \oplus e_{1(i-2)} \oplus e_{3i}$$
$$S_{2(i-1)} = r_{1(i-1)} \oplus r_{1(i-2)} \oplus r_{1(i-3)} \oplus r_{3(i-1)}$$
$$= e_{1(i-1)} \oplus e_{1(i-2)} \oplus e_{3(i-1)}$$
$$S_{2(i-2)} = r_{1(i-2)} \oplus r_{1(i-3)} \oplus r_{1(i-4)} \oplus r_{3(i-2)}$$
$$= e_{1(i-2)} \oplus e_{3(i-2)}$$

$$(2\text{-}23)$$

six syndromes are not orthogonal for $e_{1(i-2)}$, and therefore, a pattern where only $e_{1(i-2)}$ is "1" and eight patterns where $e_{1(i-2)}$ and one of eight others, e_{1i}, $e_{1(i-1)}$, e_{2i}, $e_{2(i-1)}$, $e_{2(i-2)}$, e_{3i}, $e_{3(i-1)}$ and $e_{3(i-2)}$ are "1" should be detected. These patterns are given as follows:

$$S_i = \begin{Bmatrix} 011 \\ 111 \end{Bmatrix} \quad \begin{Bmatrix} 101 \\ 001 \end{Bmatrix} \quad \begin{Bmatrix} 111 \\ 011 \end{Bmatrix}$$
$$\begin{Bmatrix} 010 \\ 111 \end{Bmatrix} \quad \begin{Bmatrix} 001 \\ 111 \end{Bmatrix} \quad \begin{Bmatrix} 111 \\ 111 \end{Bmatrix}$$
$$\begin{Bmatrix} 011 \\ 110 \end{Bmatrix} \quad \begin{Bmatrix} 011 \\ 101 \end{Bmatrix} \quad \begin{Bmatrix} 011 \\ 011 \end{Bmatrix}$$

2.5.4 Triple error correction

Triple error correction can be achieved by using a total of four differential detectors. Because of its triple error correction capability, the obtained receiver structure is more complicated compared to the previous two NEC receivers. Using the same procedure, a total of 12 syndromes can be found for triple error correction case, as shown below. These syndrome patterns are solely dependent upon the error patterns present at the differential detector outputs.

$$S_{1i} = r_{1i} \oplus r_{1(i-1)} \oplus r_{2i}$$

$$= e_{1i} \oplus e_{1(i-1)} \oplus e_{2i}$$

$$S_{1(i-1)} = r_{1(i-1)} \oplus r_{1(i-2)} \oplus r_{2(i-1)}$$

$$= e_{1(i-1)} \oplus e_{1(i-2)} \oplus e_{2(i-1)}$$

$$S_{1(i-2)} = r_{1(i-2)} \oplus r_{1(i-3)} \oplus r_{2(i-2)}$$

$$= e_{1(i-2)} \oplus e_{1(i-3)} \oplus e_{2(i-2)}$$

$$S_{1(i-3)} = r_{1(i-3)} \oplus r_{2(i-3)}$$

$$= e_{1(i-3)} \oplus e_{2(i-3)}$$

$$S_{2i} = r_{1i} \oplus r_{1(i-1)} \oplus r_{1(i-2)} \oplus r_{3i}$$

$$= e_{1i} \oplus e_{1(i-1)} \oplus e_{1(i-2)} \oplus e_{3i}$$

$$S_{2(i-1)} = r_{1(i-1)} \oplus r_{1(i-2)} \oplus r_{1(i-3)} \oplus r_{3(i-1)}$$

$$= e_{1(i-1)} \oplus e_{1(i-2)} \oplus e_{1(i-3)} \oplus e_{3(i-1)}$$

$$S_{2(i-2)} = r_{1(i-2)} \oplus r_{1(i-3)} \oplus r_{3(i-2)}$$

$$= e_{1(i-2)} \oplus e_{1(i-3)} \oplus e_{3(i-2)}$$

$$S_{2(i-3)} = r_{1(i-3)} \oplus r_{3(i-3)}$$

$$= e_{1(i-3)} \oplus e_{3(i-3)}$$

$$S_{3i} = r_{1(i-1)} \oplus r_{1(i-2)} \oplus r_{1(i-3)} \oplus r_{1i} \oplus r_{4i}$$

$$= e_{1i} \oplus e_{1(i-1)} \oplus e_{1(i-2)} \oplus e_{1(i-3)} \oplus e_{4i}$$

$$S_{3(i-1)} = r_{1(i-1)} \oplus r_{1(i-2)} \oplus r_{1(i-3)} \oplus r_{4(i-1)}$$

$$= e_{1(i-1)} \oplus e_{1(i-2)} \oplus e_{1(i-3)} \oplus e_{4(i-1)}$$

$$S_{3(i-2)} = r_{1(i-2)} \oplus r_{1(i-3)} \oplus r_{4(i-2)}$$
$$= e_{1(i-2)} \oplus e_{1(i-3)} \oplus e_{4(i-2)}$$
$$S_{3(i-3)} = r_{1(i-3)} \oplus r_{4(i-3)}$$
$$= e_{1(i-3)} \oplus e_{4(i-3)} \tag{2-24}$$

There are a total of 16 distinct error symbols resulting in 118 different syndrome patterns. The circuit diagram can be easily derived from these equations. Fig.2.36 shows two-bit differential case, and the circuit block diagram for three-bit encoding is given in Fig.2.37. The error symbol $e_{1(i-3)}$ can always be corrected if the total number of symbol errors is less than or equal to three. In these syndrome patterns, the error symbol $e_{1(i-4)}$, $e_{1(i-5)}$ and $e_{1(i-6)}$ are assumed to have been corrected through the feedback paths from the output of the pattern detectors. If any of these patterns is detected, a "1" is output from the pattern detector and EX-ORed with $d_{1(i-3)}$ so that the error symbol can be removed. Otherwise, a "0" is output from the pattern detector. The syndrome matrix for triple error correction is shown below. A general summary of these syndrome patterns can be found in Appendix C.

$$\begin{bmatrix} S_{1i} & S_{1(i-1)} & S_{1(i-2)} & S_{1(i-3)} \\ S_{2i} & S_{2(i-1)} & S_{2(i-2)} & S_{2(i-3)} \\ S_{3i} & S_{3(i-1)} & S_{3(i-2)} & S_{3(i-3)} \end{bmatrix}$$
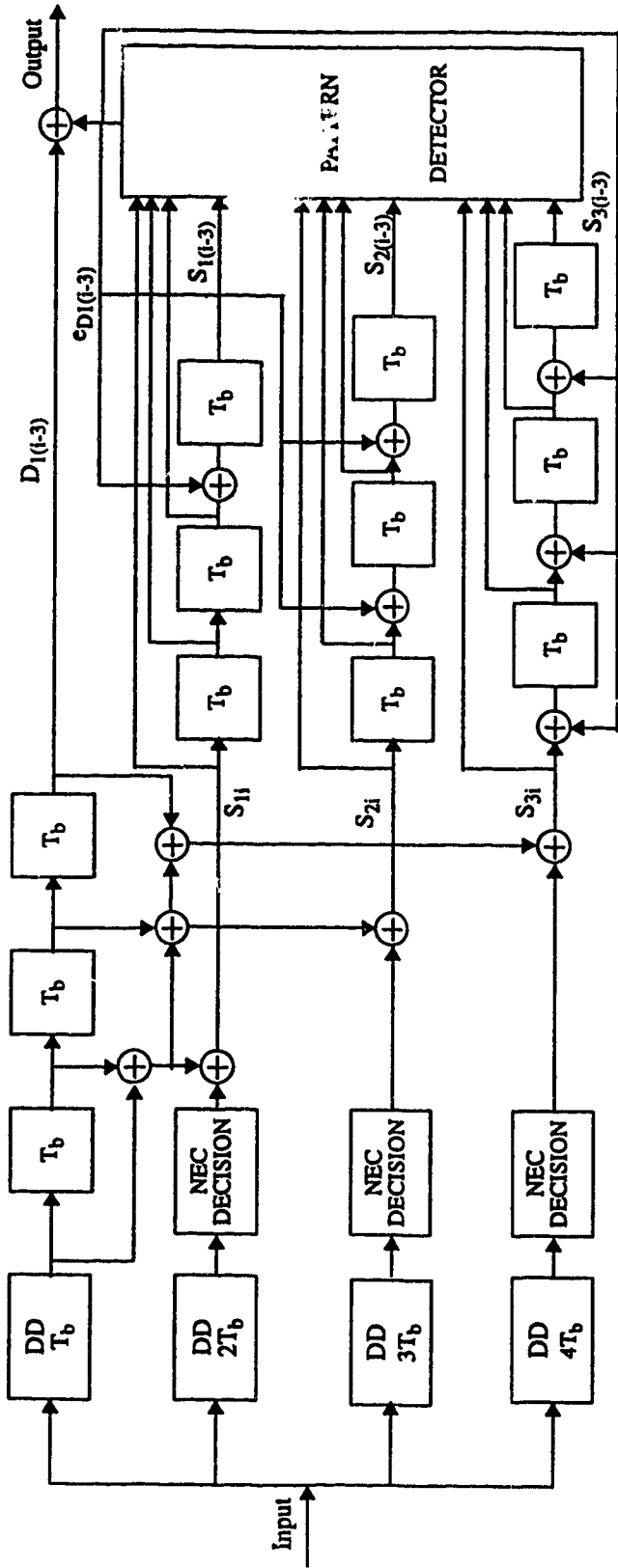
Fig.2.36 Block diagram of triple error correction for two-bit differential encoding
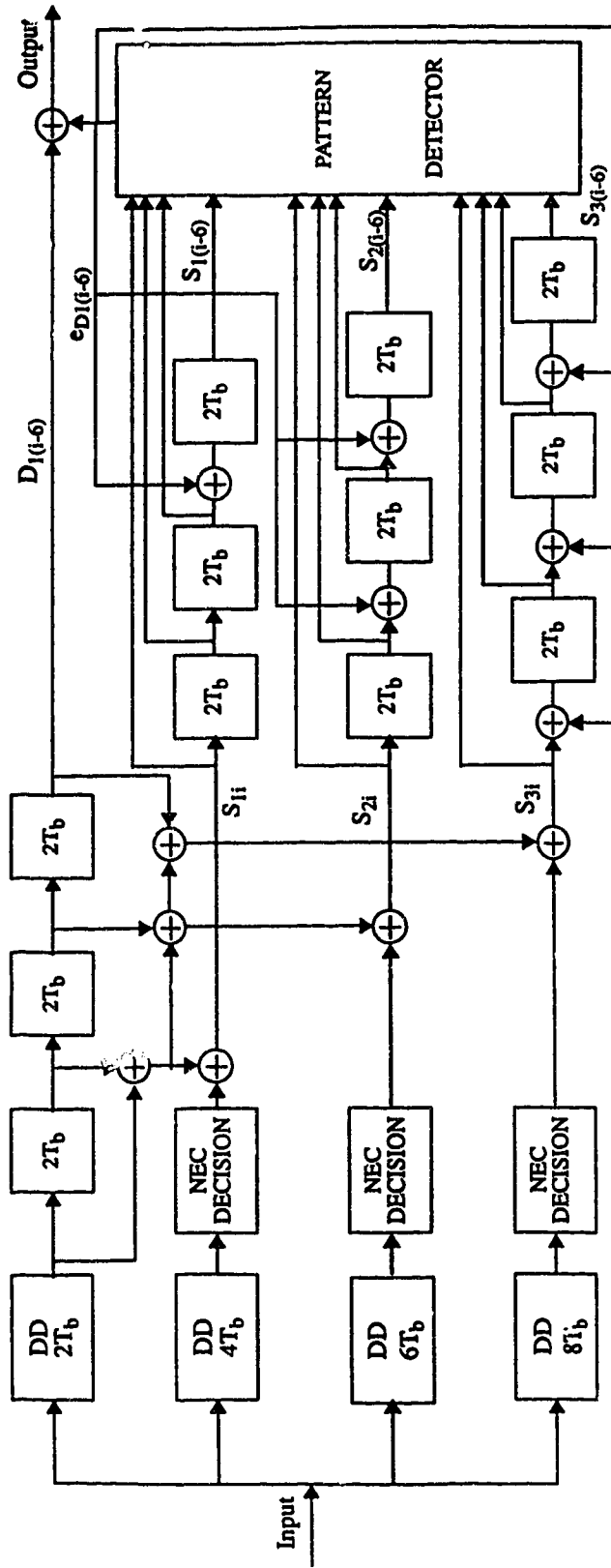
Fig.2.37 Block diagram of triple error correction
for three-bit differential encoding

CHAPTER 3   COMPUTER SIMULATION OF ODQPSK SYSTEMS

This chapter is concerned with various implementation methods for ODQPSK systems by means of computer aided design. The systems described earlier are simulated using a software simulation package called *Block Oriented System Simulator(BOSS)* by Comdisco Systems Inc. The major features of this simulation package are briefly described. Simulation block diagrams developed for different ODQPSK transceivers and mobile radio fading channels are explained in detail. Simulation methods for nonredundant error correction circuits including single, double and triple error correction and their error correction algorithms are also discussed.

3.1 Block Oriented System Simulator(BOSS) environment

The BOSS simulation package provides a complete interactive environment for simulation-based analysis and design of any system which can be represented in block diagram form. The major components of the BOSS software package are written in LISP and run under the VMS operating system on DEC VAXstations using VWS or DEC windows or, under the UNIX system on SUN or SPARC workstations using X-Windows. Although BOSS can perform waveform level simulation for any system, it is most suitable for communication system simulation. In BOSS , all systems, whether they are simple functional blocks such as transmitters or entire communication links, are described in a hierarchical form so that very complex systems can also be studied[34]. On the other hand, this structure considerably simplifies the process of testing and debugging a functional block or a whole complex system. In addition, BOSS provides a variety of post processor functions, with which a number of signal processing operations can be performed, such as time domain waveform plots,

eye diagrams, scatter diagrams, magnitude and phase spectra, correlation diagrams and histograms. In addition to a large number of modules already provided in the library along with the package, each user can also create new primitive modules(new blocks) to meet specific purposes, supported by corresponding FORTRAN subroutines. All these features of BOSS provide communication engineers with a very flexible, user friendly and powerful design and simulation environment.

3.2 General considerations in the simulation

In order to compare the proposed systems with the current second generation North American system and European systems, it is preferable to use the same parameters in these systems. Unfortunately, the bit rates in North American system and European systems are different. In the IS-54 standard, the specified data rate is 48.6kb/s, while in the DECT and GSM systems they are 1152kb/s and 271kb/s, respectively. This usually does not cause a problem in an AWGN channel. In a Rayleigh fading channel with large Doppler spread, however, different bit rates would yield different error performance. Therefore, special care must be taken to normalize the fading rate with respect to the signalling rate in order to obtain a consistent basis for performance comparisons. In addition, to obtain high computational efficiency and save simulation time, high bit rate transmission should be avoided in the simulation if an alternative approach is possible. Another factor which should be taken into consideration is that numeric values can be stored with only a finite number of binary digits. Thus, any rate or period should correspond exactly with a binary number. The BOSS manual recommends that the sampling interval ΔT be a power of 2, and that the bit rate be an integral multiple of ΔT. Hence, the internal binary representation of ΔT is the same as the entered value. The sampling interval ΔT should be small enough to avoid undue aliasing for the signals being sampled. Ideally, the corresponding

sampling rate should be greater than twice the highest frequency present in the signals to be sampled. In practice many waveforms have infinite bandwidth, and so ΔT is made small enough such that the aliased power falling into the simulation bandwidth is small compared to the noise power in the same bandwidth. For the simulation of a binary NRZ system, a sampling rate of 8 to 16 times the bit rate is adequate for accurately characterizing the signal processing processes involved.

With all this in mind, and considering that 1/48.6=0.0205761..., the bit rate used in the simulation is chosen as 50kb/s, and 16 samples are taken in every bit interval. Therefore, the sampling interval used in the simulation is:

$$\Delta T = \frac{1}{(50 \times 16 \times 10^3)} = 1.25 \times 10^{-6} s \qquad (3\text{-}1)$$

3.3 Multipath Rayleigh fading channel simulator

As mentioned in Chapter 1, although both Rayleigh fading and Log-normal fading are present in a typical land mobile radio environment, system error performance is mainly determined by Rayleigh fading. Therefore, only this kind of fading is incorporated in the simulation studies. The BOSS simulation block diagram of a flat Rayleigh fading channel is given in Fig.3.1.

As can be seen, it consists of two Gaussian random generators, two lowpass pulse shaping filters, an adjustable AWGN source and several multipliers and adders. Each Gaussian random generator has a different seed so that the output Gaussian random variables from the two generators are independent of each other. Both outputs are assumed to have zero mean and unity variance. Since the output samples from the generators take on discrete values, and contain high frequency components, they are fed into two lowpass pulse shaping

55
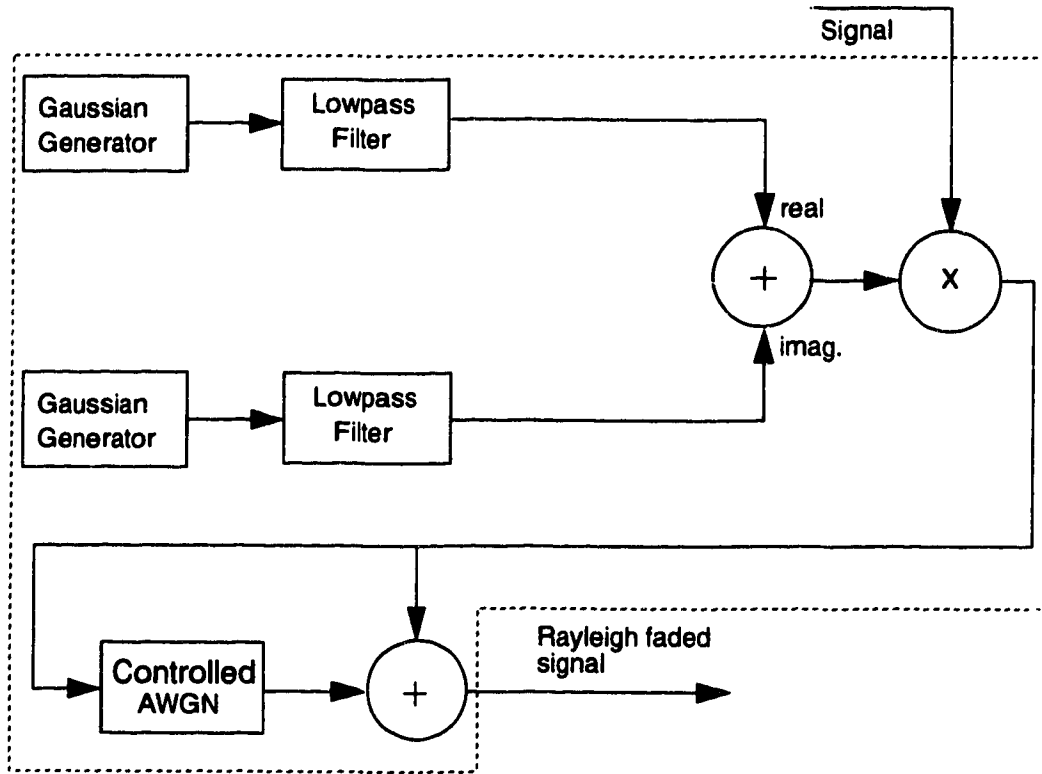
Fig.3.1 BOSS diagram of a flat Rayleigh fading channel

filters to obtain required smoothed outputs. In a practical mobile radio environment, the measured spectrum of the received signal is very close to the analytical result, provided that an omnidirectional antenna is mounted at the receiver. It has been proved that the spectrum can be formulated as follows[35]:

$$S_s(f) = \frac{C}{\sqrt{f_m^2 - f^2}} \qquad -f_m \leq f \leq f_m \qquad (3-2)$$

where $S_s(f)$ is the power spectrum of the fading signal. C is a constant depending upon the antenna gain pattern and medium attenuation factor, and f_m is the maximum Doppler frequency. The fading spectrum is sk^wn Fig.3.2.

56
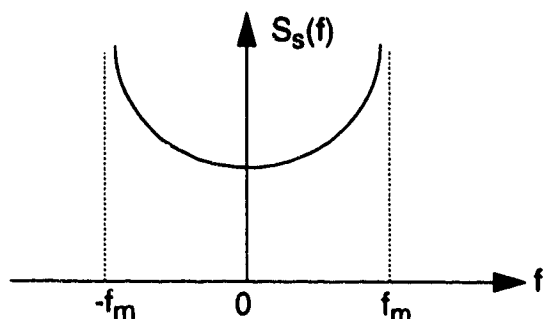
Fig.3.2 Spectrum of a typical fading signal

In the simulation, a 10th order lowpass filter has been used to approximate $S_s(f)$, and the peak frequency of the spectrum is made the same as the Doppler frequency. The power spectrum at the frequency f_m is about 10dB higher than that at $f=0$. The outputs from the two pulse shaping filters are then combined together to form a complex output with the required fading characteristics. The output bit stream from the transmitter is then multiplied with this fading signal and added to the output from a controlled AWGN source. The mean value of this AWGN source is set to zero and its variance is adjusted according to the strength of the faded signal so as to provide a specified signal-to-noise ratio over a certain noise bandwidth. For QPSK signalling, the noise bandwidth is usually set to the channel signalling rate. Therefore, the noise bandwidth is fixed at half the bit rate for all the simulations.

The block diagram for a frequency-selective Rayleigh fading channel is shown in Fig.3.3.
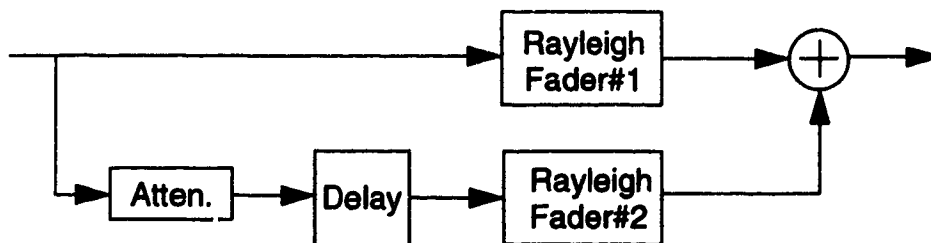
Fig.3.3 Block diagram of a two-ray Rayleigh fading channel

57

It should be noted that this model presents a rough approximation of a practical frequency-selective Rayleigh fading channel, as specified in the IS-54 recommendation. In this model, the attenuation block accounts for practical reflection losses incurred by surrounding buildings and objects, as compared to the direct path. The delay block represents the excess propagation delay of the second ray, as compared to the direct path. The two Rayleigh faders generate independent signals which have Rayleigh fading envelope and random phase characteristics. This can be achieved by choosing four distinct seeds for the four Gaussian random generators in the two faders. According to the IS-54 specifications, the two paths are of equal strength, and the delay spread ranges from 0 to one symbol duration, which is about 40µs. To more accurately model a mobile radio dispersive channel, more than two fading paths are needed, with variable path attenuations. Usually, the amount of attenuation in each path increases with the corresponding path delay, and could be as high as 20dB[11]. The BOSS implementation of a 4-ray Rayleigh fading channel in shown in Fig.3.4. Each path has a variable gain and delay to account for a number of channel scenarios. By setting some of the gain parameters to zero, a 2-ray channel can be simulated as well. For the performance study in this project, we still use the two-ray model as all the results published so far for either π/4-DQPSK or GMSK are based upon a two-ray channel model with equal strength.

3.4 SRC-ODQPSK transceiver

The block diagram for the SRC-ODQPSK system is shown in Fig.3.5. A pseudo-random binary sequence is generated from a random data source, and fed to a two-stage differential encoder. The encoded data are then split into two quadrature channels and offset modulated. After 4RRC pulse shaping is performed on each channel, they are recombined to give a complex baseband representation. This signal is then faded and corrupted by AWGN, as observed in

58
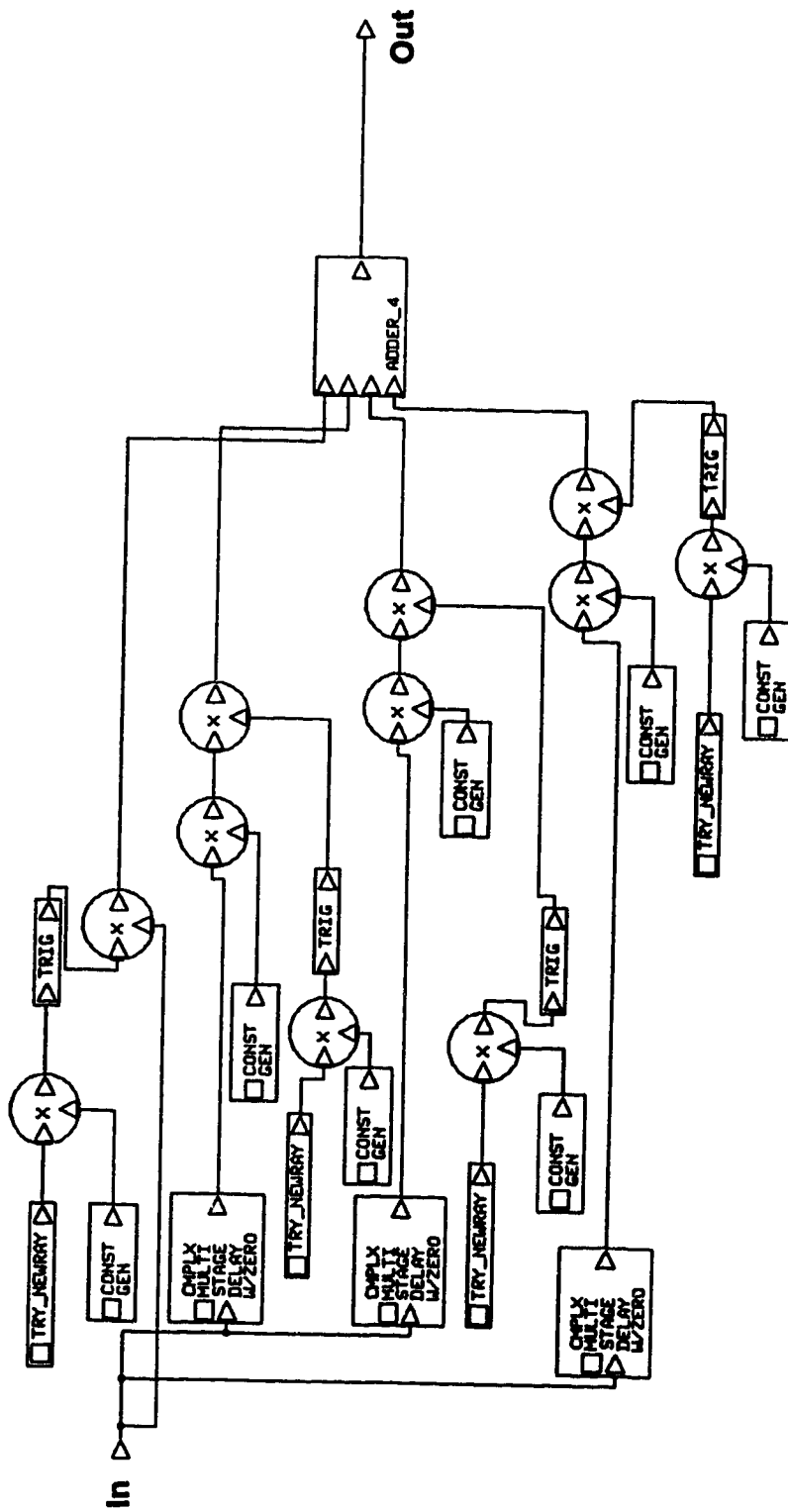
Fig.3.4 BOSS diagram of a 4-ray Rayleigh fading channel

59

a practical mobile radio channel. The receiver filter is another 4RRC filter, which can achieve ISI-free transmission in a linear AWGN channel. In a fading channel, this combination can yield sub-optimal results. The filtered signal is then demodulated using one-bit differential detection. Finally, an ei.ɔr counter is used to count the bit error rate of this system. If three-bit differential encoding is required, an additional differential encoding stage has to be inserted at the transmitter differential encoding stage, and the amount of delay involved in the receiver block CMPLX MULTI-STAGE DELAY must be doubled. If a Butterworth filter is used at the front end of the receiver instead of a 4RRC filter, the 4RRC pulse shaping at the transmitter is replaced by SRRC pulse shaping.

3.5 ST-ODQPSK transceiver

Fig.3.6 shows the block diagram of ST-ODQPSK system. The expansions of ST-ODQPSK transmitter and pulse shaping blocks are given in Fig.3.7 and Fig.3.8. In the pulse shaping circuit, a sinusoidal source is synchronized with the input data stream and used to provide the required transition waveforms. The four control signals, CLKA, CLKB, CLKC and CLKC, are generated from the input data stream and the sinusoidal source.They are fed to the multiplexer to select the correct output waveform, according to the rules formulated in Sec. 2.3.3.
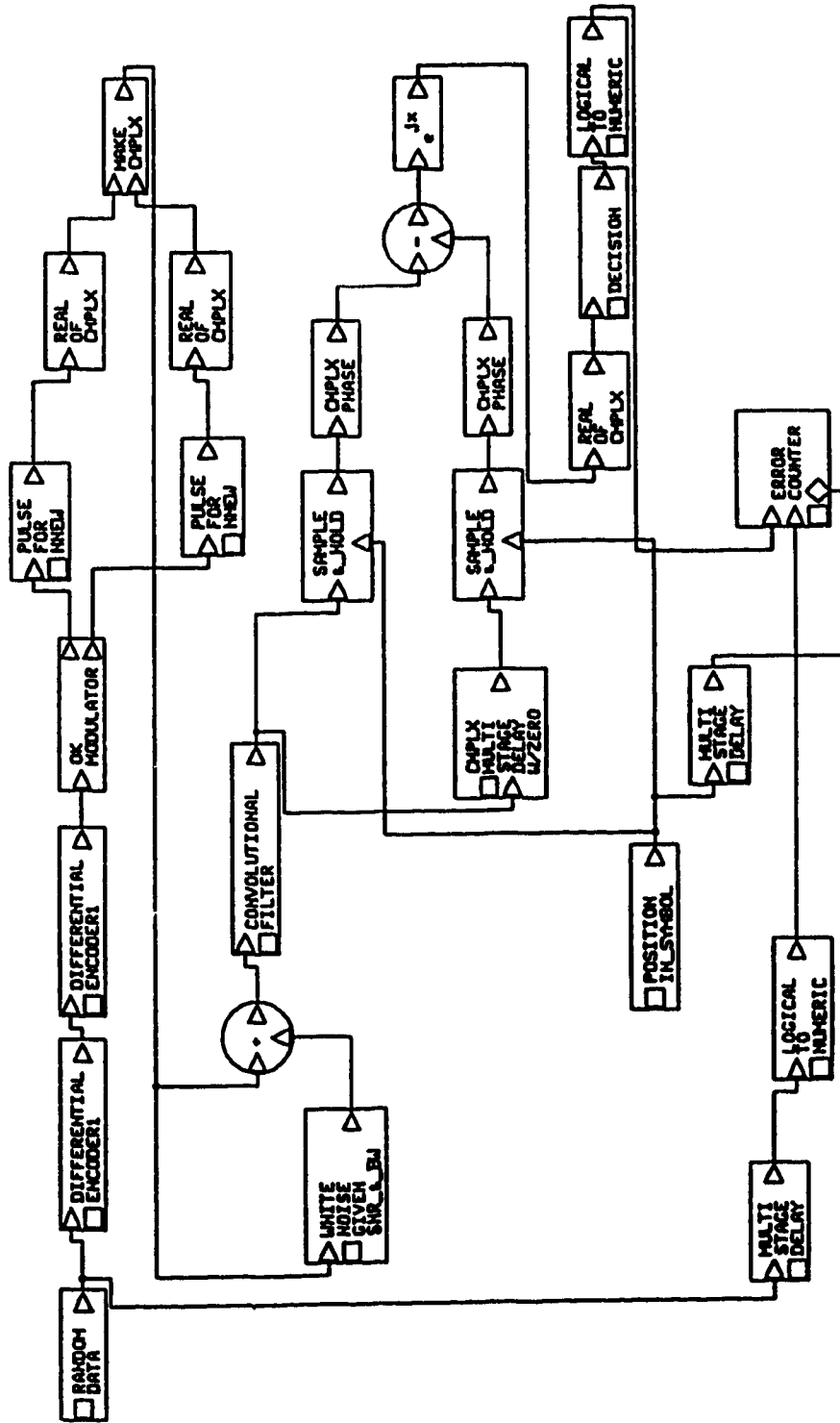
Fig.3.5 BOSS diagram of the SRC-ODQPSK system
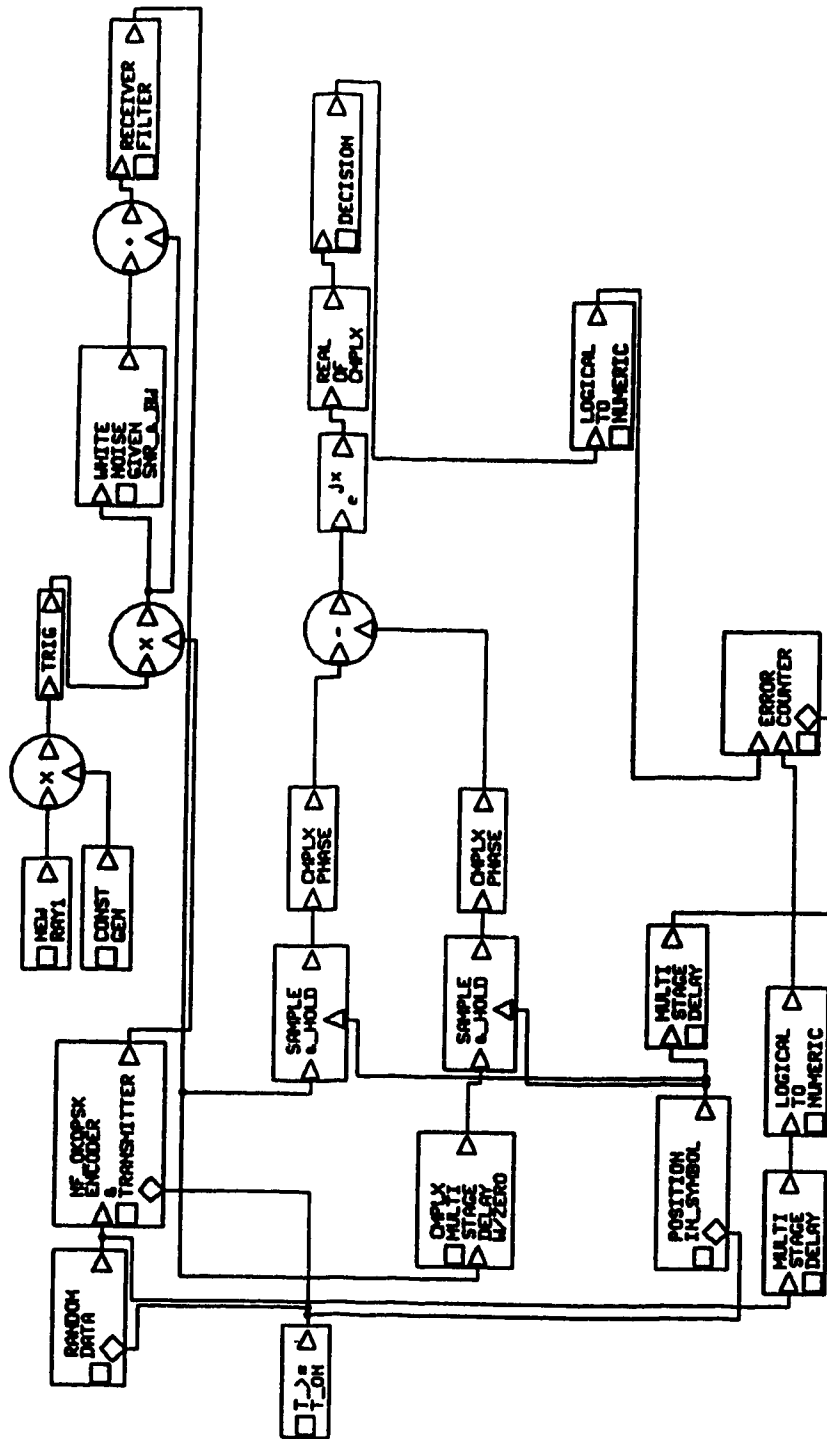
Fig.3.6 BOSS diagram of the ST-ODQPSK system
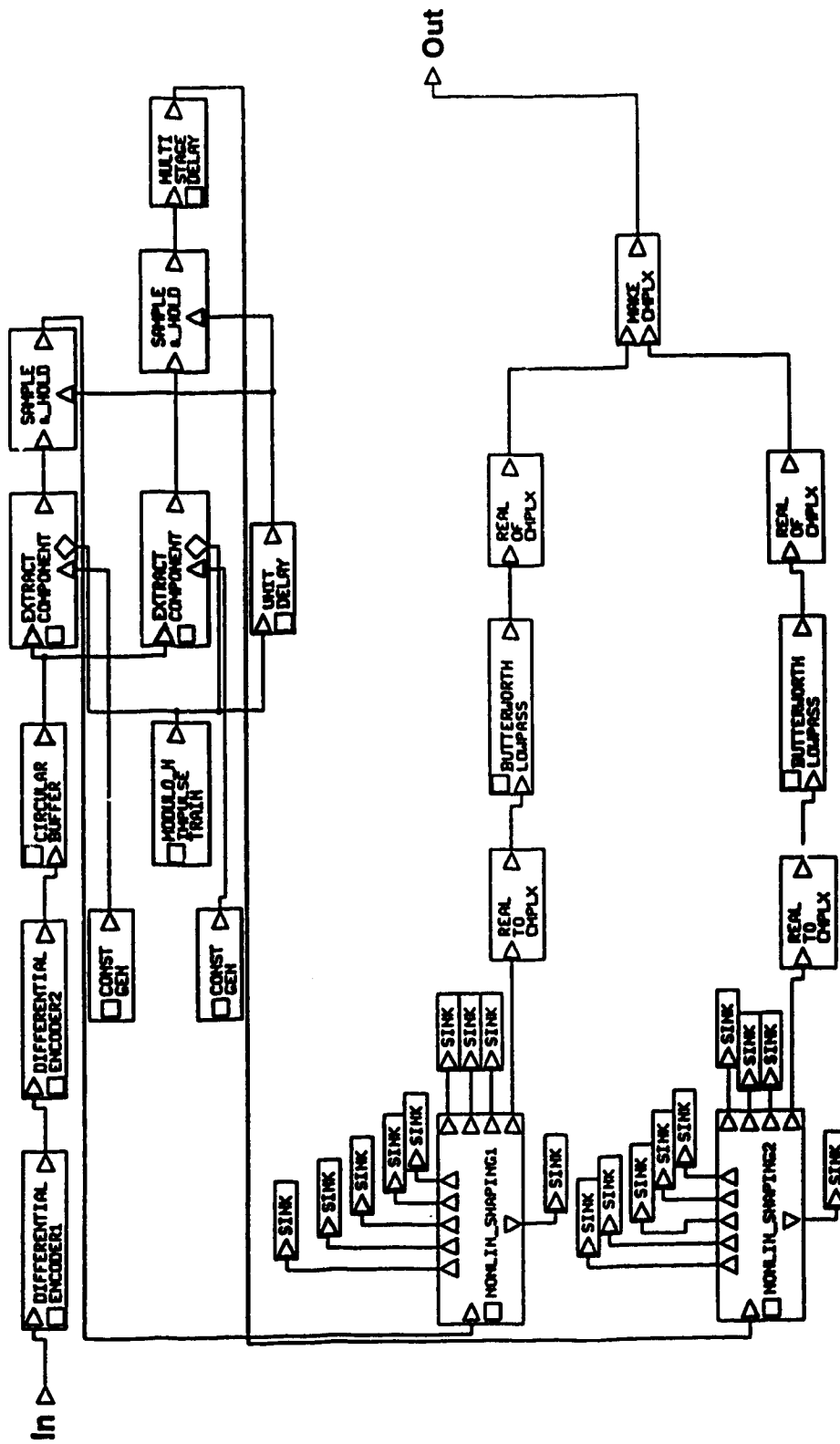
Fig.3.7 Expansion of ST-ODQPSK transmitter
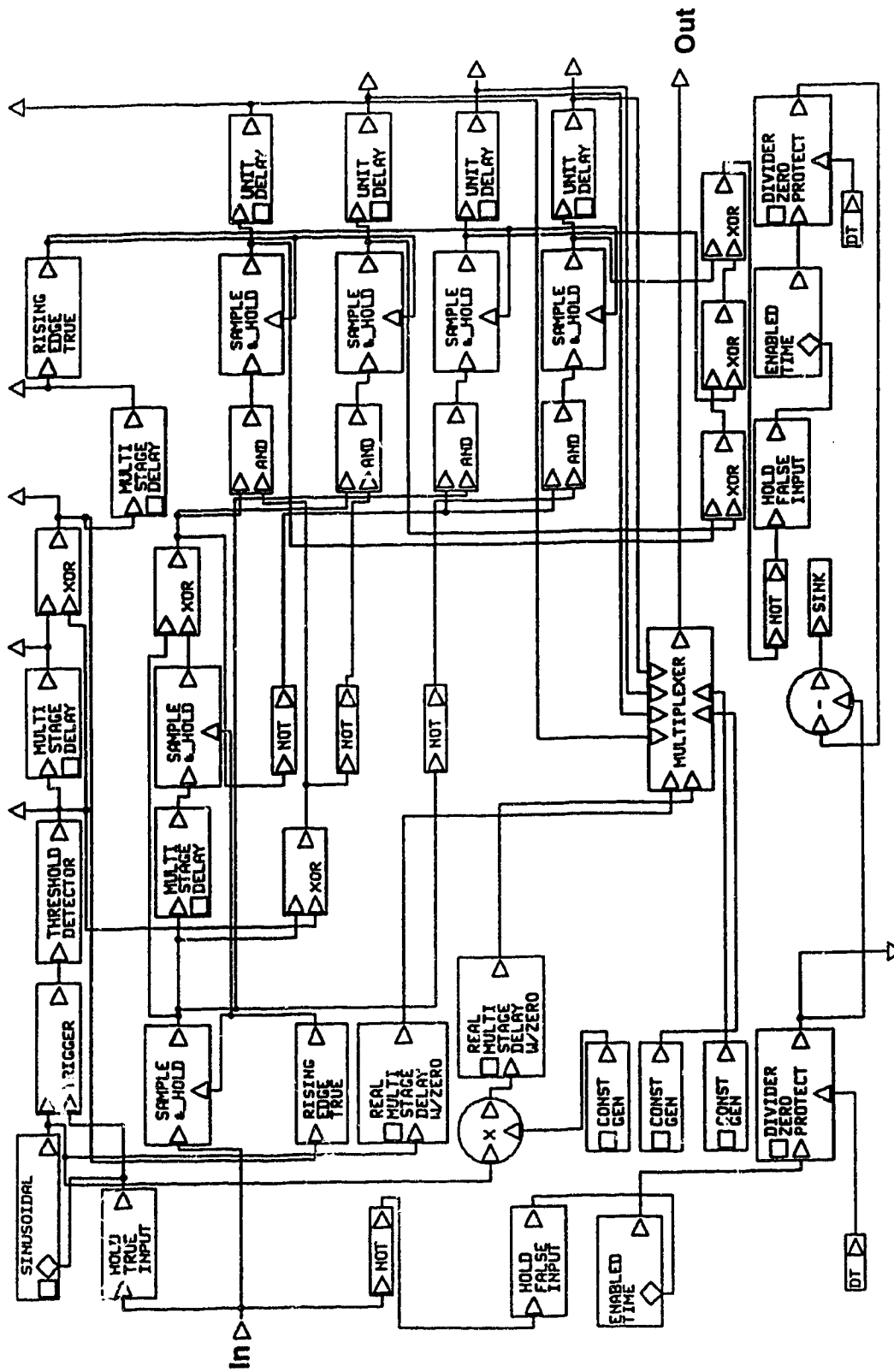
Fig.3.8 Expansion of nonlinear pulse shaping

3.6 Simulation of nonredundant error correction schemes

For the discussion of the NEC receiver structure, only the ST-ODQPSK system is presented here as the same configuration also applies to SRC-ODQPSK systems. Fig.3.9 shows the BOSS block diagrams of the ST-ODQPSK system with single error correction in an AWGN channel. As there are only two syndromes, namely S_i and S_{i-1}, involved in the detection of error symbol $e_{1(i-1)}$, only two differential detectors are needed and a relatively simple realization can be achieved. It may also be noted that the decision blocks are different for the two differential detectors; this is not the case for general phase shift keying modulation. As a matter of fact, this is only true for ODQPSK modulation schemes. Specifically, the decision strategy employed in the first-order differential detector is the same as for one-bit differential detection of ODQPSK, while the detection method used in the second or higher order differential detectors is actually the same as for two-bit differential detection of ODQPSK, assuming that three-bit differential encoding is performed at the transmitter. In the BOSS diagram these detectors are represented by blocks DECISION and NEC_DECISION, followed by a NOT gate. The block diagrams for double and triple error correction are shown in Fig.3.10 and Fig.3.11, respectively. In the case of multiple error correction, a pattern detector is needed as there are a number of syndrome patterns which can be detected from the outputs of the syndrome generating circuit. For double error correction, there are three parallel differential detectors following the receiver filter. In the syndrome generating part, six syndromes, namely S_{1i}, $S_{1(i-1)}$, $S_{1(i-2)}$, S_{2i}, $S_{2(i-1)}$ and $S_{2(i-2)}$, are created from nine error symbols e_{1i}, $e_{1(i-1)}$, $e_{1(i-2)}$, e_{2i}, $e_{2(i-1)}$, $e_{2(i-2)}$, e_{3i}, $e_{3(i-1)}$ and $e_{3(i-2)}$, which are present at the outputs of the three differential detectors. These syndromes form the inputs to the syndrome detection circuit. As has been discussed earlier, although there are as many as 2^6 distinct patterns which can be formed, only nine

of them are legal syndrome patterns effective for error correction. These patterns are stored and detected by the created BOSS primitive modules PATTERN DETECTOR, as shown in the diagram. If the input noisy pattern matches any one of these stored patterns, a correction pulse, namely "1", is generated by the pattern detector and is modulo-2 added to the delayed data stream detected from the first-order differential detector. The amount of delay is equal to twice the delay introduced in the first-order differential detector. As long as the number of simultaneous errors in the nine error symbols is less than or equal to two, any error can be corrected. For triple error correction, four differential detectors are employed at the receiver. As many as 12 syndromes can be generated from 16 error symbols, namely, e_{1i}, $e_{1(i-1)}$, $e_{1(i-2)}$, $e_{1(i-3)}$, e_{2i}, $e_{2(i-1)}$, $e_{2(i-2)}$, $e_{2(i-3)}$, e_{3i}, $e_{3(i-1)}$, $e_{3(i-2)}$ and $e_{3(i-3)}$. The syndromes include S_{1i}, $S_{1(i-1)}$, $S_{1(i-2)}$, $S_{1(i-3)}$, S_{2i}, $S_{2(i-1)}$, $S_{2(i-2)}$, $S_{2(i-3)}$, S_{3i}, $S_{3(i-1)}$, $S_{3(i-2)}$ and $S_{3(i-3)}$. A total of 118 legal syndrome patterns can be found from the 2^{12} possible patterns. As long as there are no more than three concurrent errors in the 12 error symbols, these errors can always be corrected. The data stream from the first-order detector is further delayed by three times the delay in the previous detection process, and EX-ORed with the correction pulse to yield the true output. When going through the error correction procedure, we also have to bear in mind that the illustrated BOSS implementation diagrams can apply to both two-bit and three-bit differentially encoded ODQPSK schemes, the only difference being that, for three-bit detection case, the amount of delay in all the delay elements at the receiver should be doubled.
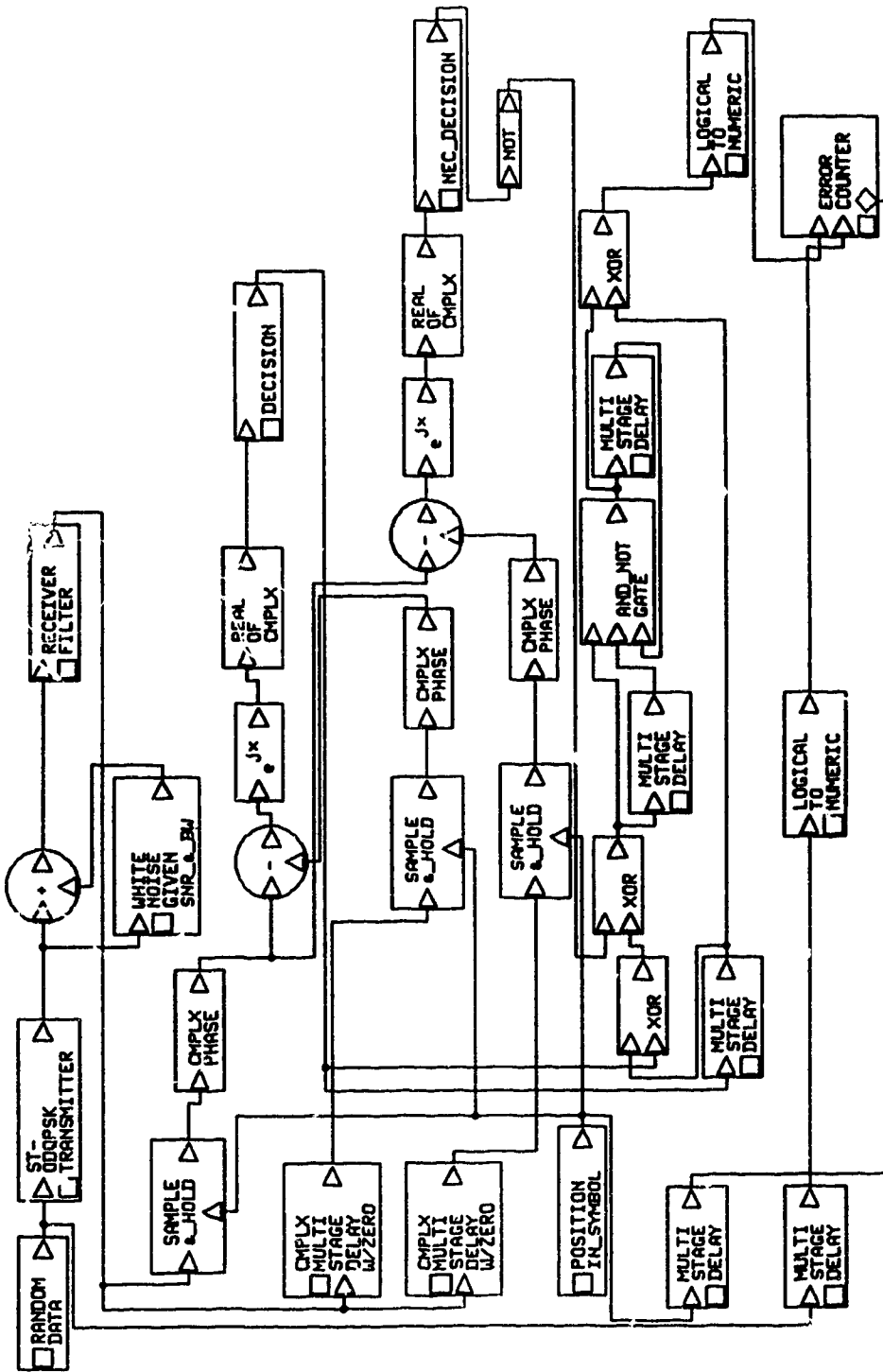
Fig.3.9 BOSS diagram of the single NEC receiver

67
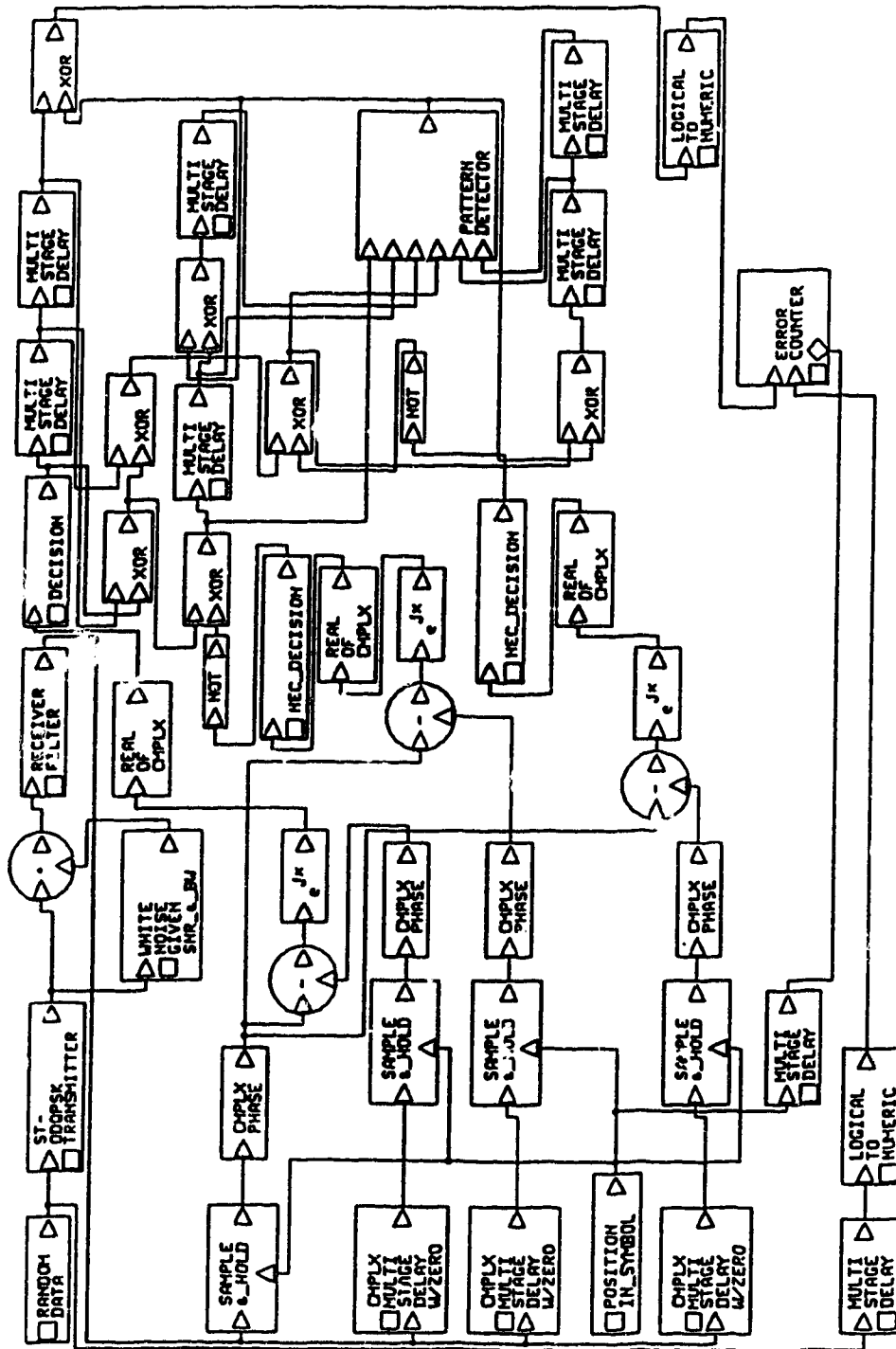
Fig.3.10 BOSS diagram of the double NEC receiver

68
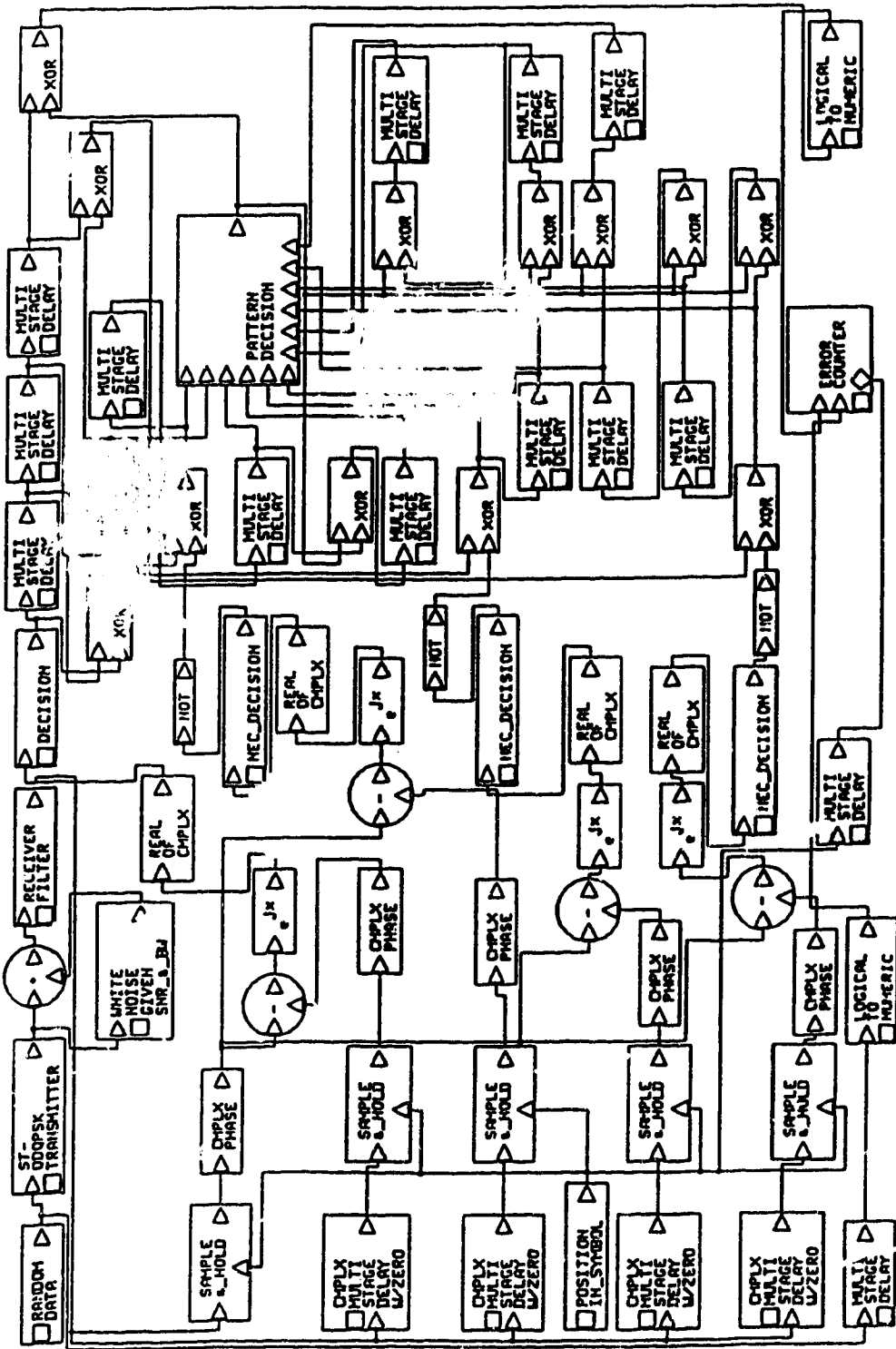
Fig.3.11 BOSS Jiagram of the triple NEC receiver

69

3.7 Bit error rate estimation

There are a number of ways to arrive at an estimate of the BER, each with its own advantages and disadvantages. Some of the popular techniques used in the computer aided analysis of error performance of communication systems include Monte Carlo simulation, modified Monte Carlo simulation or importance sampling, extreme-value theory, tail extrapolation, and a quasi-analytical approach. The Monte Carlo simulation method has been the most widely used technique due to its simplicity and intuitiveness. Therefore, this method is adopted in the evaluation of the BER of ODQPSK systems. It has been proved[44] that, in order to achieve a confidence level of 95%, the number of bits used in the simulation run should be at least $10/P_e$, where P_e is the estimated bit error rate. This produces a confidence interval of approximately $(2P_e, 0.5P_e)$, which is generally considered an acceptable estimate. This criterion is used in the simulation of ODQPSK systems in both AWGN and Rayleigh fading channels. Also, for a given channel signal-to-noise ratio, three independent simulation runs are conducted, and then the results are averaged to give the BER.

3.8 Summary

This chapter has presented the computer simulation models for the multipath-path Rayleigh fading channel and three ODQPSK systems. As well, a system simulation package called BOSS developed for communication systems was briefly introduced. The BOSS implementations of single, double and triple NEC schemes for ODQPSK systems have been discussed. The simulated system error performance and characteristics will be discussed in the next chapter.

CHAPTER 4   SIMULATION RESULTS

In this chapter, results of simulations described in the previous chapter are presented and compared with two standard second generation digital cellular modulation schemes, $\pi/4$-DQPSK and Gaussian MSK, under different channel conditions. The investigations involve BER performance, envelope variation of the transmitted signals, and power spectral density characteristics. As has been mentioned earlier, the simulated land mobile radio channel is characterized by single path or flat Rayleigh fading, and multi-path or frequency-selective Rayleigh fading. In order to conform to the IS-54 recommendation, the two-path Rayleigh fading channel is used for the simulation studies, and the two paths are allowed to have variable attenuation factors to account for different fading scenarios. The excess channel delay spread has been chosen to range from 0 to one symbol duration(T_s=2T_b). In order to analyze the effect of nonlinear amplification of the transmitter of power amplifier, an ideal hardlimiter is also incorporated in the simulation model. The effect of channel white noise is simulated by injecting AWGN at the receiver input, with its noise variance dependent upon the specified signal-to-noise ratio and the signal strength in the channel. The performance improvement achieved by single, double and triple NEC techniques used with different ODQPSK schemes is also discussed in this chapter for both linear and nonlinear channels.

71

4.1 Performance of SRC-ODQPSK with 4RRC filter receiver

The error performance of a SRC-ODQPSK system with 4RRC baseband pulse shaping is discussed in this section for linear, nonlinear, flat Rayleigh fading and frequency-selective Rayleigh fading channels. One-bit differential d·· ction is assumed at the receiver. Two-bit differential detection will be analyzed, along with NEC schemes, in a subsequent section.

4.1.1 Linear AWGN channel

Fig.4.1 shows the BER performance of a SRC-ODQPSK system with 4RRC transmitter baseband pulse shaping in a linear AWGN channel. The corresponding error performance of π/4-DQPSK and Gaussian DMSK (premodulation bandwidth BT=0.32) are also plotted in this graph, for comparison.
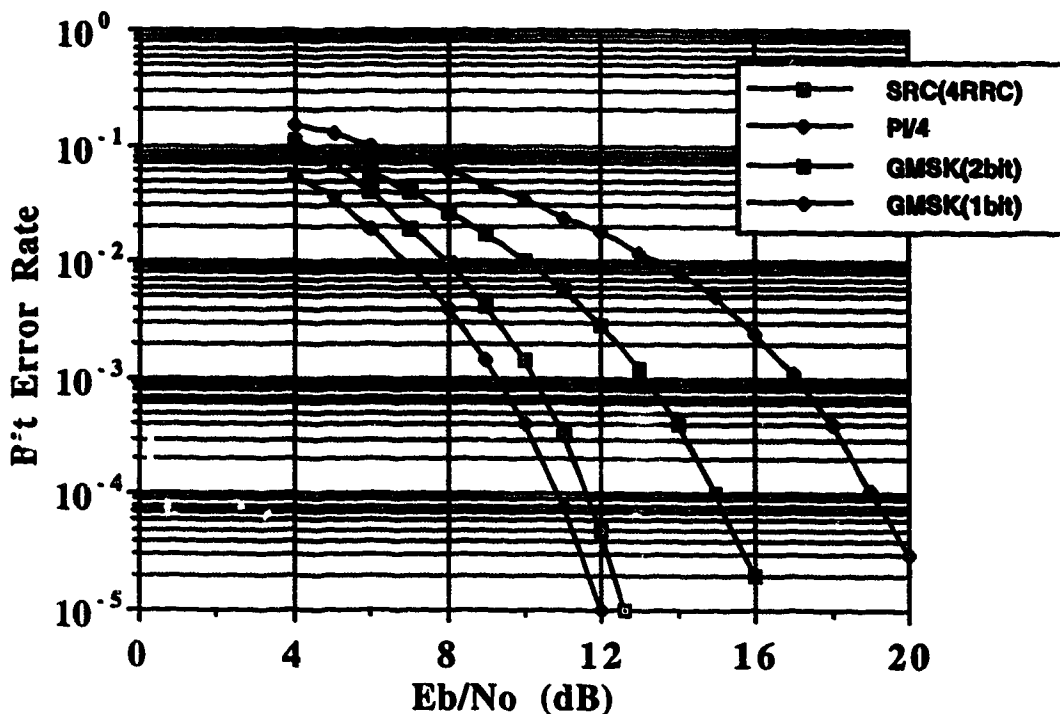
Fig.4.1 BER performance of a SRC-ODQPSK system with 4RRC pulse shaping, π/4-DQPSK and GMSK in a linear AWGN channel

As can be seen, in a linear AWGN channel, $\pi/4$-DQPSK can achieve the best error performance, while Gaussian DMSK has the poorest performance. SRC-ODQPSK is slightly worse than $\pi/4$-DQPSK. For a BER lower than 10^{-3}, the performance penalty of SRC-ODQPSK is within 1dB in terms of E_b/N_o, as compared with $\pi/4$-DQPSK, and this difference becomes even smaller with increasing signal energy per bit. One-bit differentially detected Gaussian DMSK is inferior to SRC-ODQPSK by at least 7dB for a BER below 10^{-3}, and two-bit differentially detected Gaussian DMSK by more than 3dB. It should be noted that two-bit differential detection of Gaussian DMSK requires adaptive optimization of the decision threshold for each E_b/N_o; this necessitates a sophisticated receiver circuit and may not be a practical approach for the detection of Gaussian DMSK signals.

The reason why SRC-ODQPSK exhibits a slightly poorer error performance than $\pi/4$-DQPSK can be easily observed by referring to the eye diagram of the pre-detected SRC-ODQPSK signals(Fig.2.17). Although ISI-free transmission can be satisfied in a SRC-ODQPSK system by equal partitioning of the transmitter and receiver filters, the sampled signal levels do not yield the optimal signal-to-noise ratio, as observed in many other matched filter transmission systems. In a $\pi/4$-DQPSK system, a matched filter and Gray encoding are used at the receiver and transmitter, respectively. It can be shown that the amplitude of SRC-ODQPSK signals, at each sampling instant, is only 78.5% of the peak signal amplitude. This translates into a 20Log(0.785)=2dB penalty in E_b/N_o, as compared to $\pi/4$-DQPSK and other matched filter systems. On the other hand, bit-by-bit detection is employed in the SRC-ODQPSK system. The minimum phase margin for the detection of bit "1" and "0" is 45 degrees, but the maximum phase margin for bit "1" is 225 degrees. This is superior to $\pi/4$-DQPSK system, in which both maximum and minimum phase margins are 45

degrees. Although Gray encoding helps reduce the equivalent bit error rate of a symbol-based detection system such as the $\pi/4$-DQPSK system, bit-by-bit detection still provides a net E_b/N_0 gain over symbol-by-symbol detection. Therefore, the combined effect of the above receiver sampling and detection strategies is that the E_b/N_0 gain of $\pi/4$-DQPSK over SRC-ODQPSK can be reduced from 2dB to within 1dB. At high E_b/N_0, the detection strategy has a dominant effect on system error performance. Hence, this penalty will monotonically decrease with the increase of signal power.

4.1.2 Hardlimited AWGN channel

Fig.4.2 shows the error performance of the SRC-ODQPSK system in a nonlinearly amplified AWGN channel. As the worst case of nonlinear distortion, a hardlimiter is used to approximate a Class C high power transmitter amplifier.
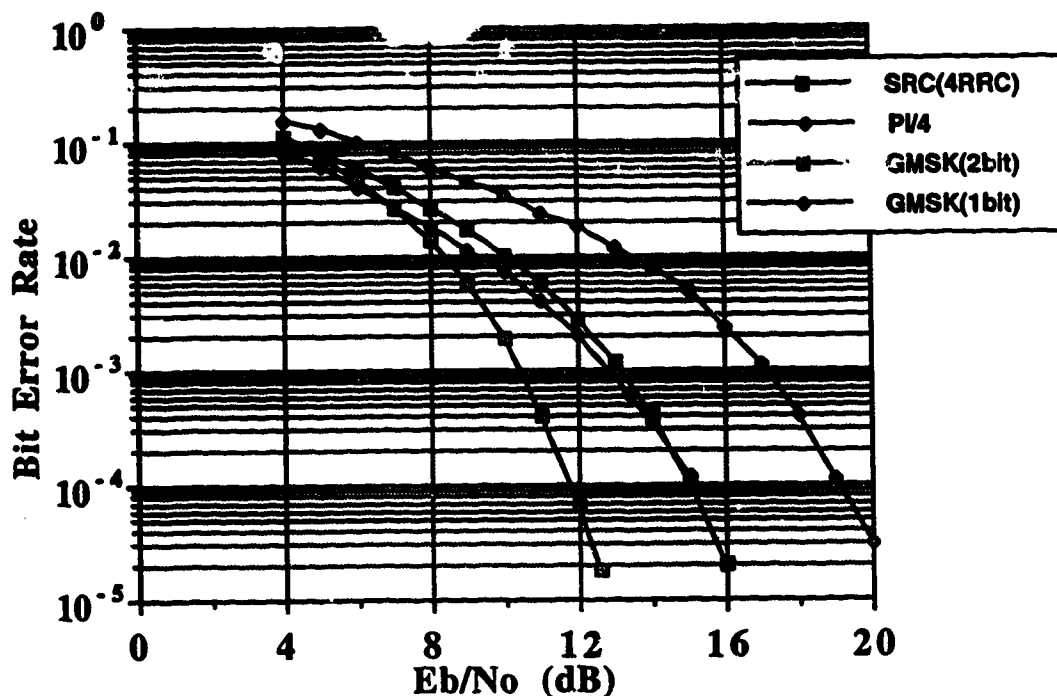
Fig.4.2 BER performance of SRC-ODQPSK with 4RRC
pulse shaping,$\pi/4$-DQPSK and Gaussian DMSK
in a hardlimited AWGN channel

74

When nonlinear distortion caused by the hardlimiter is taken into account, the SRC-ODQPSK scheme exhibits much better error performance than both the π/4-DQPSK and Gaussian DMSK schemes. Specifically, at a BER of 10^{-4}, the SRC-ODQPSK system has a gain of more than 3dB over π/4-DQPSK, of 3dB over two-bit differentially detected Gaussian DMSK, and of 7dB over one-bit differentially detected Gaussian DMSK. For the SRC-ODQPSK scheme, the hardlimiting operation only causes about 0.5dB degradation in performance, even at high E_b/N_o, as compared to the linear channel case. However, for π/4-DQPSK, the degradation increases dramatically at high E_b/N_o. For example, at a BER of 10^{-4}, it is already more than 4dB. Gaussian DMSK schemes do not suffer any deterioration from nonlinear distortion. Therefore, their performance remains the same as in a linear AWGN channel.

Generally, if the nonlinear device is envelope-driven, the amount of distortion will depend largely upon the envelope characteristics of the input signal. Since transmitter nonlinear power amplifiers belong to this type of nonlinear device, the envelope properties of the modulated signals become very important. As mentioned earlier, π/4-DQPSK signals have a 20dB power fluctuation at the modulator output, so that the degradation caused by the hardlimiter is severe. SRC-ODQPSK signals have only a 5dB envelope variation when the 4RRC pulse shaping technique is used at the transmitter. This explains why its error performance is only worse by about 0.5dB. Gaussian DMSK schemes have the advantage of constant envelope characteristics. Hence hardlimiting has no deleterious effect on their BER performance. In mobile radio communications, perfect linearization of transmitter power amplifiers is very difficult to achieve, and is subject to many factors. Even linearized power amplifiers still possess a small amount of inherent nonlinearities. Therefore, it is desirable that the modulated signals have as small a power variation as possible. Of all the QPSK modulation

schemes, offset keying modulation produces the smallest envelope fluctuation. Therefore, they are far less sensitive to channel nonlinear disrtortion than other QPSK schemes.

4.1.3 Flat Rayleigh fading channel

If the channel is non-dispersive in time or has a flat Rayleigh fading characteristic, the system performance depends upon three factors: Rayleigh fading, Doppler spread and AWGN. Fig.4.3 shows the BER in a flat Rayleigh fading channel. The simulated Doppler frequency is 90Hz, which corresponds to a vehicle speed of 114km/h at a carrier frequency of 850MHz.
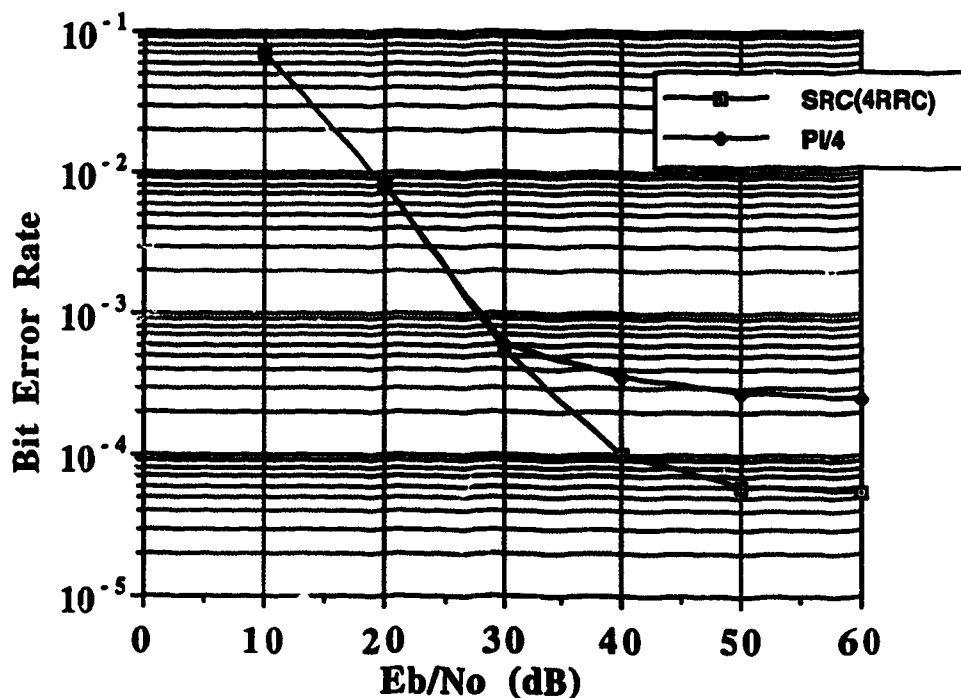
Fig.4.3 BER of SRC-ODQPSK with 4RRC pulse shaping and π/4-DQPSK in a flat Rayleigh fading channel

From this graph, it is seen that both SRC-ODQPSK and π/4-DQPSK systems have irreducible error floors when the level of signal power is increased beyond certain values. Any further increment of signal power has no effect of

reducing the BER. SRC-ODQPSK exhibits a lower irreducible error floor than π/4-DQPSK.

It is also noted that the error performance of SRC-ODQPSK is essentially the same as that of π/4-DQPSK at relatively small E_b/N_o. The reason is given as follows. In a land mobile radio fading environment characterized by severe Rayleigh fading, the error rate is mainly determined by both the fading and AWGN effects when the channel SNR is small. Rayleigh fading also makes ISI-free transmission impossible for both the π/4-DQPSK and SRC-ODQPSK systems. As a result, different filtering schemes manifest similar reception effect, although the SRC-ODQPSK system is slightly inferior to the π/ DQPSK system in a linear channel. On the other hand, the advantage gained by using bit-by-bit detection in the SRC-ODQPSK system is merely 1dB, as previously discussed. This is actually negligible when the SNR is small, i.e., the signal itself is in deep fades and also completely immersed in AWGN. Due to the two-fold factors, π/4-DQPSK and SRC-ODQPSK have almost the same BER characteristics for E_b/N_o up to 30dB.

For even larger E_b/N_o values, the fading effects tend to have the major impact on the BER, which involve both Rayleigh fading and random phase modulation. Eventually, the effect of increasing signal strength would make the BER independent of channel AWGN and solely related to the phase disturbance caused by the fading process. As the characteristics of random phase modulation are closely associated with the Doppler spread, i.e., the vehicle speed and carrier frequency, this disturbance can never be eliminat d by increasing the signal strength, resulting in the so-called irreducible error floor for a system operating in a mobile radio channel. It is noted that the SRC-ODQPSK system has twice the sampling frequency as used in the π/4-DQPSK system. Thus it is more robust against fast random phase modulation than π/4-DQPSK, as verified in the

simulation. In Fig.4.3, it is shown that SRC-ODQPSK has an error floor around 6×10^{-5}, while the error floor for $\pi/4$-DQPSK is about 2×10^{-4}.

4.1.4 Frequency-selective Rayleigh fading channel

The frequency-selective fading channel used for the SRC-ODQPSK system is the two-ray channel of equal strength, as specified in the IS-54 recommendation.

Fig.4.4 shows the BER floor versus channel delay spread characteristic of the SRC-ODQPSK system. The E_b/N_0 is fixed at 50dB in order to obtain the required error floor. The channel delay spread is selected from the following values: 1/16T, 1/8T, 3/16T, 1/4T, 1/2T and T, where T is the channel signalling interval equal to 40μs. It can be seen from the graph that the BER floor is very sensitive to channel delay spread. With the delay spread increasing from 0 to 1/16T, the corresponding BER goes up by more than one order of magnitude. A BER ceiling appears when the delay spread reaches one symbol duration.

Fig.4.5 shows the BER versus channel E_b/N_0 curve for a delay spread of 1/16T. It is seen that an irreducible error floor exists when the E_b/N_0 is larger than 40dB. This error floor is mainly caused by the severe intersymbol interference due to the channel frequency-selectivity. As well, it is observed that a BER of 3×10^{-2} requires an E_b/N_0 of about 15dB. In the IS-54B recommendation[42], it is specified that, for mobile voice communications, a BER of 3×10^{-2} is required with a channel E_b/N_0 of 17dB. Therefore, a delay spread of one sixteenth of a symbol duration can be tolerated by this system, which is about 3μs.

Fig.4.6 shows the BER versus the channel E_b/N_0 for a delay spread of 1/4T. The error rate is nearly a constant over the whole range of E_b/N_0 from 10dB to 50dB. Therefore, it can be determined that, for a large delay spread, the BER is actually independent of the channel signal strength as a result of severe ISI. This

is different from the case shown in Fig.4.5, where the frequency-selectivity shows dominant effects only in the error floor region.
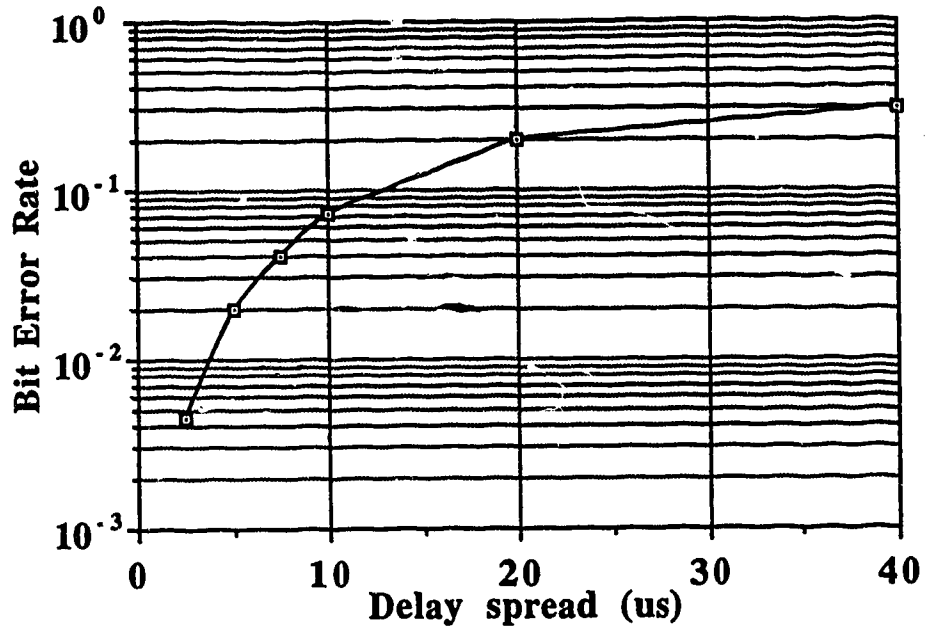
Fig.4.4 BER floor vs. channel delay spread for a SRC-ODQPSK system with 4RRC pulse shaping
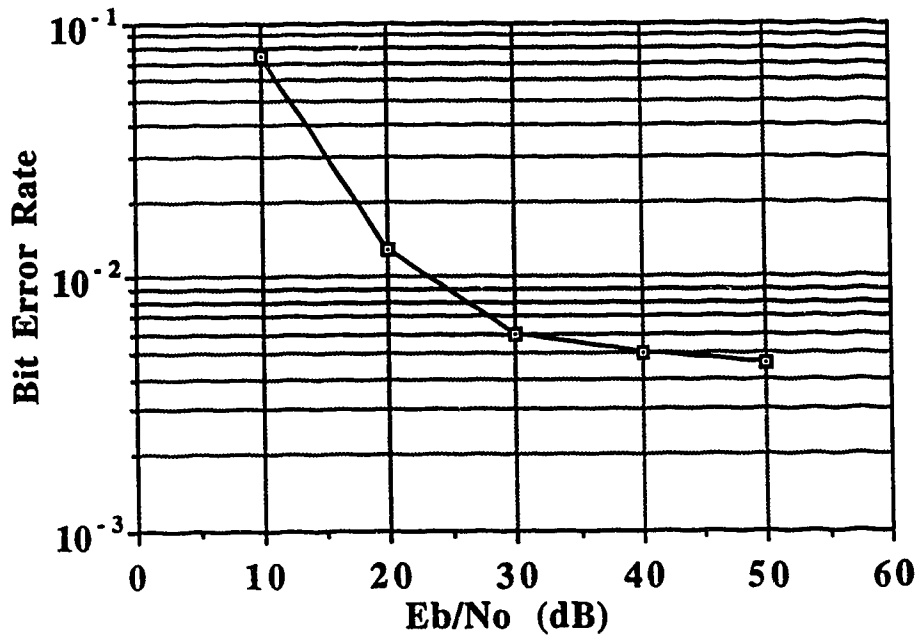
Fig.4.5 BER vs. Eb/No for a delay spread of 1/16T
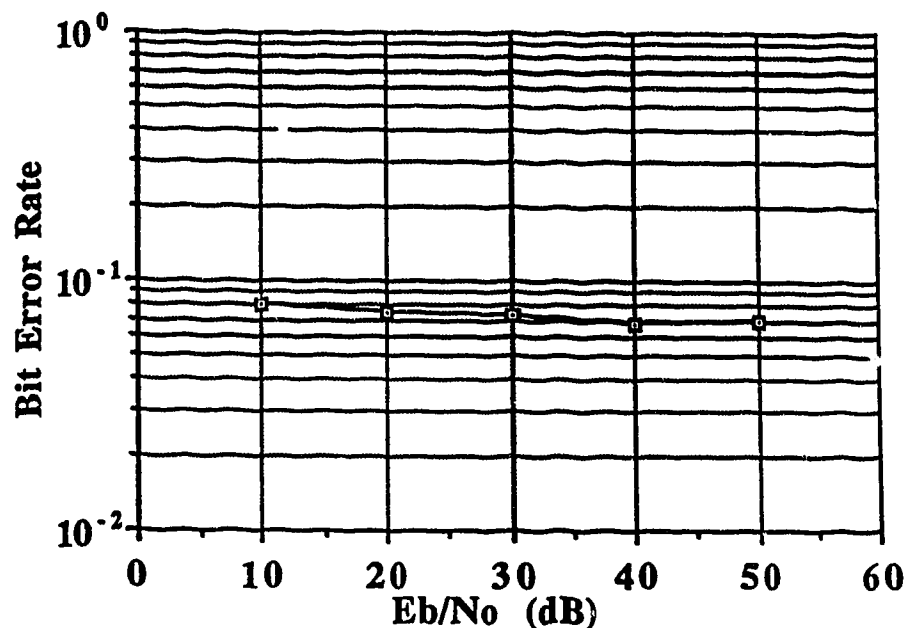
Fig.4.6 BER vs. E_b/N_o for a delay spread of 1/4T

4.2 Performance of SRC-ODQPSK with Butterworth filter receiver

As described in chapter 2, this system is basically the same as the previous one, except that the transmitter baseband pulse shaping is of square-root-raised-cosine type, and the receiver filter is a 4th order Butterworth filter.

4.2.1 Linear AWGN channel

Fig.4.7 shows the BER versus E_b/N_o curve for a linear AWGN channel. As for the case where 4RRC pulse shaping is used, its error performance also lies in between that of $\pi/4$-DQPSK and Gaussian DMSK with a premodulation bandwidth of 0.32. Specifically, for a BER=10^{-3}, it is approximately 1.5dB poorer than $\pi/4$-DQPSK, 2dB better than Gaussian DMSK with two-bit differential detection, and 6dB better than Gaussian DMSK with one-bit differential detection. For BER=10^{-5}, it is worse than $\pi/4$-DQPSK by about 2dB, better than two-bit differentially detected Gaussian DMSK by more than 2dB and one-bit differentially detected

Gaussian DMSK by more than 7dB. It is realized that the receiver fourth order Butterworth filter will introduce a certain amount of intersymbol interference, which would contribute to the 1.5dB performance penalty, compared to the π/4-DQPSK system.
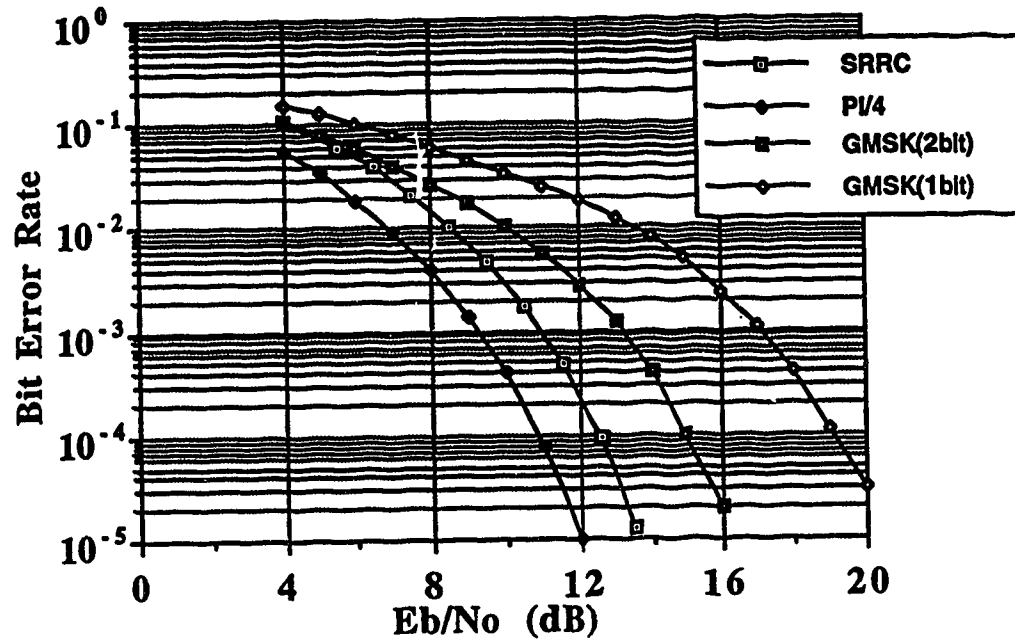
Fig.4.7 BER performance of SRC-ODQPSK with a Butterworth filter receiver, π/4-DQPSK and GMSK in linear AWGN channel

4.2.2 Hardlimited AWGN channel

Fig.4.8 shows the error performance in a hardlimited AWGN channel. It is seen that this system outperforms both Gaussian DMSK and π/4-DQPSK systems. For BER=10^{-3}, the nonlinear-distortion-induced degradation is found to be 0.5dB, which is much less than that of π/4-DQPSK. The performance gain is about 1.5dB over π/4-DQPSK, 2dB over Gaussian DMSK with two-bit differential detection and 6dB over Gaussian DMSK with one-bit differential detection.
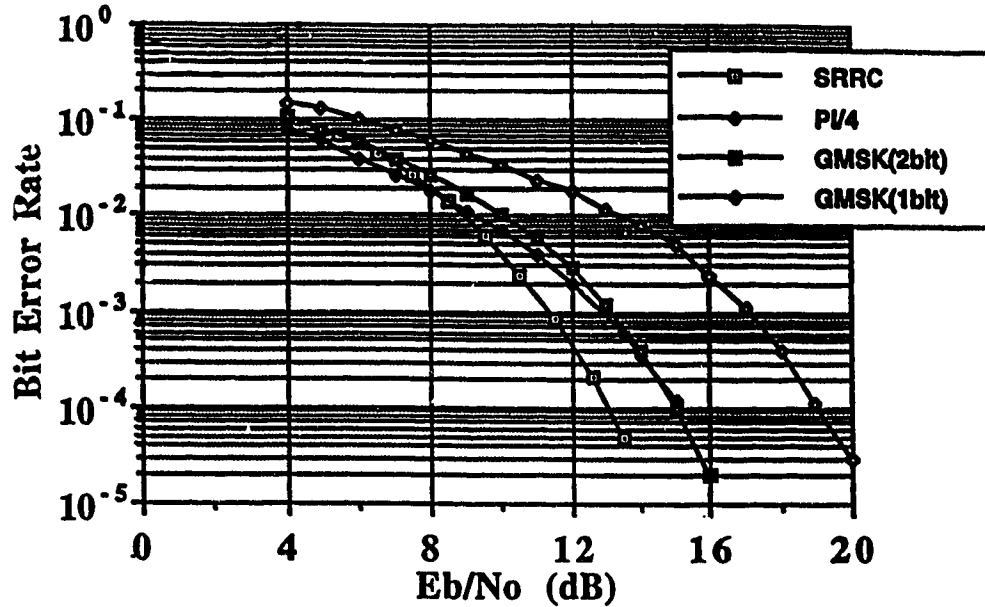
Fig.4.8 BER of SRC-ODQPSK with a Butterworth filter receiver, π/4-DQPSK and GMSK in hardlimited AWGN channel

4.2.3 Flat Rayleigh fading channel

The BER versus channel E_b/N_0 curve is shown in Fig.4.9. The Doppler frequency is 90Hz, corresponding to a vehicle speed of 114km/h at a carrier frequency of 850MHz. As can be seen, when channel E_b/N_0 is less than 30dB, the π/4-DQPSK and SRC-ODQPSK systems almost have the same error performance. Both systems exhibit irreducible error floors when E_b/N_0 is large enough, e.g., 50dB. As with the case of using 4RRC pulse shaping, this SRC-ODQPSK system has an error floor of about 6×10^{-5}, which is also lower than that of the π/4-DQPSK system. It is interesting to note that the type of receiver filtering has little effect on the system error performance in a severe Rayleigh fading channel. If the system is operating in small signal-to-noise ratio region, the error performance is predominantly determined by the fading process. Therefore, although the two SRC-ODQPSK systems and π/4-DQPSK system have different error performance in a linear channel, they turn out to achieve rather similar error

rates in a Rayleigh fading channel. For a large signal-to-noise ratio, the sampling frequency and ISI inherent in the system become important. Remember that moderate ISI always exists for these systems due to the fading effect. Consequently, a higher sampling frequency is expected to play a major role in reducing the irreducible error floor. This explains why both 4RRC filtered and Butterworth filtered SRC-ODQPSK systems have almost the same error floor, and have better performance than the π/4-DQPSK system.
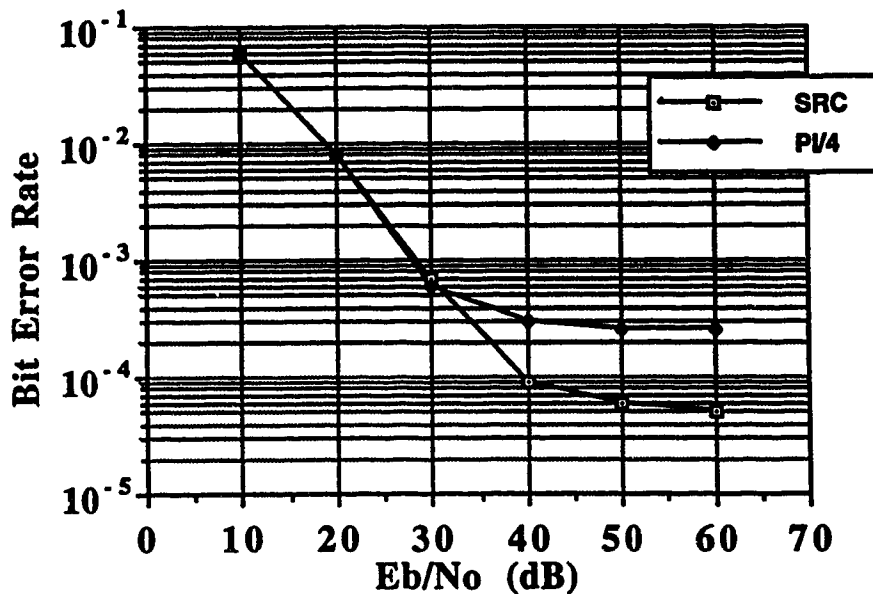
Fig.4.9 BER of SRC-ODQPSK with Butterwoth filter receiver and π/4-DQPSK in a flat fast Rayleigh fading channel

4.2.4 Frequency-selective Rayleigh fading channel

As before, the two-ray channel model has been used for performance evaluation. Fig.4.10 shows the BER versus channel delay spread for an E_b/N_0 of 100dB. As can be seen, when the delay spread increases from 0 to one symbol duration(T), the BER goes up from about $5x10^{-5}$ to 0.28. The most dramatic

increase in BER corresponds to the change in the delay spread from 0μs to about 4μs. When the delay spread exceeds one-bit duration, the BER reaches a ceiling.

Fig.4.11 shows the BER versus channel E_b/N_0 curve for channel delay spreads of 1/4T and 3/32T. The delay spread of 1/4T and 3/32T corresponds to 10μs and 3.75μs, respectively. It is seen that a delay spread of 3 ~ 4μs can still be tolerated for the system to meet the 17dB SNR requirement at a BER of 3×10^{-2}, as stipulated in IS-54B documents. Also observed is that an increase from 3.75μs to 10μs in the delay spread would boost the BER floor by more than one order of magnitude.

Fig.4.12 shows the BER floor versus direct-path-to-delay-path power ratio(C/D). The E_b/N_0 is chosen as 100dB, and the delay spread is fixed at 3/32T=3.75μs. As the ratio increases from 0dB to 50dB, the error floor is reduced from 9.5×10^{-3} to 5×10^{-5}. When the power ratio exceeds 30dB, the channel actually becomes a flat Rayleigh fading channel. Therefore, the simulated BER stays around 5×10^{-5}, which is also the BER floor seen in a flat Rayleigh fading channel.
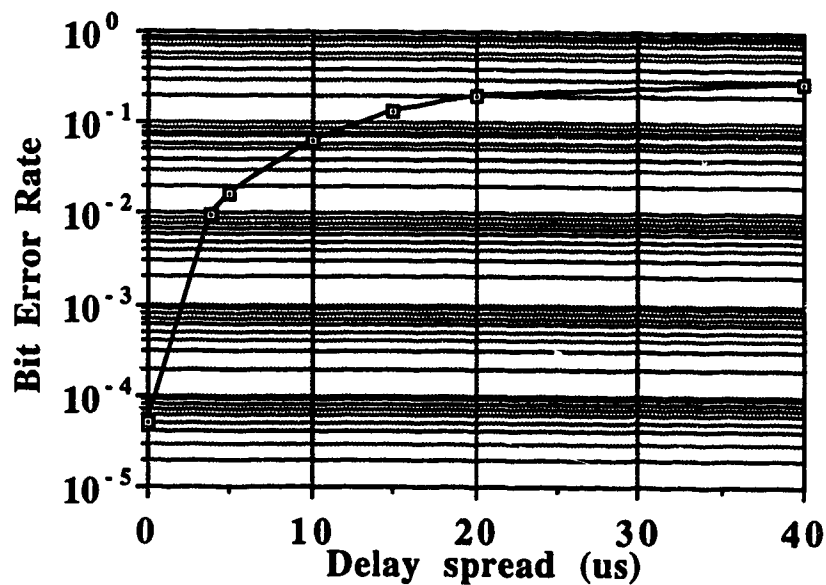
Fig.4.10 BER vs. delay spread performance in a two-ray channel
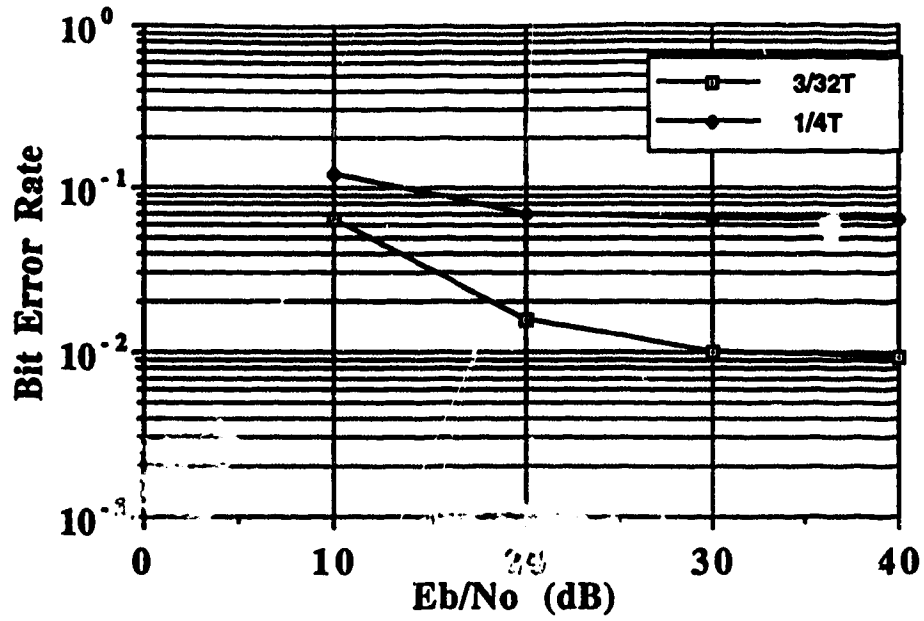
Fig.4.11 BER vs. channel E_b/N_o in a two-ray channel
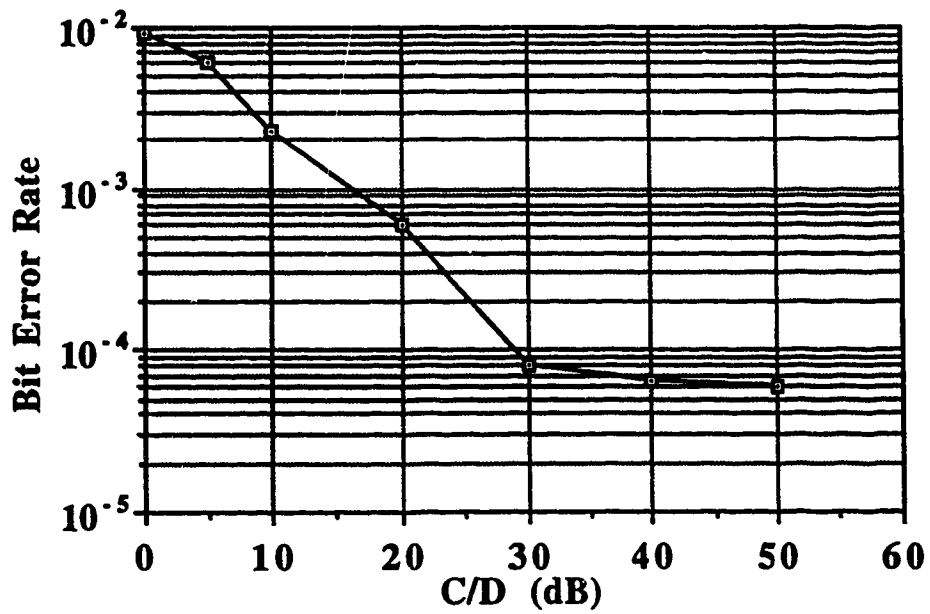
Fig.4.12 BER floor vs. C/D in a two-ray channel

4.3 Performance of ST-ODQPSK

The following sections present the error performance of the ST-ODQPSK system in linear, hardlimited, flat Rayleigh fading and frequency-selective fading channels.

4.3.1 Linear AWGN channel

Fig.4.13 shows the BER versus E_b/N_0 performance. For a BER of 10^{-3}, the ST-ODQPSK system is poorer than $\pi/4$-DQPSK by 2dB. On the other hand, it is better than Gaussian DMSK with two-bit and one-bit differential detection by 2dB and 6dB, respectively. The 2dB performance penalty, as compared to the $\pi/4$-DQPSK system is mainly due to the transmitter and receiver Butterworth filtering operations.
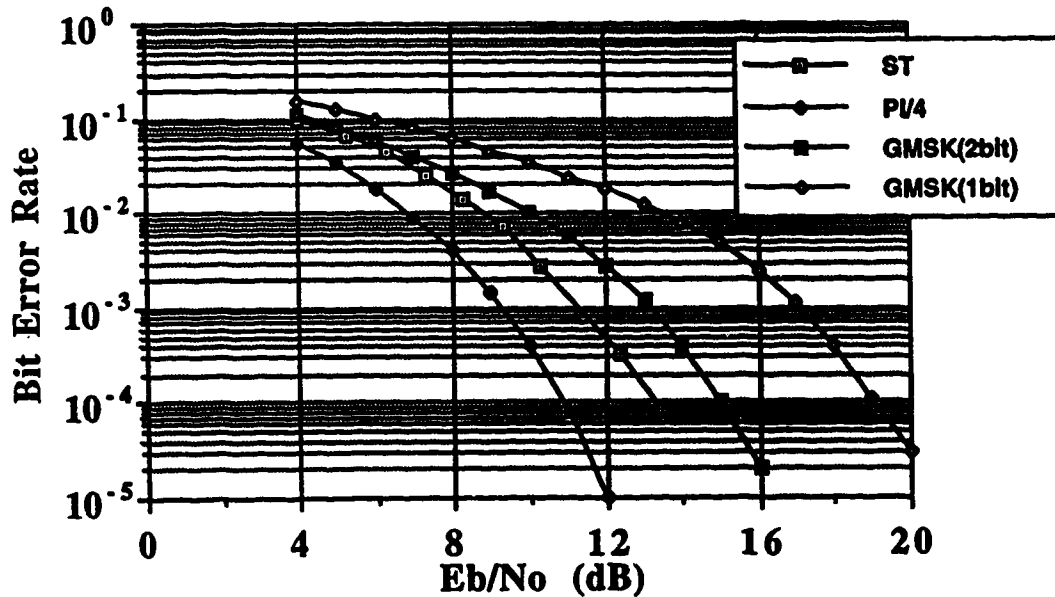
Fig.4.13 BER vs. channel E_b/N_0 in a linear AWGN channel

4.3.2 Hardlimited AWGN channel

Fig.4.14 shows the error performance of the ST-ODQPSK system in a hardlimited AWGN channel. For a BER of 10^{-3}, it is superior to $\pi/4$-DQPSK and

Gaussian DMSK with two-bit differential detection by about 1dB, and better than Gaussian DMSK with one-bit differential detection by about 5dB. The degradation incurred by the hardlimiting is only 0.2dB at a BER of 10^{-3} and 0.4dB at a BER of 10^{-4} in the ST-ODQPSK system. This is due to its sm; 'l envelope fluctuation, which makes it insensitive to the nonlinear envelope distortion. Therefore, ST-ODQPSK appears to be very suitable for use with nonlinear power amplifiers.

4.3.3 Flat Rayleigh fading channel

The error performance is shown in Fig.4.15. The simulated Doppler frequencies are 90Hz and 60Hz, which correspond to vehicle speeds of 114km/h and 76km/h, respectively. It is observed that, for channel E_b/N_0 below 36dB, $\pi/4$-DQPSK is slightly better than ST-ODQPSK by 1 1.5dB. When E_b/N_0 increases up to 50dB, the error rates reach the error floor region, which are about 7.5×10^{-5} and 3.5×10^{-5} for Doppler frequencies of 90Hz and 60Hz, respectively. Like the previously discussed SRC-ODQPSK systems, the lower BER floor of the ST-ODQPSK system is attributed to the fact that it has double the sampling frequency of the $\pi/4$-DQPSK system at the receiver.
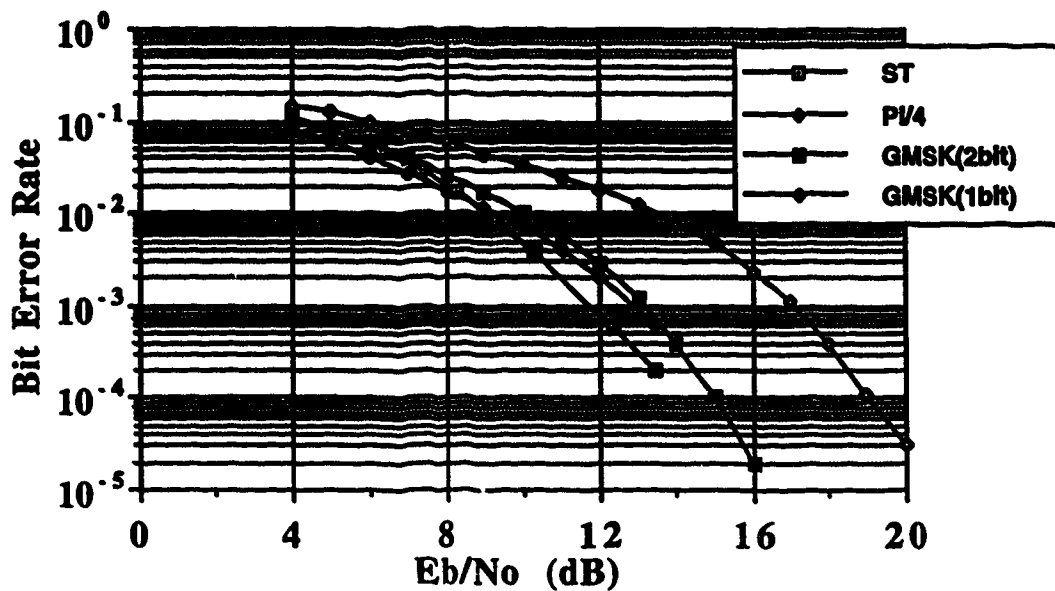
Fig.4.14 BER performance of ST-ODQPSK in a hardlimited channel
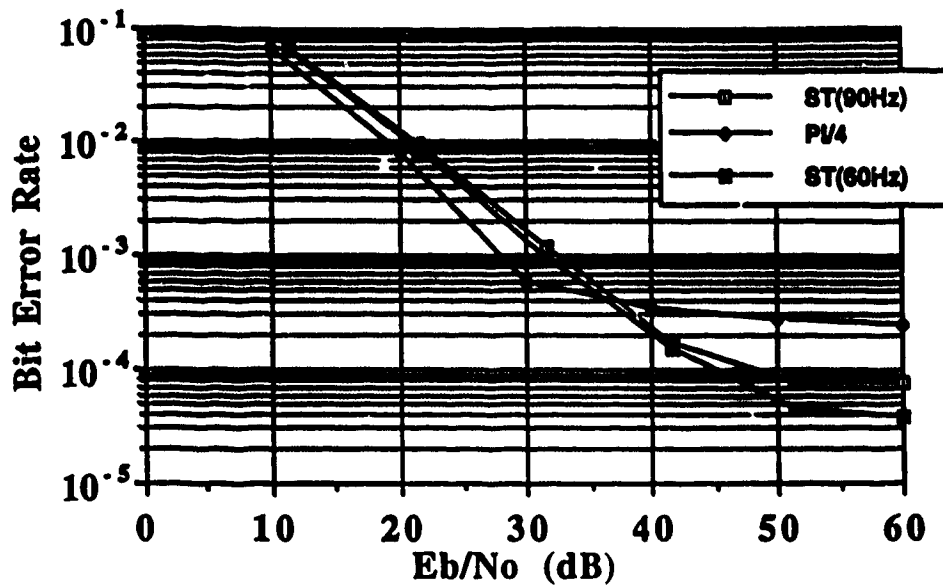
Fig.4.15 BER of ST-ODQPSK in a flat Rayleigh fading channel

4.3.4 Frequency-selective fading channel

The same channel as used in SRC-ODQPSK systems was also used in the simulation of ST-ODQPSK system. The direct-path-to-delay-path power ratio (C/D) can vary from 0dB to 60dB. Fig.4.16 shows the BER floor versus channel delay spread performance of this system. The simulated Doppler frequency is 90Hz. E_b/N_0=100dB and C/D=0dB. It is noted that the BER floor is 7.5×10^{-5} when no channel delay spread is present. It rises to 0.208 when the delay is one-bit duration and 0.29 when one-symbol delay is present. When the delay spread exceeds one bit, the BER approaches a ceiling. The most dramatic degradation of BER occurs with delay spread changing from 0 to 1/16T(~2.5μs).

Fig.4.17 shows the BER floor versus C/D performance for two different channel delay spread values, 10μs and 40μs. Again, the channel E_b/N_0 is 100dB. The two curves are seen to merge into one with the increase of C/D. This is because, at very high power ratio, the second path actually has little effect on the
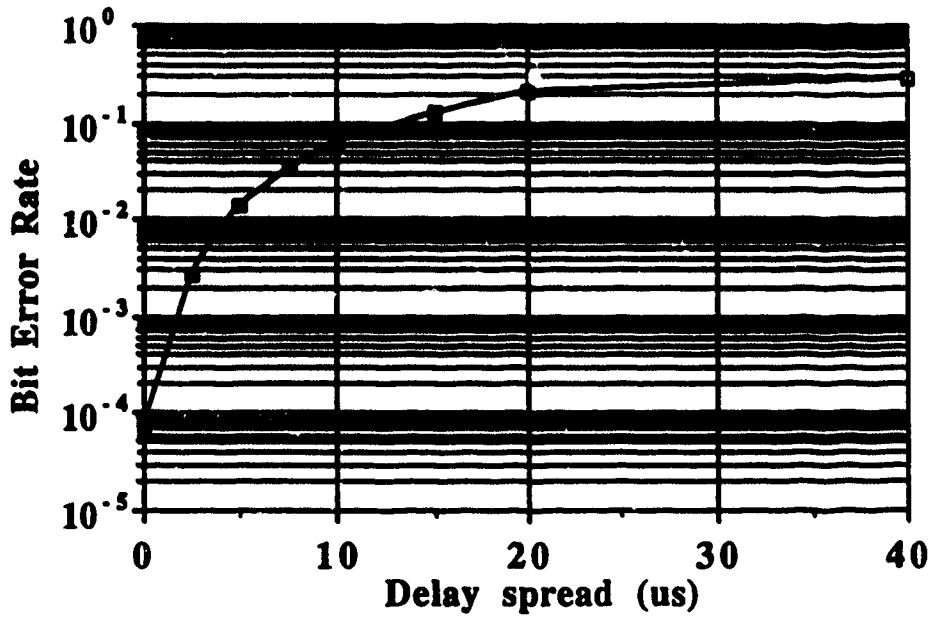
Fig.4.16 BER vs. delay spread performance
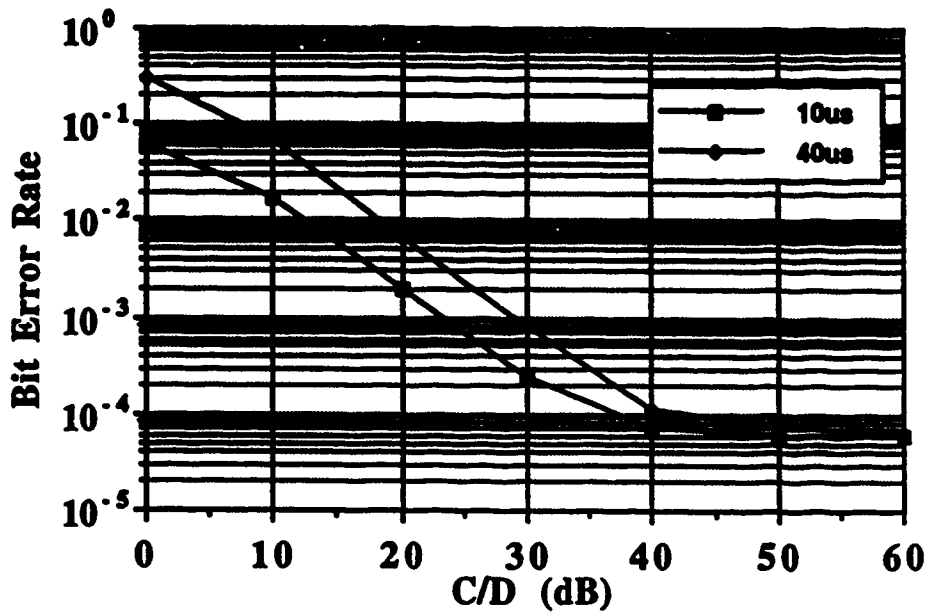
Fig.4.17 BER vs. C/D performance

direct path, i.e., the channel has turned into a flat Rayleigh fading channel. Hence, the amount of delay spread does not count at all in this situation. For small C/D, the channel is characterized by frequency-selectivity. The more severe the channel frequency-selectivity, the worse error performance. This is why the error rate with a delay spread of 10μs is much better than that with a delay spread of 40μs at the low C/D region.

Fig.4.18 shows the BER versus channel E_b/N_0 for delay spread of 4us and 20us, respectively. The power ratios (C/D) are 0dB and 10dB. It is observed that if the channel E_b/N_0 is increased by 30dB, the BER can be correspondingly reduced by one order of magnitude for small delay spread. However, in the case of 20μs channel delay, the BER is hardly reduced. Also, if the second path is attenuated by 10dB with respect to the direct path, the improvement in BER is more noticeable for delay spread of 20μs than for 4μs. For E_b/N_0 of 40dB, the BER is lowered by almost one order of magnitude for 20us delay when C/D changes from 0dB to 10dB, while it is only reduced from 7.8×10^{-3} to 3.6×10^{-3} for the case of 4μs delay spread
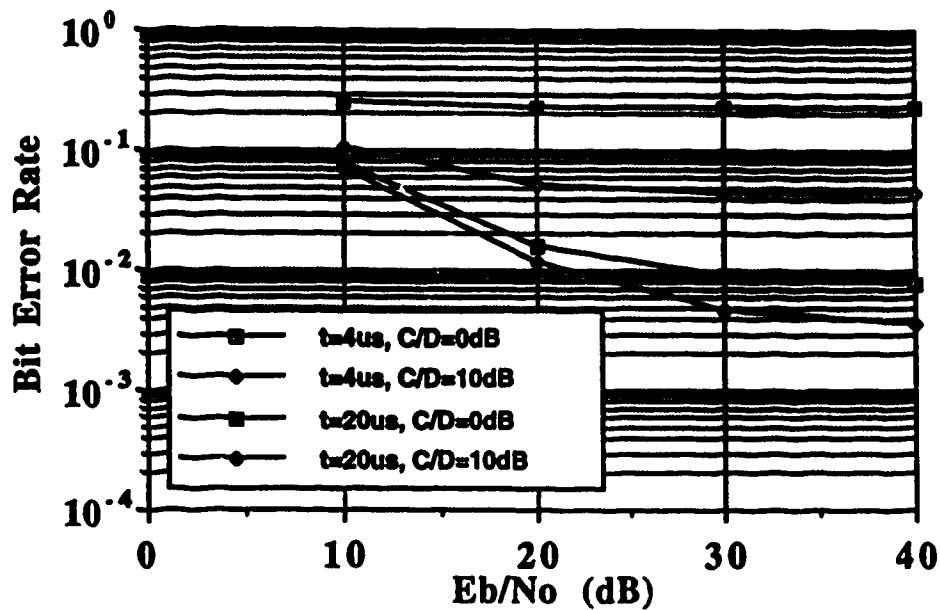
Fig.4.18 BER vs. channel Eb/No performance

4.4 Power spectral density

Computer simulated power spectral density functions of SRC-ODQPSK, ST-ODQPSK, π/4-DQPSK and Gaussian DMSK signals are illustrated in Fig.4.19(a)-(e). The bit rate is 50kb/s. As shown in the graph, π/4-DQPSK signals occupy the smallest transmission channel bandwidth. The single-sided bandwidth is about 20kHz where the power spectrum drops down to below -60dB. SRC-ODQPSK systems with 4RRC pulse shaping and SRRC pulse shaping basically occupy the same amount of bandwidth. For power spectrum below -60dB, the single-sided frequency bandwidth can be found to be 25kHz. ST-ODQPSK signals occupy a broader spectrum than SRC-ODQPSK signals because the first side lobe is still present. Gaussian DMSK signals with a pre-modulation bandwidth of 0.32 have the widest spectrum. Also, there is no zero at 25kHz in the spectrum of Gaussian DMSK signals, as seen in the other spectra. Therefore, the bandwidth efficiencies of the proposed schemes lie between π/4-DQPSK and Gaussian DMSK schemes. For the current outdoor land mobile radio applications, the allowed channel bandwidth is only 30kHz. This requires a bandwidth efficiency slightly larger than that provided by SRC-ODQPSK. However, these modulation schemes may still find applications in many other scenarios such as indoor mobile radio communications.
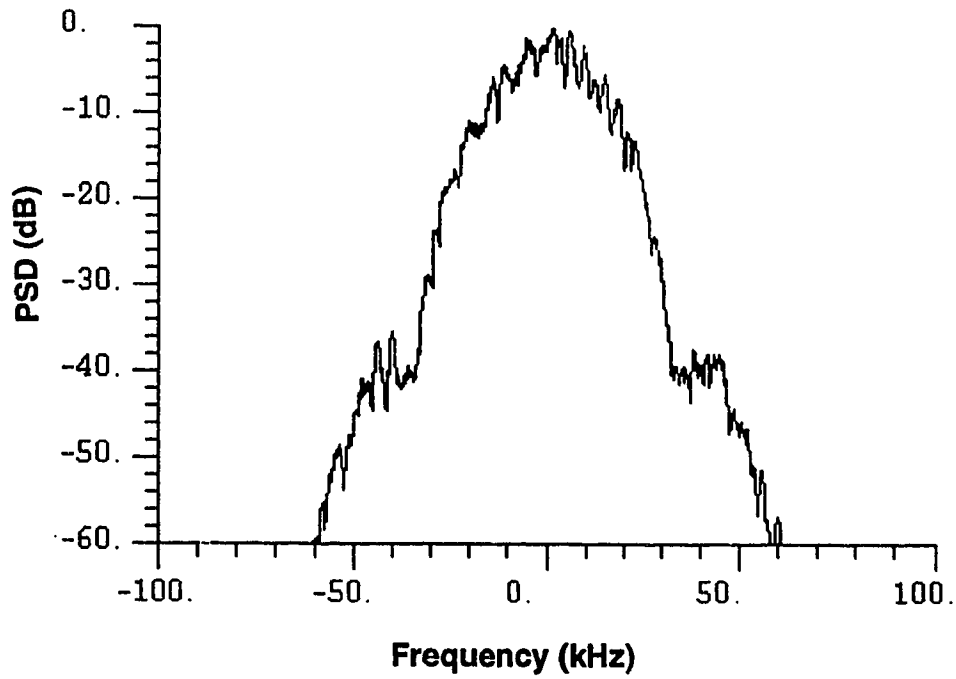
(a) Gaussian DMSK (pre-modulation bandwidth=0.32)

(b) SRC-ODQPSK(4RRC)

92
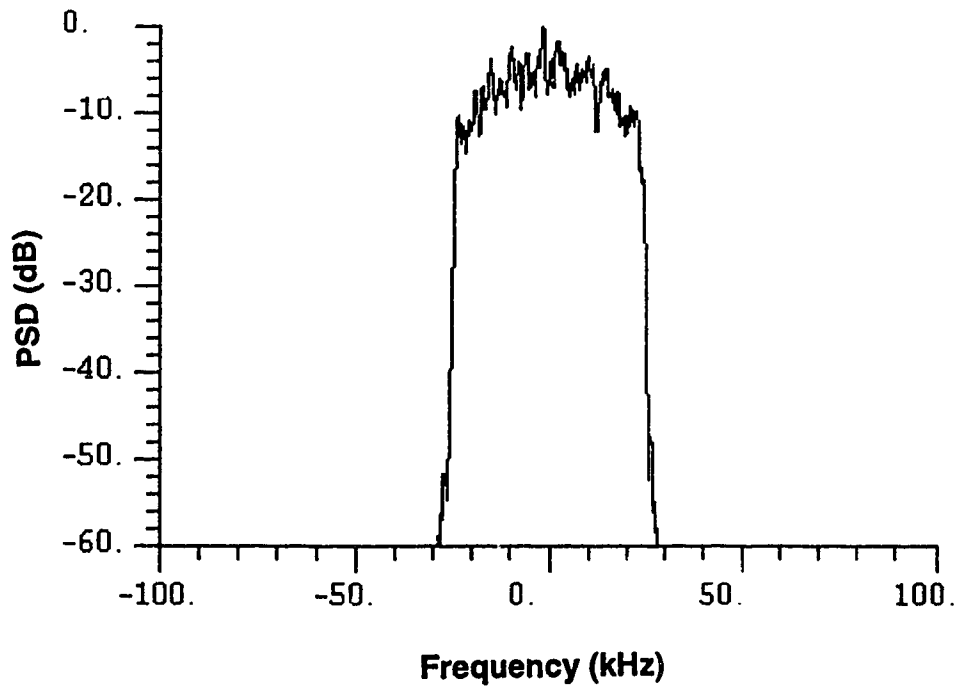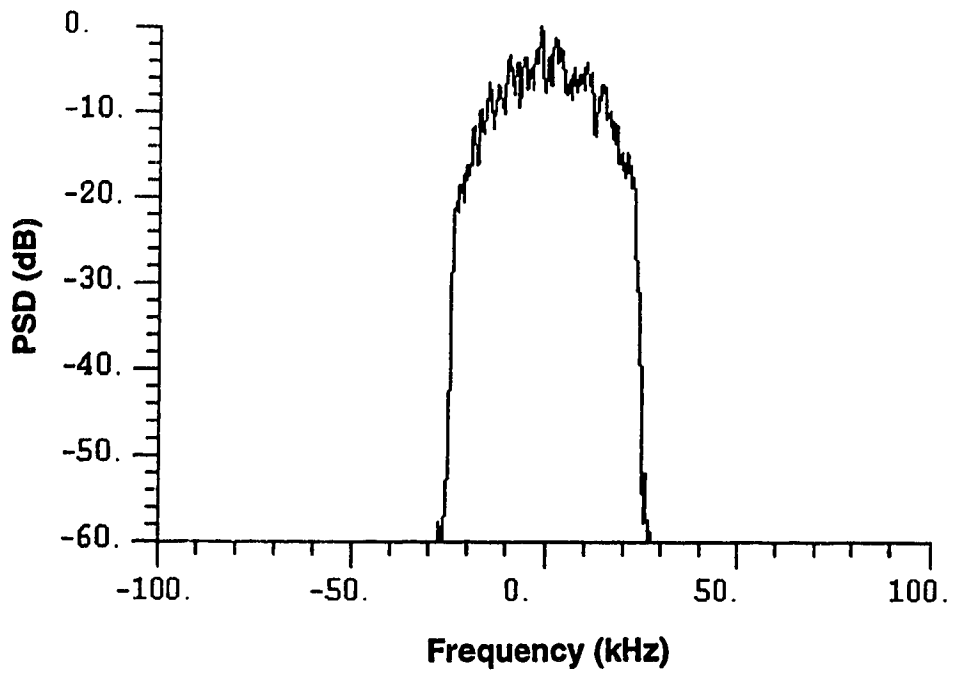
(c) SRC-ODQPSK(Butterworth)
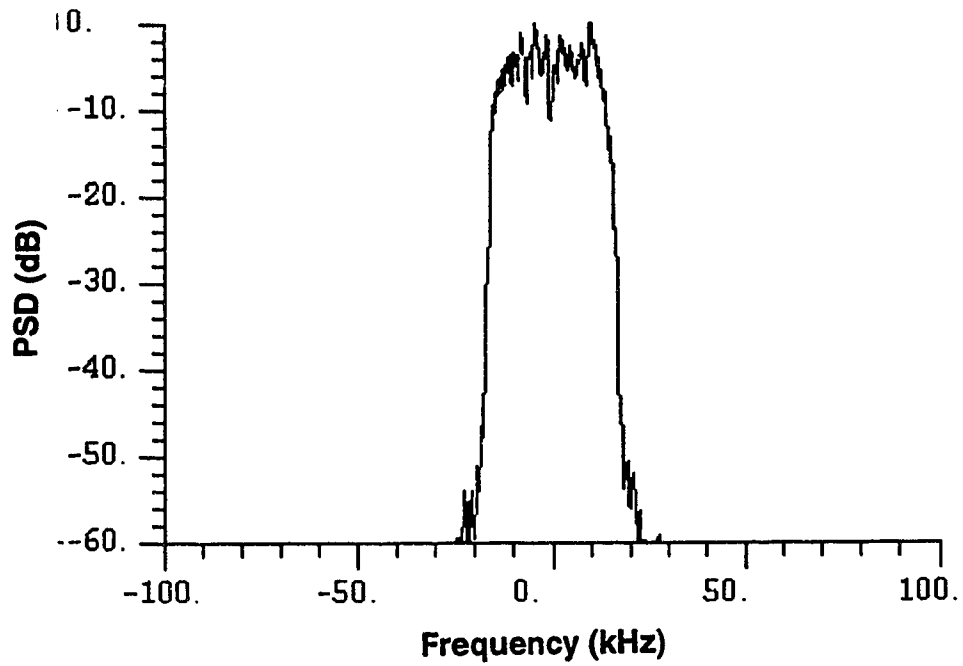
(d) π/4-DQPSK
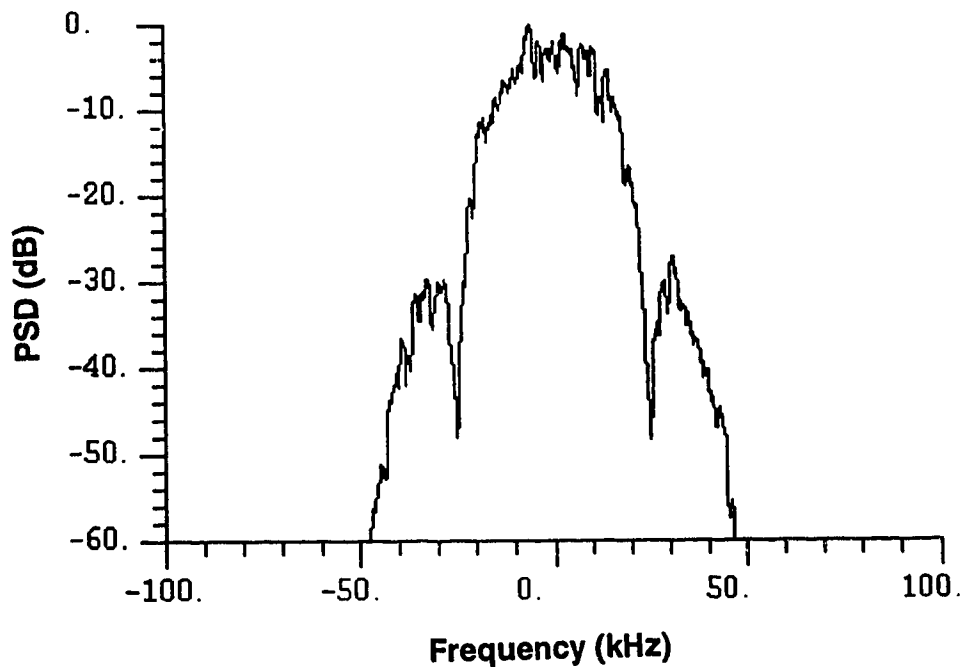
(e) ST-ODQPSK

Fig.4.19 Simulated power spectral density functions

4.5 Power variation

Power variation characteristics of the modulated signals are important because the transmitter amplifiers used in mobile radio systems are usually nonlinear, envelope-driven devices. It is always desired for the modulator output signals to have as little envelope fluctuation as possible. The peak-to-peak power variation of several kinds of modulated signals has been calculated and is listed in Table 4.1.

As can be seen, $\pi/4$-DQPSK has the largest envelope variation, and Gaussian DMSK has no envelope variation at all. The other three schemes all have very small power variation. It is therefore reasonable to expect that all these schemes, except for $\pi/4$-DQPSK, will suffer only a little nonlinear distortion by

power amplifiers. The spectral spreading due to nonlinear amplification should also be significantly less than that of the π/4-DQPSK scheme.

Modulation Scheme	Min-Max Power Variation
SRC-ODQPSK (4RRC)	5dB
SRC-ODQPSK (Butterworth)	4dB
ST-ODQPSK	3.5dB
π/4-DQPSK	20dB
Gaussian DMSK	0dB

Table 4.1 Power fluctuation characteristic

4.6 Performance comparison

The SRC-ODQPSK and ST-ODQPSK systems use different filtering schemes at the transmitter and receiver. Their error performance in different channel conditions have been presented in previous sections, and compared to two standard modulation schemes for digital mobile radio, namely, π/4-DQPSK and Gaussian DMSK. In this section, the comprehensive performance of SRC-ODQPSK and ST-ODQPSK is summarized.

Fig.4.20 shows the BER performance for the three studied systems in a linear AWGN channel. SRC-ODQPSK with 4RRC pulse shaping is seen to have

the best error performance. At a BER of 10^{-3}, it has an E_b/N_0 gain of 1dB over the one with SRRC pulse shaping, and 1.5dB over ST-ODQPSK. Therefore, equal partitioning of a SRRC filter at the transmitter and receiver will yield the best error rate results for ODQPSK modulation.

Fig.4.21 shows the BER performance in a hardlimited channel. It is noted that, for the BER of 10^{-3}, the performance gain of SRC-ODQPSK with 4RRC pulse shaping over the other two schemes still remains the same as in Fig.19. Therefore, it is found that the hardlimiting operation causes nearly the same deterioration of the error rates in each of the three systems.

Fig.4.22 shows the BER performance in the flat Rayleigh channel, where the Doppler spread is 90Hz. It is found that the two SRC-ODQPSK systems have almost the same BER performance in such a channel. They are both slightly better than ST-ODQPSK system. Therefore, equal partitioning of 4RRC filters can not yield any performance gain over SRRC filtering in association with receiver Butterworth filtering in a Rayleigh fading channel. However, the use of SRRC filtering or 4RRC filtering does reduce the system-inherent intersymbol interference, as compared to ST-ODQPSK. Hence, those systems have lower error floors.

Table 4.2 gives some important characteristics of the three systems and comparisons with π/4-DQPSK and Gaussian DMSK systems.
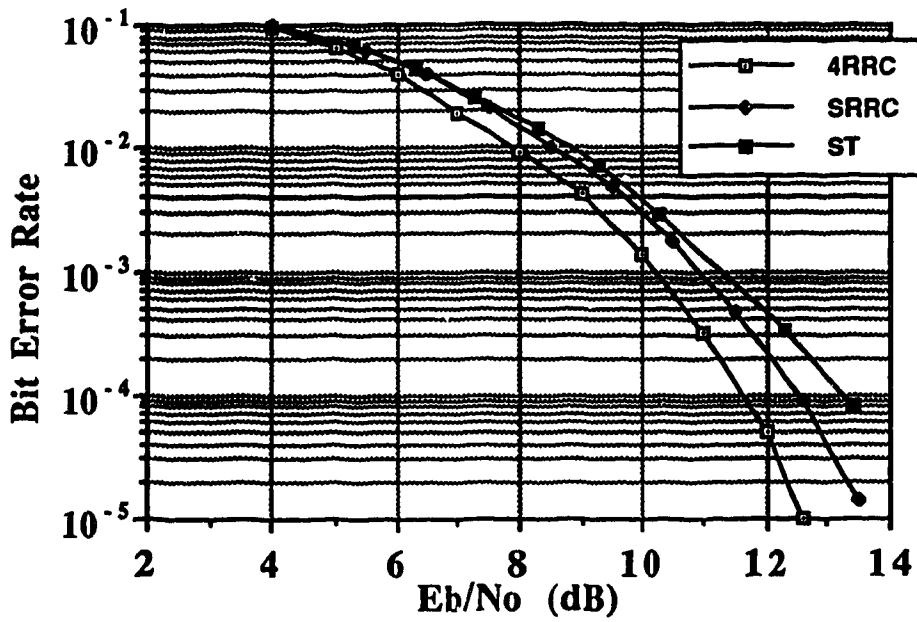
Fig.4.20 BER performance in a linear AWGN channel
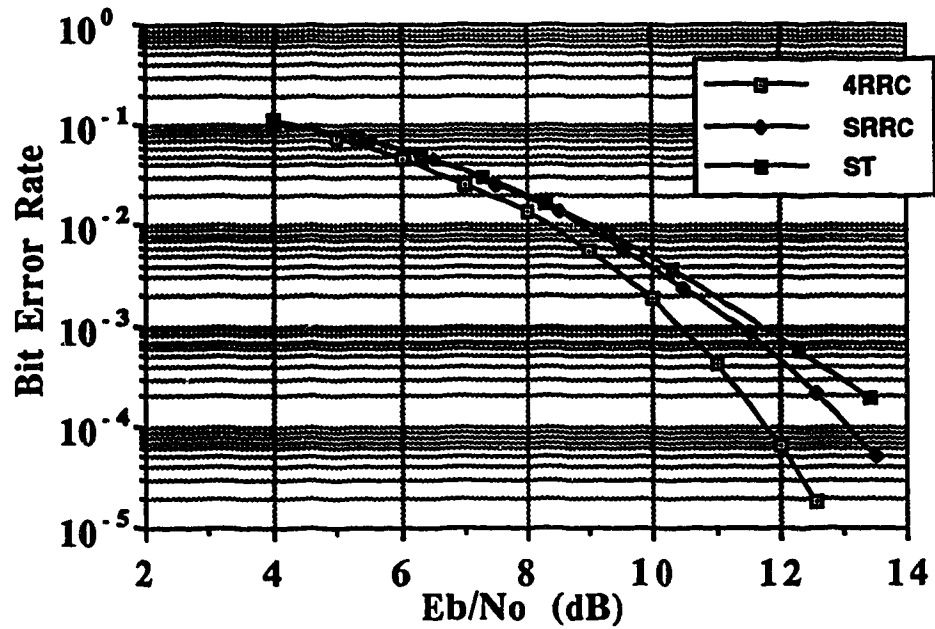
Fig.4.21 BER performance in a hardlimited channel
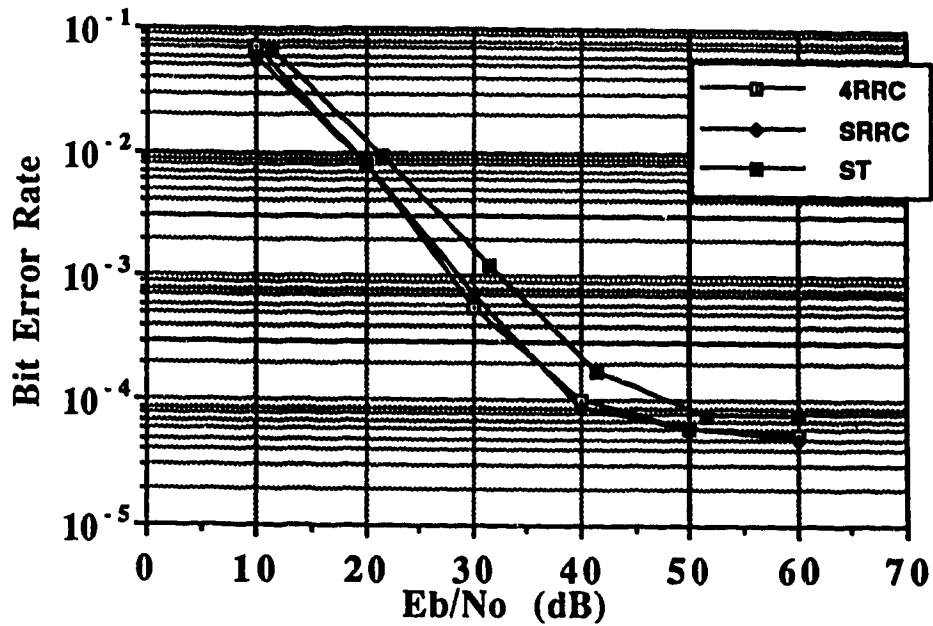
Fig.4.22 BER performance in a Rayleigh fading channel

Modulation Scheme	E_b/N_0 for BER $=10^{-3}$ (linear)	E_b/N_0 for BER $=10^{-3}$(nonlin.)	Error floor in fading	Power variation
SRC-ODQPSK (4RRC)	10.3dB	10.5dB	5.5×10^{-5}	5dB
SRC-ODQPSK (Butterworth)	11dB	11.4dB	5.5×10^{-5}	4dB
ST-ODQPSK	11.5dB	11.8dB	7.5×10^{-5}	3.5dB
π/4-DQPSK	9.5dB	12.7dB	2×10^{-4}	20dB
Gaussian DMSK (two-bit detect.)	13.5dB	13.5dB		0dB
Gaussian DMSK (one-bit detect.)	17.5dB	17.5dB		0dB

Table 4.2 Summary of performance

98

4.7 Error performance of NEC schemes

Using the BOSS simulation models described in Chapter 3, single, double and triple NEC schemes were evaluated for the ST-ODQPSK system in both linear AWGN and hardlimited AWGN channels. Two-bit and one-bit differential detection were used at the receiver, along with NEC schemes, and their error performance was investigated and compared.

Fig.4.23 shows the error rate improvement for one-bit differentially detected ST-ODQPSK in a linear channel. With single error correction, 0.6dB E_b/N_0 gain can be achieved at a BER of 10^{-3}. Double and triple error correction schemes have nearly equal error correcting performance. At the same BER, the amount of improvement in E_b/N_0 is about 1.3dB, compared to the case without NEC. This gives the implication that many of the errors present in the detection process occur in pairs, but that triple errors occur only rarely.

Fig.4.24 shows the error performance of NEC schemes for two-bit differential detection. It is seen that, at a BER of 10^{-3}, single error correction can produce an E_b/N_0 gain of 1dB. The Double and triple error correction schemes have almost the same performance. The improvement is 1.8dB for double error correction, and 2dB for triple error correction. If we compare Fig.4.23 with Fig.4.24, it can be noted that, in a linear AWGN channel, the triple error correction scheme used with two-bit differential detection performs best, while double or triple error correction with one-bit differential detection is second to it. In addition, It can be seen that, although one-bit differential detection proves to be superior to two-bit differential detection without NEC schemes, as discussed in Chapter 2, the reverse turns out to be true when NEC methods are applied to ST-ODQPSK. The effect of NEC is particularly noticeable when the system is operating at large signal-to-noise ratio, and it is almost negligible when the ratio is small.
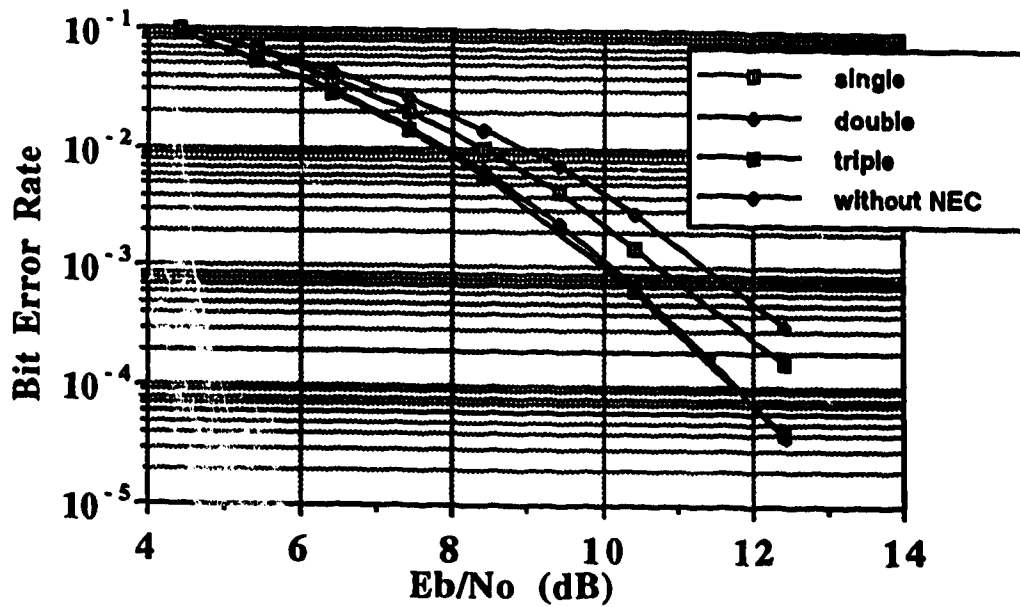
Fig.4.23 BER performance of NEC with one-bit detection
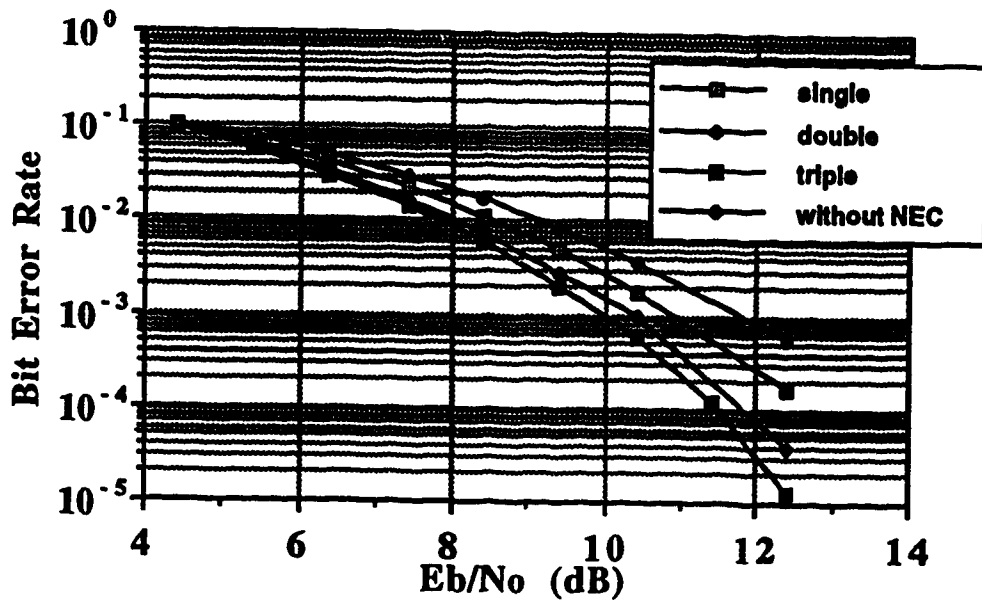
Fig.4.24 BER performance of NEC with two-bit detection

The error performance of NEC with two-bit differential detection in a hardlimited AWGN channel is illustrated in Fig.4.25. As can be seen, if the BER is

10^{-3}, single, double and triple error correction can achieve an improvement in E_b/N_0 of 1.2dB, 2dB and 2.5dB, respectively. The most significant improvement is made by single error correction.   can be justified from the fact that the E_b/N_0 gains from single to double error correction and from double to triple error correction are only 0.8dB and 0.5dB, while single error correction yields a gain of 1.2dB. Therefore, in a hardlimited channel, single errors occur most frequently when two-bit differential detection is used at the receiver.

Fig.4.26 gives the performance for a one-bit differential detection NEC receiver. The amount of improvement achieved by single, double and triple error correction schemes at a BER of 10^{-3} is 1dB, 1.5dB and 2dB, respectively. Single errors are the most likely errors in one-bit differential detection process. Comparing Fig.4.25 with Fig.4.26, it is observed that one-bit detection appears to be better than two-bit detection in any case, and that with triple error correction it performs best. This is just contrary to the linear channel case where two-bit detection turns out to be better than one-bit detection with the use of triple NEC.

Generally speaking, the improvement due to the use of NEC depends upon several factors. Firstly, the modulation and demodulation schemes have large effect on the performance of NEC. This is because NEC techniques are mainly aimed at reducing the intersymbol-interference-induced burst errors. In other words, they perform best in a system where severe intersymbol interference exists, which is most likely caused by the transmitter/receiver filtering, cochannel interference and nonlinear distortion in the transmitter power amplifier. Therefore, in a system using matched filter receiver such as the $\pi/4$-DQPSK system and operating in a linear AWGN channel, there will be little gain obtained from the use of NEC methods. Secondly, the type of channel we are dealing with is also crucial to NEC. Since NEC techniques make use of redundant receiver structure and large syndrome matrices, they tend to be very sensitive to the number of errors in

the error matrices. For example, if triple error correction is used, there could be 16 error symbols present in each error matrix derived from the receiver. A total of 2^{16} error patterns will result! However, only 121 of them uniquely correspond to detectable syndrome patterns. In a hostile channel such as a Rayleigh fading channel, deep fades may cause more than three successive errors to occur. As a result, the number of errors would be far more than three in the error matrix, resulting in the output of an erroneous correction pulse. If this kind of severe condition happens frequently, the use of NEC can only worsen the system error performance. Thirdly, even though the encountered channel is a linear AWGN channel, there are still some practical considerations which limit the use of high-order NEC schemes. On one hand, the use of high-order NEC scheme needs a more complex receiver. Usually, the number of differential detection branches is equal to the order of the NEC scheme used. On the other hand, increasing the order beyond three actually only results in a minor improvement of the error performance. This is because the number of error symbols increases dramatically with the square of the order. Fourthly, differential detection methods also affect the best achievable performance gain, since the differential detection method always affects the pattern of error occurrence in the error matrix, which will in turn affect the detected syndrome pattern.

In this project, NEC methods have been applied to ODQPSK modulation in linear and hardlimited channels, and have proved to be able to produce considerable performance gain. They have also been investigated in a Rayleigh fading channel. Unfortunately, for this case, NEC schemes degrade the system performance since severe Rayleigh fading disrupts the previously-mentioned conditions for employing NEC techniques. Hence, the corresponding results are not included in this thesis. In a Rician fading channel as encountered in mobile satellite communications, however, NEC methods have been reported[30] to be

able to reduce error rates significantly. Since these techniques successfully avoid introducing redundancy into either bit stream or symbol space, it is felt that they are still very attractive for bandwidth-limited applications such as mobile radio communications.
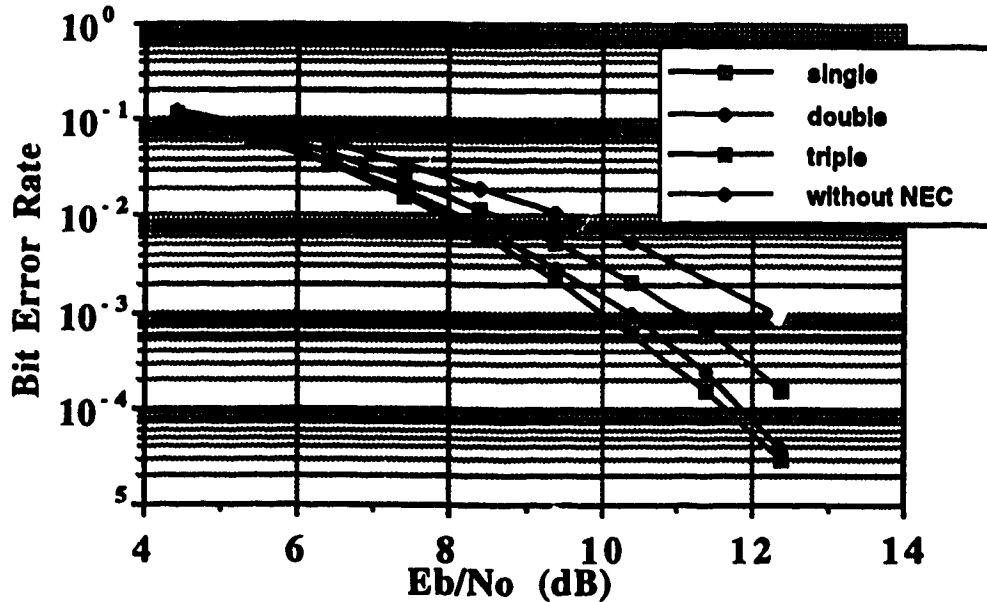
Fig.4.25 BER of two-bit detection in hardlimited channel
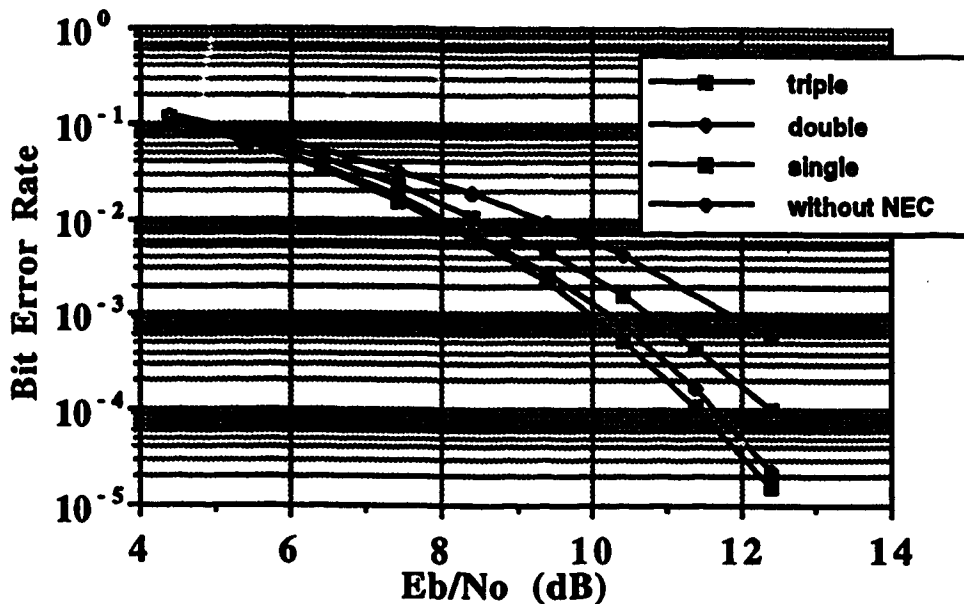
Fig.4.26 BER of one-bit detection in hardlimited channel

Chapter 5   CONCLUSIONS AND DISCUSSION

This chapter summarizes the results of the computer simulation and performance analyses conducted in this project. First, in Section 5.1, SRC-ODQPSK and ST-ODQPSK systems and NEC techniques are summarized, and the computer simulation strategies are described. Then, system performance and improvement obtained by using NEC techniques are discussed in Section 5.2. Finally, some topics on future research work related to this project are recommended.

5.1 System and simulation strategies

The simulation tool used in this project to develop the investigated communication systems is a simulation software package called BOSS by COMDISCO, SYSTEMS Inc. It provides a complete interactive and user-friendly environment for communication engineers to conduct simulation-based system performance analyses. This package has a built-in signal processing development library. Also, it provides users with a convenient and powerful approach to build up new basic BOSS modules in order to achieve more complicated signal processing functions. FORTRAN support programs are used for all the user-defined modules. For the studied systems, the complex baseband equivalents were simulated on a SUN SPARC2 station so as to improve simulation efficiency. The Monte Carlo error counting technique was adopted to obtain the bit error rate performance of the simulated systems.

This project investigated two systems, SRC-ODQPSK and ST-ODQPSK, for land mobile radio communications. Currently, two standard modulation schemes, $\pi/4$-DQPSK and Gaussian DMSK, have been proposed in North American and Europe respectively, for second generation land mobile radio

applications. Compared to the first generation FM systems, they have the major advantage of providing significantly increased channel capacity and diverse services. Comparing π/4-DQPSK with Gaussian DMSK, it can be found that π/4-DQPSK system offers a higher spectral efficiency, while Gaussian DMSK system has the advantage of constant envelope, which precludes the use of transmitter linearization techniques. On the contrary, the severe envelope fluctuation of π/4-DQPSK signals necessitates considerable effort to linearize the transmitter power amplifier. SRC-ODQPSK and ST-ODQPSK systems are therefore proposed to achieve the best trade-off between the π/4-DQPSK and Gaussian DMSK systems. In other word, they should have largely reduced power variation in the modulated signals compared to π/4-DQPSK modulation, offer high spectral efficiency as the two standard schemes, and also achieve comparable or better error performance in all kinds of channel scenarios.

In addtion to modulation/demodulation techniques, error control encoding techniques are also important for the realization of reliable transmission in mobile radio channels. Nonredundant error correction(NEC) schemes have the advantage that they do not need any transmission bandwidth expansion or signal constellation expansion. This project pursued the application of NEC techniques to ODQPSK modulation scheme. Single, double and triple error correction schemes have been developed for ODQPSK modulation. Their performance has been evaluated in linear, nonlinear and Rayleigh fading channels.

Two types of differential encoding strategies, two-bit and three-bit differential encoding, have been proposed in this work for ODQPSK modulation. The performance has been evaluated along with NEC schemes in linear, nonlinear channels.

In the SRC-ODQPSK system, two kinds of filtering techniques were investigated. One uses SRRC pulse shaping at the transmitter baseband, and

Butterworth filtering as the receiver filter. Another uses 4RRC filtering both at the transmitter and receiver. In the ST-ODQPSK system, transmitter baseband pulse shaping is replaced by sinusoidal waveshaping according to a specific rule. A 4-th order Butterworth filter was used as the receiver filter. The whole system is analogous to the SRC-ODQPSK system except for the different filtering operations used at transmitter and receiver.

The land mobile radio channel used in the simulation was a two-ray channel, as recommended in IS-54 documents. Fast flat Rayleigh fading with a Doppler frequency of 90Hz and frequency-selective Rayleigh fading were simulated. By using this channel model, the effects of fast random phase and frequency modulation phenomenon have been investigated.

5.2 Simulated performance

Power spectral density and envelope variation were simulated for $\pi/4$-DQPSK, Gaussian ⊔MSK, SRC-ODQPSK and ST-ODQPSK schemes. The BER performance of the proposed systems were also evaluated in linear AWGN, hardlimited AWGN and flat Rayleigh fading as well as frequency-selective Rayleigh fading channels. NEC techniques were studied under linear, nonlinear and Rayleigh fading channel conditions for ST-ODQPSK.

In terms of power variation of the modulated signals, ST-ODQPSK has the smallest one, which is only about 3.5dB. The SRRC-filtered and 4RRC-filtered SRC-ODQPSK schemes have 4dB and 5dB fluctuation, respectively. This means that a very small envelope fluctuation is achievable with the ODQPSK modulation format. This is close to the 0dB power variation achieved by Gaussian DMSK, and significantly lower than that of $\pi/4$-DQPSK, which is 20dB.

All three schemes have more compact spectra than Gaussian DMSK. SRC-ODQPSK is more spectrally efficient than ST-ODQPSK as its spectrum has no sidelobes. The theoretical bandwidth occupied by the π/4-DQPSK signal is lower than that of SRC-ODQPSK. However, when transmitter nonlinear power amplifiers are used, spectral spreading will result in a broader occupied bandwidth even though linearization techniques are employed. SRC-ODQPSK will see much less spectral spreading, thus easing the amplifier linearization problem. It is reasonable to expect that the actual spectral efficiencies of SRC-ODQPSK and π/4-DQPSK systems will be close to each other.

The error rate of 4RRC-filtered SRC-ODQPSK appears to be the best of the proposed schemes in a linear AWGN channel. At a BER of 10^{-3}, it is 0.8dB poorer than π/4-DQPSK, 0.7dB better than SRRC-filtered SRC-ODQPSK, 1.2dB better than ST-ODQPSK and 3.2dB better than two-bit detected Gaussian DMSK. Two-bit differentially detected Gaussian DMSK was assumed to have adaptive threshold adjustment for each E_b/N_0, which is not practical. However, one-bit differentially detected Gaussian DMSK gives a worse error rate. It is inferior to 4RRC-filtered SRC-ODQPSK by 7.2dB.

In a hardlimited AWGN channel, 4RRC-filtered SRC-ODQPSK also performs best. At a BER of 10^{-3}, it is 0.9dB better than SRRC-filtered SRC-ODQPSK, 1.3dB better than ST-ODQPSK, 2.2dB better than π/4-DQPSK, 3dB better than two-bit GMSK and 7dB better than one-bit GMSK. From this, it is felt that SRC-ODQPSK is very robust against AM-AM nonlinear distortion.

In a flat fast Rayleigh fading channel, the three schemes exhibit lower irreducible error floors than π/4-DQPSK. For 4RRC-filtered SRC-ODQPSK, SRRC-filtered SRC-ODQPSK, ST-ODQPSK and π/4-DQPSK, the error floors were found to be 5.5×10^{-5}, 5.5×10^{-5}, 7.5×10^{-5} and 2×10^{-4}, respectively. It is observed that 4RRC and SRRC pulse shaping operations lead to almost the

same bit error performance in a flat Rayleigh fading channel, and SRC-ODQPSK is comparable or better than $\pi/4$-DQPSK for all E_b/N_o values. Therefore, equally partitioning a SRRC filter into two 4RRC filters does not produce any E_b/N_o gain at all in the case of Rayleigh fading. ST-ODQPSK is seen to be slightly worse than $\pi/4$-DQPSK for $E_b/N_o < 35$dB, beyond which it enters the lower error floor region. The reason why ODQPSK systems have lower error floors than $\pi/4$-DQPSK system can be attributed to the fact that the sampling frequency of the former at the decision circuit is twice as much as that of the latter, which partially offsets the deleterious effect of fast random phase modulation.

Nonredundant error correction schemes yield different error correcting capabilities for different differential encoding used at the transmitter. In a linear AWGN channel, triple error correction performs best with three-bit differential encoding; it can produce a 2dB gain in E_b/N_o at a BER of 10^{-3}. In a hardlimited AWGN channel, the reverse appears to be correct. Triple error correction yields the most gain when used with two-bit differential encoding. For this case, a 2.5dB gain can be achieved at a BER of 10^{-3}. It is also found that single and double errors are the most frequent errors in a linear AWGN channel, while in a hardlimited AWGN channel, only single errors are dominant. Therefore, considering the circuit complexity and amount of error rate improvement, there is no point in using high order NEC schemes in practice. Also, in a system where intersymbol interference is small, such as $\pi/4$-DQPSK, and operating in a linear AWGN channel, there is no need for using NEC techniques. In a mobile radio channel characterized by Rician fading, NEC methods have also been proved to be able to improve the system error performance. In the author's opinion, NEC techniques are particularly suitable for use in bandwidth-efficient and reliable communications, which, of course, also include mobile radio applications.

In conclusion, SRC-ODQPSK has been found to be a promising modulation scheme for increased capacity digital mobile radio applications, due to its small envelope variation, compact power spectrum and excellent error performance. Besides, the very simple receiver configuration allows cost-effective implementation of the mobile portable unit. ST-ODQPSK may also find applications in situations where bandwidth efficiency is less stringent and power efficiency is of major concern. NEC techniques are powerful means of reducing error rates caused by cochannel interference and transmitter/receiver filtering. They may find a variety of applications in cases where cochannel interference caused by cell-site frequency re-use is strong and the channels are not characterized by Rayleigh fading, such as those found in indoor and land mobile satellite communications.

5.3 Suggested future research

As a result of this research work and considering the evolvement of mobile radio communications, future research emphases may be placed in the following areas:

❑ High-level digital modulation schemes such as M-ary QAM and M-ary PSK. These schemes can be used to dramatically enhance spectral efficiency. One of the major disadvantages of employing these schemes is that they need efficient amplifier linearization since severe power variation is present on the modulated signal. Their error performance also needs to be improved in a mobile fading channel.

❑ Combined modulation and coding schemes such as TCM. As they require little or no bandwidth expansion, and can also produce considerable coding gain to combat the fading effects, these techniques could be usefully applied to mobile radio and other wireless communication systems.

BIBLIOGRAPHY

[1] William C.Y. Lee, *Mobile Communications Engineering*. McGraw Hill, New York, 1982, p.2.

[2] G. Calhoun, *Digital Cellular Radio*. Artech House, MA, 1988, p. 26.

[3] *Ibid.*, p. 63.

[4] EIA/TIA: " Cellular System Dual-Mode Mobile Station - Base Station Compatibility Standard," Electronic Industries Association(EIA), May 1990.

[5] DECT: " Digital European Cordless Telecommunication System," Code: RES-3(89), DECT, 1989.

[6] G.S.M.: " Physical Layer On The Radio Path," GSM 05.04; Release GSM/PN; ETSI-European Telecommunications Standards Institute, Nice, France, July 1988.

[7] G.L. Stuber, C. Kchao, " Capacity of direct-sequence CDMA for cellular radio," IEEE International Conference on Selected Topics in Wireless Communications, pp. 199-202, 1992.

[8] Hirofumi Suzuki, " A statistical model for urban radio propagation," IEEE Trans. Commun., Vol. COM-25, No.7, pp. 673-680, 1977.

[9] G. Turin, F. Clapp, T. Johnston, S. Fine, D. Lavry, " A statistical model of urban multipath propagation," IEEE Trans. Veh. Tech., Vol. VT-21, No.1, pp. 1-8, 1972.

[10] S. Stapleton, J. Cavers, " A new technique for adaptation of linearizing predistorters," IEEE Veh. Tech. Conf., pp. 753-758, 1991.

[11] M. Faulkner, T. Mattsson, W. Yates, " Adaptive linearization using pre-distortion," IEEE Veh. Tech. Conf., pp. 35-39, 1990.

[12] Y. Nagata, " Linear amplification technique for digital mobile communications," IEEE Veh. Tech. Conf., pp. 159-164, 1989.

[13] Y. Akaiwa, Y. Nagata, " Highly efficient digital mobile communications with a linear modulation method," IEEE Journal Selected Areas Commun., Vol. SAC-5, No. 5, pp. 890-895, June 1987.

[14] Y. Yamao, S. Saito, H. Suzuki, T. Nojima, " Performance of π/4-QPSK transmission for digital mobile radio applications," IEEE GLOBECOMM., pp. 443-447, 1989.

[15] S. Chennakeshu, G. Saulnier, " Differential detection of π/4-DQPSK for digital cellular radio," IEEE Veh. Tech. Conf., pp. 186-191, 1991.

[16] F. Patenaude, J. Lodge, " Non-coherent detection of hardlimited OQPSK," IEEE International Conference on Wireless Communications, pp. 93-97, 1992.

[17] J. Hagenauer, N. Seshadri, C. Sundberg, " The performance of rate-compatible punctured convolutional codes for digital mobile radio," IEEE Trans. Commun., Vol. 38, No. 7, pp. 966-980, July 1990.

[18] P. Chow, D. Ko, " Improving DCPSK transmission by means of error control," IEEE Trans. Commun., Vol. COM-19, pp. 715-719, 1971.

[19] S. Samejima, K. Enomoto, Y. Watenabe, " Differential PSK system with nonredundant error correction," IEEE Journal Select Areas Commun. Vol. SAC-1, No.1, pp. 74-81, 1983.

[20] T. Masamura, " Intersymbol interference reduction for differential MSK by nonredundant error correction," IEEE Trans Veh. Tech., Vol. 39, No. 1, pp. 27-36, 1990.

[21] J. Yang, K. Feher, " Nonredundant error correction for π/4-QPSK in mobile satellite channels," IEEE Veh. Tech. Conf., pp. 782-787, 1991.

[22] T. Tezcan, K. Feher, " Performance evaluation of differential MSK with nonredundant error correction in an AWGN and ACI environment," IEEE Trans. Commun., Vol. COM-34, pp. 727-733, July 1986.

[23] K. Feher, Advanced Digital Communication: Systems and Signal Processing Techniques. Prentice-Hall Inc., 1987.

[24] P. Varshney, S. Kumar, " Performance of GMSK in a land mobile radio channel," IEEE Trans. Veh. Tech., Vol. 40, No. 3, pp. 607-614, August 1991.

[25] K. Murota, K. Hirade, " GMSK modulation for digital radio telephony," IEEE Trans. Commun., Vol. COM-29, No.7, pp. 1044-1050, July 1981.

[26] K. Defly, M. Lecours, N. Boutin, " Differential detection of the OQPSK signals: coding and decoding," IEEE International Conference Commun., pp. 1660-1664, 1989.

[27] T. Le-Ngoc, K. Feher, H. Phamvan, " New modualtion techniques for low-cost power and bandwidth efficient satellite earth stations," IEEE Trans. Commun., pp. 275-283, Jan. 1982.

[28] M. El-Torky, K. Feher, " Analysis and design of bandlimiting filters to meet FCC restrictions for digital QPSK radio systems in an interference environment," IEEE International Conference Commun., pp. 15.3.1- 15.3.5, June 1978.

[29] D. Wiggert, Codes For Error Control And Synchronization, Artech House Inc., 1988.

[30] J. Walker, Mobile Information Systems, Artech House Inc., 1990.

[31] J. Tarallo, G. Zysman, " Modulation techniques for digital cellular systems," IEEE Veh. Tech. Conf., pp. 245-247, 1990.

[32] C. Schlegel, D. Costello, " Bandwidth efficient coding for fading channels: code construction and performance analysis," IEEE Journal Selected Areas Commun., Vol. 7, No. 9, pp. 1356-1368, Dec. 1989.

[33] C. Liu, K. Feher, " Non-coherent detection of π/4-QPSK systems in a CCI-AWGN combined interference environment," IEEE Veh. Tech. Conf., 1989.

[34] COMDISCO Systems, Inc., Block Oriented System Simulator(BOSS) User's Guide, COMDISCO Systems, Inc., Foster City, CA, 1989.

[35] W.C. Jakes, Microwave Mobile Communications, New York, John Wiley & Sons, 1974.

[36] C. Liu, K. Feher, " Performance of non-coherent π/4-QPSK in a frequency-selective fast Rayleigh fading channel," IEEE International Conference Commun., pp. 1369-1371, 1990.

[37] S. Elnoubi, " Analysis of GMSK with two-bit differential detection in land mobile radio channels," IEEE Trans. Commun., Vol. COM-35, No. 2, pp. 237-240, Feb. 1987.

[38] S. Elnoubi, " Analysis of GMSK with differential detection in land mobile radio channels," IEEE Veh. Tech. Conf., pp. 96-101, 1986.

[39] J. Smith, " A computer generated multipath fading simulation for mobile radio," IEEE Trans. Veh. Tech., pp. 39-40, 1975.

[40] M. Kavehrad, P. Balaban, " Digital radio transmission modeling and simulation," IEEE Veh. Tech. Conf., pp. 1289-1294, 1989.

[41] M. Simon, C. Wang, " Differential detection of Gaussian MSK in a mobile radio environment," IEEE Trans. Veh. Tech., Vol. VT-33, No.4, pp. 307-320, 1984.

114

[42] V. Fung, T. Rappaport, " Bit-error simulation of π/4 DQPSK in flat and frequency-selective fading nobile radio channels with real time applications," IEEE International Commun. Conference, pp. 553-557, 1991.

[43] Proakis, *Digital Communications*, McGraw-Hill Inc., 1989.

[44] M. Jeruchim, " Techniques for estimating the bit error rate in the simulation of digital communication systems," IEEE Journal Selected Areas Commun., Vol. SAC-2, No. 1, pp. 153-170, January 1984.

APPENDIX A:

Derivation of the PSD function of ST-ODQPSK signals

Since the output of the pulse shaping filter for ST-ODQPSK signals depends not only upon the current input, but also upon the output in the previous time slot, the modulated signals can be regarded as being generated from a Markov chain. Therefore, the power spectral density function can be derived by the same methods as used in some modulation techniques which have memory such as Manchester coding and Miller coding. Assuming that the data stream is a stationary random process and bit "1" and "0" are equally probable, the following state transition diagram can be easily obtained:
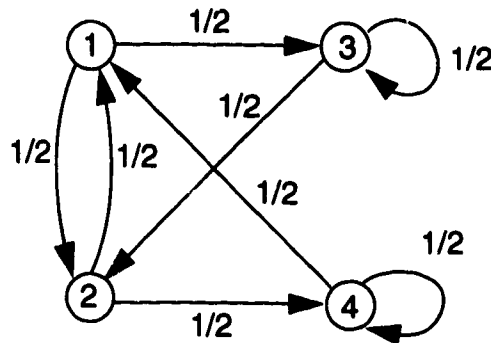
In this diagram, each circled number indicates one state. Therefore, the process can be represented by a finite state Markov chain model. The transition from one state to another is also labelled with the corresponding state transition probability. The four states given in the graph correspond to four unique waveform transitions. The four transitions are given as follows:
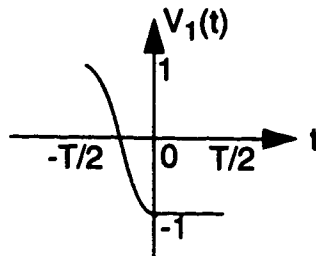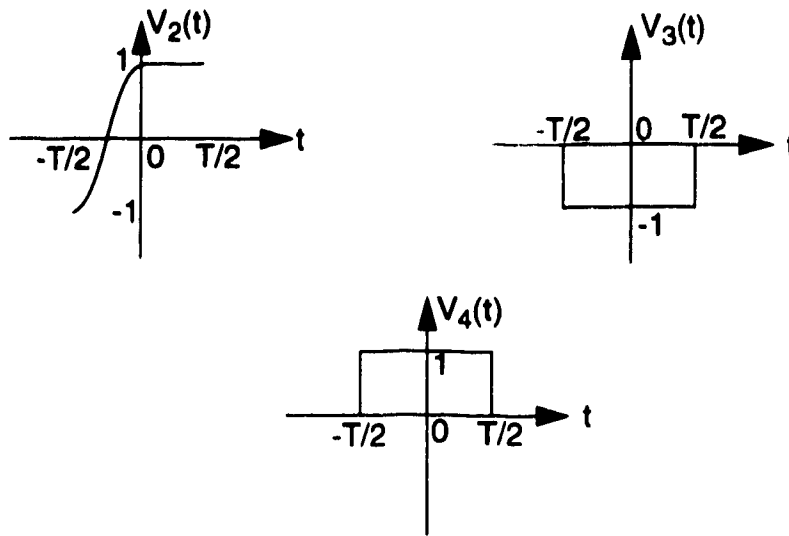
$V_1(t)$, $V_2(t)$, $V_3(t)$ and $V_4(t)$ indicate four possible waveform transitions relating to the waveform shaping operation. T is one symbol duration, which is twice one bit duration. The maximum amplitude of these waveforms is normalized without loss of generality. The state transition probability matrix Q can be found according to the state transition diagram shown above:

$$Q = \begin{bmatrix} 0 & \frac{1}{2} & \frac{1}{2} & 0 \\ \frac{1}{2} & 0 & 0 & \frac{1}{2} \\ 0 & \frac{1}{2} & \frac{1}{2} & 0 \\ \frac{1}{2} & 0 & 0 & \frac{1}{2} \end{bmatrix}$$

It can be easily proved that the n-step state transition matrix is:

$$Q^n = \frac{1}{4}\begin{bmatrix} 1 & 1 & 1 & 1 \\ 1 & 1 & 1 & 1 \\ 1 & 1 & 1 & 1 \\ 1 & 1 & 1 & 1 \end{bmatrix}$$

The stationary state probabilities can be calculated using the balance equations in terms of probability flows:

$$\begin{cases} p_1 = \frac{1}{2}p_4 + \frac{1}{2}p_2 \\ p_2 = \frac{1}{2}p_1 + \frac{1}{2}p_3 \\ p_3 = \frac{1}{2}p_1 + \frac{1}{2}p_3 \\ p_4 = \frac{1}{2}p_4 + \frac{1}{2}p_2 \end{cases}$$

Solving for these equations leads to $p_1 = p_2 = p_3 = p_4 = 1/4$. Considering the four waveform transitions, it is reasonable to formulate the output y(t) from the waveform shaping circuit as follows:

$$y(t) = \sum_{n=-\infty}^{\infty} V_n(t - nT)$$

The general form of the power spectral density of a signal generated from a finite state Markov chain model has been derived in [40]. By using the same procedure, the power spectral density of process y(t) can be found to be:

$$y(f) = \frac{1}{T^2}\sum_{n=-\infty}^{\infty}\left|\sum_{i=1}^{4}p_i V_i\left(\frac{n}{T}\right)\right|^2 \delta\left(f - \frac{n}{T}\right) + \frac{1}{T}\sum_{i=1}^{4}p_i|V_i(f)|^2$$

$$-\frac{2}{T}Re\left\{\sum_{i=1}^{4}\sum_{k=1}^{4}p_i V_i^*(f)\, V_k(f)\, V_{ik}(-1)\right\}$$

where

$$V_{ik} = \sum_{n=1}^{\infty} p_{ik}^{(n)} e^{-j2\pi fT} = p_{ik}^{(1)} e^{-j2\pi fT} + \sum_{n=2}^{\infty} p_{ik}^{(n)} e^{-j2\pi fT}$$

In the above equation, $p_{ik}^{(n)}$ is the n-step state transition probability from state i to k, which can be found from the state transition matrices. $V_i(f)$ is the Fourier transformation of $V_i(t)$.

Substituting the values of state transition probabilities and stationary state probabilities into the equation, y(t) can be simplified as follows:

$$
\begin{aligned}
Y(f) &= \frac{1}{2T}(|V_1(f)|^2 + |V_3(f)|^2) + \frac{1}{2T}Re\Big\{ \Big[\frac{1}{2}V_1^*(f)(V_3(f) - V_1(f)) \\
&\quad - \frac{1}{2}V_2^*(f)(V_3(f) - V_1(f)) + \frac{1}{2}V_3^*(f)(V_3(f) - V_1(f)) \\
&\quad - \frac{1}{2}V_4^*(f)(V_3(f) - V_1(f)) \Big] e^{-j2\pi fT} \Big\} \\
&= \frac{1}{2T}(|V_1|^2 + |V_3|^2) + \frac{1}{2T}Re\Big\{ (V_1 + V_3)^*(V_3 - V_1) e^{-j2\pi fT} \Big\} \\
&= \frac{1}{2T}(V_1 V_1^* + V_3 V_3^* + jV_1 V_3^* \sin(2\pi fT) - V_1 V_1^* \cos(2\pi fT)) \\
&\quad - \frac{1}{2T}(jV_1^* V_3 \sin(2\pi fT) + V_3 V_3^* \cos(2\pi fT)) \\
&= \frac{1}{T}\Big\{ V_3^2 \cos^2(\pi fT) - Im(V_1)V_3 \sin(2\pi fT) + V_1 V_1^* \sin^2(\pi fT) \Big\}
\end{aligned}
$$

The Fourier transformations of V_1 and V_3 are calculated as follows:

$$V_3 = \int_{-\frac{T}{2}}^{\frac{T}{2}} (-1) e^{-j2\pi ft} dt = -\frac{1}{\pi f}\sin(\pi fT)$$

$$V_1 = \int_{-\frac{T}{2}}^{0} (-1) \cos\left(\frac{2\pi}{T} t\right) e^{-j2\pi ft} dt + \int_{0}^{\frac{T}{2}} (-1) e^{-j2\pi ft} dt$$

$$= -\int_{-\frac{T}{2}}^{0} \cos\left(\frac{2\pi}{T} t\right) \cos(wt) \, dt + j\int_{-\frac{T}{2}}^{0} \cos\left(\frac{2\pi}{T} t\right) \sin(wt) \, dt$$
$$-\int_{0}^{\frac{T}{2}} e^{-jwt} dt$$

$$= \frac{1}{2}\left[\frac{\sin\left(\frac{wT}{2}\right)}{w+\frac{2\pi}{T}} - \frac{\sin\left(\frac{wT}{2}\right)}{\frac{2\pi}{T}-w}\right] - \frac{j}{2}\left[\frac{2w}{w^2-\left(\frac{2\pi}{T}\right)^2} + \frac{\cos\left(\frac{wT}{2}\right)}{w+\frac{2\pi}{T}}\right]$$

$$-\frac{j}{2}\frac{\cos\left(\frac{wT}{2}\right)}{w-\frac{2\pi}{T}} - \frac{2\sin\left(\frac{wT}{2}\right)}{w} e^{-\frac{jwT}{4}}$$

$$= \frac{w}{w^2-\left(\frac{2\pi}{T}\right)^2}\sin\left(\frac{wT}{2}\right) - j\frac{w}{w^2-\left(\frac{2\pi}{T}\right)^2} - j\frac{w}{w^2-\left(\frac{2\pi}{T}\right)^2}\cos\left(\frac{wT}{2}\right)$$

$$-\frac{2}{w}\sin\left(\frac{wT}{4}\right) e^{-\frac{jwT}{4}}$$

Substituting the expressions for V_1 and V_3 into $Y(f)$ yields:

$$Y(f) = \frac{1}{T}\left\{ \cos^2(\pi fT) \frac{4}{w^2}\sin^2(\pi fT) + (\sin\pi fT)^2 \cos(\pi fT) \sin^2\left(\frac{wT}{4}\right)\frac{8}{w^2}\right\}$$

$$-\frac{1}{T}\frac{4}{w}\frac{w}{w^2-\left(\frac{2\pi}{T}\right)^2}\cos\left(\frac{wT}{2}\right)\sin^2(\pi fT)\cos(\pi fT)$$

120

$$-\frac{1}{T}\sin^2(\pi fT)\;(-1)\left[\frac{w}{w^2-\left(\frac{2\pi}{T}\right)^2}\sin\left(\frac{wT}{2}\right)-\frac{2}{w}\sin\left(\frac{wT}{4}\right)\cos\left(\frac{wT}{4}\right)\right]^2$$

$$-\frac{1}{T}(-1)\sin^2(\pi fT)\left[\sin^2\left(\frac{wT}{4}\right)\frac{2}{w}-\frac{w}{w^2-\left(\frac{2\pi}{T}\right)^2}-\frac{w}{w^2-\left(\frac{2\pi}{T}\right)^2}\cos\left(\frac{wT}{2}\right)\right]^2$$

$$=\frac{1}{T}\left\{T\frac{\sin(\pi fT)}{2\pi fT}\,(1+\cos(\pi fT))-\frac{T}{\pi}\sin(\pi fT)\cos^2\left(\frac{\pi fT}{2}\right)\frac{fT}{T^2 f^2-1}\right\}^2$$

$$-\frac{(2\pi)^4}{T^5}\sin^4(\pi fT)\frac{T^6}{(4\pi^2)^3 f^2 T^2 (f^2 T^2-1)^2}$$

letting fT = x, the power spectral density is thus normalized in the frequency domain:

$$y(x)=T\left[\frac{\sin(\pi x)}{2\pi x}\,(1+\cos(\pi x))-\frac{1}{\pi}\sin(\pi x)\cos^2\left(\frac{\pi x}{2}\right)\frac{x}{x^2-1}\right]^2$$

$$-\frac{T}{4\pi^2}(-1)\sin^4(\pi x)\frac{1}{x^2(x^2-1)^2}$$

It can be easily verified that y(x) is an even function with respect to x, and the maximum point corresponds to dc, i.e., x=0. Some particularly important points of the PSD are given below: (magnitude of the PSD has been normalized)

y(0) = 0dB,   y(0.5) = -4.4dB

y(1.5) = -18.4dB,   y(2.5) = -35dB

y(3.5) = -45dB,   y(4.5) = -52dB

y(5.5) = -57dB,   y(n) = -infinite dB

n=nonzero integer

Appendix B:

Computer programs for simulating double and triple NEC schemes

In this part, some Fortran subroutines, which are used for generating and detecting the error patterns and syndrome patterns in double and triple NEC schemes, are given. Since there are a relatively small number of detectable syndrome patterns in double error correction scheme, only one subroutine is needed to realize the syndrome pattern detection operation. All the corresponding error patterns leading to these syndrome patterns can be previously calculated. BOSS supports user-defined primitive modules, provided that their corresponding subroutines conform to certain constraints. A primitive module called PATTERN DETECTOR is therefore built up using the subroutine for double error correction. To achieve triple correction, a large number of syndrome patterns exists. For the purpose of avoiding time-consuming calculation of numerous error and syndrome patterns, several computer programs were written to automatically generate all the required patterns efficiently. Similar to double error correction, a syndrome detection subroutine is written to construct a user defined primitive module called PATTERN DECISION to achieve triple error correction. All these programs are listed as follows.

```
CCCCCCCCCCCCCCCCCCCCCCCCCCCCCCCCCCCCCCCCCCCCC
C This program is used to detect all the syndrome C
C patterns for double NEC scheme. It can be used  C
C for either two-bit or three-bit differentially  C
C encoded ODQPSK modulation schemes. The BOSS     C
C primitive module PATTERN DETECTOR uses this     C
C subroutine to decide whether to ouput a correc- C
C pulse or not. A total of 9 distinct syndrome    C
C patterns, each of which contains 6 syndromes,   C
C can be detected in this subroutine.             C
CCCCCCCCCCCCCCCCCCCCCCCCCCCCCCCCCCCCCCCCCCCCCCCCC
      subroutine pattern(in1,in2,in3,in4,in5,in6,out)
      logical*1 in1,in2,in3,in4,in5,in6,out
      out=.false.
C     The following each IF block detects one syndrome
C     pattern
      if (in1.eq..false.) then
      if(in2.eq..true.) then
      if(in3.eq..true.) then
      if(in4.eq..true.) then
      if(in5.eq..true.) then
      if(in6.eq..true.) then
      out= .true.
      else
      endif
      else
      endif
      else
      endif
      else
      endif
      else
      endif
      else
      endif
      if(in1.eq..true.) then
      if(in2.eq..false.) then
      if(in3.eq..true.) then
      if(in4.eq..false.) then
      if(in5.eq..false.) then
      if(in6.eq..true.) then
      out=.true.
      else
      endif
      else
      endif
      else
      endif
      else
      endif
      else
      endif
      else
      endif
      if(in1.eq..true.) then
```

```
if(in2.eq..true.) then
if(in3.eq..true.) then
if(in4.eq..false.) then
if(in5.eq..true.) then
if(in6.eq..true.) then
out=.true.
else
endif
else
endif
else
endif
else
endif
else
endif
else
endif
if(in1.eq..false.) then
if(in2.eq..true.) then
if(in3.eq..false.) then
if(in4.eq..true.) then
if(in5.eq..true.) then
if(in6.eq..true.) then
out=.true.
else
endif
else
endif
else
endif
else
endif
else
endif
else
endif
if(in1.eq..false.) then
if(in2.eq..false.) then
if(in3.eq..true.) then
if(in4.eq..true.) then
if(in5.eq..true.) then
if(in6.eq..true.) then
out=.true.
else
endif
else
endif
else
endif
else
endif
else
endif
else
```

```
endif
if(in1.eq..true.) then
if(in2.eq..true.) then
if(in3.eq..true.) then
if(in4.eq..true.) then
if(in5.eq..true.) then
if(in6.eq..true.) then
out=.true.
else
endif
else
endif
else
endif
else
endif
else
endif
else
endif
if(in1.eq..false.) then
if(in2.eq..true.) then
if(in3.eq..true.) then
if(in4.eq..true.) then
if(in5.eq..true.) then
if(in6.eq..false.) then
out=.true.
else
endif
else
endif
else
endif
else
endif
else
endif
else
endif
if(in1.eq..false.) then
if(in2.eq..true.) then
if(in3.eq..true.) then
if(in4.eq..true.) then
if(in5.eq..false.) then
if(in6.eq..true.) then
out=.true.
else
endif
else
endif
else
endif
else
endif
else
endif
else
```

```
            endif
            else
            endif
            if(in1.eq..false.) then
            if(in2.eq..true.) then
            if(in3.eq..true.) then
            if(in4.eq..false.) then
            if(in5.eq..true.) then
            if(in6.eq..true.) then
            out=.true.
            else
            endif
            else
            endif
            else
            endif
            else
            endif
            else
            endif
            else
            endif
            return
            end
```

```
CCCCCCCCCCCCCCCCCCCCCCCCCCCCCCCCCCCCCCCCCCC
C This program generates all the required C
C 4x4 error matrices which are used to     C
C create the correctable syndrome patternsC
C for double NEC scheme. There are a totalC
C of 121 legal error patterns generated    C
C from this program.                        C
CCCCCCCCCCCCCCCCCCCCCCCCCCCCCCCCCCCCCCCCCCC
        PROGRAM EMATRIX
        INTEGER E(16),MOV,REF,I
        E(1)=1
        REF=2
        MOV=2
        DATA (E(I),I=2,16)/15*0/
C       CREATE AN ERROR FILE TO STORE PATTERNS
        OPEN(UNIT=6,FILE='ERROR',STATUS='NEW')
C       WRITE ERROR PATTERNS TO FILE
        WRITE(6,*) (E(I),I=1,16)
5       DO 10 I=2,16
        E(I)=0
10      CONTINUE
        E(MOV)=1
C       WRITE ERROR PATTERNS TO FILE
        WRITE(6,*) (E(I),I=1,16)
        MOV=MOV+1
        IF (MOV.GT.16) GO TO 40
        GO TO 5
40      REF=2
        MOV=3
50      DO 100 I=2,16
        E(I)=0
100     CONTINUE
        E(REF)=1
        E(MOV)=1
C       WRITE ERROR PATTERNS TO FILE
        WRITE(6,*) (E(I),I=1,16)
        MOV=MOV+1
        IF (MOV.GT.16) THEN
        REF=REF+1
        MOV=REF+1
        ENDIF
        IF (REF.GT.15) GO TO 200
        GO TO 50
200     END
```

```
1 0 0 0 0 0 0 0 0 0 0 0 0 0 0 0
1 1 0 0 0 0 0 0 0 0 0 0 0 0 0 0
1 0 1 0 0 0 0 0 0 0 0 0 0 0 0 0
1 0 0 1 0 0 0 0 0 0 0 0 0 0 0 0
1 0 0 0 1 0 0 0 0 0 0 0 0 0 0 0
1 0 0 0 0 1 0 0 0 0 0 0 0 0 0 0
1 0 0 0 0 0 1 0 0 0 0 0 0 0 0 0
1 0 0 0 0 0 0 1 0 0 0 0 0 0 0 0
1 0 0 0 0 0 0 0 1 0 0 0 0 0 0 0
1 0 0 0 0 0 0 0 0 1 0 0 0 0 0 0
1 0 0 0 0 0 0 0 0 0 1 0 0 0 0 0
1 0 0 0 0 0 0 0 0 0 0 1 0 0 0 0
1 0 0 0 0 0 0 0 0 0 0 0 1 0 0 0
1 0 0 0 0 0 0 0 0 0 0 0 0 1 0 0
1 0 0 0 0 0 0 0 0 0 0 0 0 0 1 0
1 0 0 0 0 0 0 0 0 0 0 0 0 0 0 1
1 1 1 0 0 0 0 0 0 0 0 0 0 0 0 0
1 1 0 1 0 0 0 0 0 0 0 0 0 0 0 0
1 1 0 0 1 0 0 0 0 0 0 0 0 0 0 0
1 1 0 0 0 1 0 0 0 0 0 0 0 0 0 0
1 1 0 0 0 0 1 0 0 0 0 0 0 0 0 0
1 1 0 0 0 0 0 1 0 0 0 0 0 0 0 0
1 1 0 0 0 0 0 0 1 0 0 0 0 0 0 0
1 1 0 0 0 0 0 0 0 1 0 0 0 0 0 0
1 1 0 0 0 0 0 0 0 0 1 0 0 0 0 0
1 1 0 0 0 0 0 0 0 0 0 1 0 0 0 0
1 1 0 0 0 0 0 0 0 0 0 0 1 0 0 0
1 1 0 0 0 0 0 0 0 0 0 0 0 1 0 0
1 1 0 0 0 0 0 0 0 0 0 0 0 0 1 0
1 1 0 0 0 0 0 0 0 0 0 0 0 0 0 1
1 0 1 1 0 0 0 0 0 0 0 0 0 0 0 0
1 0 1 0 1 0 0 0 0 0 0 0 0 0 0 0
1 0 1 0 0 1 0 0 0 0 0 0 0 0 0 0
1 0 1 0 0 0 1 0 0 0 0 0 0 0 0 0
1 0 1 0 0 0 0 1 0 0 0 0 0 0 0 0
1 0 1 0 0 0 0 0 1 0 0 0 0 0 0 0
1 0 1 0 0 0 0 0 0 1 0 0 0 0 0 0
1 0 1 0 0 0 0 0 0 0 1 0 0 0 0 0
1 0 1 0 0 0 0 0 0 0 0 1 0 0 0 0
1 0 1 0 0 0 0 0 0 0 0 0 1 0 0 0
1 0 1 0 0 0 0 0 0 0 0 0 0 1 0 0
1 0 1 0 0 0 0 0 0 0 0 0 0 0 1 0
1 0 1 0 0 0 0 0 0 0 0 0 0 0 0 1
1 0 0 1 1 0 0 0 0 0 0 0 0 0 0 0
1 0 0 1 0 1 0 0 0 0 0 0 0 0 0 0
1 0 0 1 0 0 1 0 0 0 0 0 0 0 0 0
1 0 0 1 0 0 0 1 0 0 0 0 0 0 0 0
1 0 0 1 0 0 0 0 1 0 0 0 0 0 0 0
```

129

```
1 0 0 1 0 0 0 0 0 1 0 0 0 0 0 0
1 0 0 1 0 0 0 0 0 0 1 0 0 0 0 0
1 0 0 1 0 0 0 0 0 0 0 1 0 0 0 0
1 0 0 1 0 0 0 0 0 0 0 0 1 0 0 0
1 0 0 1 0 0 0 0 0 0 0 0 0 1 0 0
1 0 0 1 0 0 0 0 0 0 0 0 0 0 1 0
1 0 0 1 0 0 0 0 0 0 0 0 0 0 0 1
1 0 0 0 1 1 0 0 0 0 0 0 0 0 0 0
1 0 0 0 1 0 1 0 0 0 0 0 0 0 0 0
1 0 0 0 1 0 0 1 0 0 0 0 0 0 0 0
1 0 0 0 1 0 0 0 1 0 0 0 0 0 0 0
1 0 0 0 1 0 0 0 0 1 0 0 0 0 0 0
1 0 0 0 1 0 0 0 0 0 1 0 0 0 0 0
1 0 0 0 1 0 0 0 0 0 0 1 0 0 0 0
1 0 0 0 1 0 0 0 0 0 0 0 1 0 0 0
1 0 0 0 1 0 0 0 0 0 0 0 0 1 0 0
1 0 0 0 1 0 0 0 0 0 0 0 0 0 1 0
1 0 0 0 1 0 0 0 0 0 0 0 0 0 0 1
1 0 0 0 0 1 1 0 0 0 0 0 0 0 0 0
1 0 0 0 0 1 0 1 0 0 0 0 0 0 0 0
1 0 0 0 0 1 0 0 1 0 0 0 0 0 0 0
1 0 0 0 0 1 0 0 0 1 0 0 0 0 0 0
1 0 0 0 0 1 0 0 0 0 1 0 0 0 0 0
1 0 0 0 0 1 0 0 0 0 0 1 0 0 0 0
1 0 0 0 0 1 0 0 0 0 0 0 1 0 0 0
1 0 0 0 0 1 0 0 0 0 0 0 0 1 0 0
1 0 0 0 0 1 0 0 0 0 0 0 0 0 1 0
1 0 0 0 0 1 0 0 0 0 0 0 0 0 0 1
1 0 0 0 0 0 1 1 0 0 0 0 0 0 0 0
1 0 0 0 0 0 1 0 1 0 0 0 0 0 0 0
1 0 0 0 0 0 1 0 0 1 0 0 0 0 0 0
1 0 0 0 0 0 1 0 0 0 1 0 0 0 0 0
1 0 0 0 0 0 1 0 0 0 0 1 0 0 0 0
1 0 0 0 0 0 1 0 0 0 0 0 1 0 0 0
1 0 0 0 0 0 1 0 0 0 0 0 0 1 0 0
1 0 0 0 0 0 1 0 0 0 0 0 0 0 1 0
1 0 0 0 0 0 1 0 0 0 0 0 0 0 0 1
1 0 0 0 0 0 0 1 1 0 0 0 0 0 0 0
1 0 0 0 0 0 0 1 0 1 0 0 0 0 0 0
1 0 0 0 0 0 0 1 0 0 1 0 0 0 0 0
1 0 0 0 0 0 0 1 0 0 0 1 0 0 0 0
1 0 0 0 0 0 0 1 0 0 0 0 1 0 0 0
1 0 0 0 0 0 0 1 0 0 0 0 0 1 0 0
1 0 0 0 0 0 0 1 0 0 0 0 0 0 1 0
1 0 0 0 0 0 0 1 0 0 0 0 0 0 0 1
1 0 0 0 0 0 0 0 1 1 0 0 0 0 0 0
1 0 0 0 0 0 0 0 1 0 1 0 0 0 0 0
1 0 0 0 0 0 0 0 1 0 0 1 0 0 0 0
1 0 0 0 0 0 0 0 1 0 0 0 1 0 0 0
1 0 0 0 0 0 0 0 1 0 0 0 0 1 0 0
1 0 0 0 0 0 0 0 1 0 0 0 0 0 1 0
1 0 0 0 0 0 0 0 1 0 0 0 0 0 0 1
1 0 0 0 0 0 0 0 0 1 1 0 0 0 0 0
1 0 0 0 0 0 0 0 0 1 0 1 0 0 0 0
1 0 0 0 0 0 0 0 0 1 0 0 1 0 0 0
```

```
1  0  0  0  0  0  0  0  0  1  0  0  0  1  0  0
1  0  0  0  0  0  0  0  0  1  0  0  0  0  1  0
1  0  0  0  0  0  0  0  0  1  0  0  0  0  0  1
1  0  0  0  0  0  0  0  0  0  1  1  0  0  0  0
1  0  0  0  0  0  0  0  0  0  1  0  1  0  0  0
1  0  0  0  0  0  0  0  0  0  1  0  0  1  0  0
1  0  0  0  0  0  0  0  0  0  1  0  0  0  1  0
1  0  0  0  0  0  0  0  0  0  1  0  0  0  0  1
1  0  0  0  0  0  0  0  0  0  0  1  1  0  0  0
1  0  0  0  0  0  0  0  0  0  0  1  0  1  0  0
1  0  0  0  0  0  0  0  0  0  0  1  0  0  1  0
1  0  0  0  0  0  0  0  0  0  0  1  0  0  0  1
1  0  0  0  0  0  0  0  0  0  0  0  1  1  0  0
1  0  0  0  0  0  0  0  0  0  0  0  1  0  1  0
1  0  0  0  0  0  0  0  0  0  0  0  1  0  0  1
1  0  0  0  0  0  0  0  0  0  0  0  0  1  1  0
1  0  0  0  0  0  0  0  0  0  0  0  0  1  0  1
1  0  0  0  0  0  0  0  0  0  0  0  0  0  1  1
```

```
CCCCCCCCCCCCCCCCCCCCCCCCCCCCCCCCCCCCCCCCCCCCC
C This program is used to create all the      C
C syndrome patterns from the error patterns   C
C for triple error correction. A total of 118C
C unique syndrome patterns can be obtained    C
C from this progeram.                          C
CCCCCCCCCCCCCCCCCCCCCCCCCCCCCCCCCCCCCCCCCCCCC
      PROGRAM SYNMATRX
      INTEGER E(121,16),S(12),I,J,K
C     READ IN ERROR PATTERNS FROM FILE
      OPEN (UNIT=5,FILE='ERROR',STATUS='OLD')
C     CREATE FILE TO STORE SYNDROME PATTERNS IN
      OPEN (UNIT=6,FILE='SYND',STATUS='NEW')
      DO 100 I=1,121
      READ (5,*) (E(I,J),J=1,16)
C     GENERATE SYNDROME PATTERNS
      S(1)=MOD(E(I,4)+E(I,3)+E(I,8),2)
      S(2)=MOD(E(I,3)+E(I,2)+E(I,7),2)
      S(3)=MOD(E(I,2)+E(I,1)+E(I,6),2)
      S(4)=MOD(E(I,1)+E(I,5),2)
      S(5)=MOD(E(I,4)+E(I,3)+E(I,2)+E(I,12),2)
      S(6)=MOD(E(I,3)+E(I,2)+E(I,1)+E(I,11),2)
      S(7)=MOD(E(I,2)+E(I,1)+E(I,10),2)
      S(8)=MOD(E(I,1)+E(I,9),2)
      S(9)=MOD(E(I,4)+E(I,3)+E(I,2)+E(I,1)+E(I,16),2)
      S(10)=MOD(E(I,3)+E(I,2)+E(I,1)+E(I,15),2)
      S(11)=MOD(E(I,2)+E(I,1)+E(I,14),2)
      S(12)=MOD(E(I,1)+E(I,13),2)
      WRITE (6,*) (S(K),K=1,12)
100   CONTINUE
      END
```

```
*******************************************
* The following is a list of all the 118*
* distinct syndrome patterns generated  *
* from the program for triple NEC. Each  *
* line represents a 3x4 syndrome matrix,*
* starting left to right.                *
*******************************************
0  0  1  1  0  1  1  1  1  1  1  1
0  1  0  1  1  0  0  1  0  0  0  1
1  1  1  1  1  0  1  1  0  0  1  1
1  0  1  1  1  1  1  1  0  1  1  1
0  0  1  0  0  1  1  1  1  1  1  1
0  0  0  1  0  1  1  1  1  1  1  1
0  1  1  1  0  1  1  1  1  1  1  1
1  0  1  1  0  1  1  1  1  1  1  1
0  0  1  1  0  1  1  0  1  1  1  1
0  0  1  1  0  1  0  1  1  1  1  1
0  0  1  1  0  0  1  1  1     1  1
0  0  1  1  1  1  1  1  1  1     1
0  0  1  1  0  1  1  1  1  1     0
0  0  1  1  0  1  1  1  1     0  1
0  0  1  1  0  1  1  1  1  0  1  1
0  0  1  1  0  1  1  1  0  1  1  1
1  0  0  1  0  1  0  1  1  1  0  1
1  1  0  1  0  0  0  1  1  0  0  1
0  1  0  0  1  0  0  1  0  0  0  1
0  1  1  1  1  0  0  1  0  0  0  1
0  0  0  1  1  0  0  1  0  0  0  1
1  1  0  1  1  0  0  1  0  0  0  1
0  1  0  1  1  0  0  0  0  0  0  1
0  1  0  1  1  0  1  1  0  0  0  1
0  1  0  1  1  1  0  1  0  0  0  1
0  1  0  1  0  0  0  1  0  0  0  1
0  1  0  1  1  0  0  1  0  0  0  0
0  1  0  1  1  0  0  1  0  0  1  1
0  1  0  1  1  0  0  1  0  1  0  1
0  1  0  1  1  0  0  1  1  0  0  1
0  1  1  1  0  0  1  1  1  0  1  1
1  1  1  0  1  0  1  1  0  0  1  1
1  1  0  1  1  0  1  1  0  0  1  1
1  0  1  1  1  0  1  1  0  0  1  1
0  1  1  1  1  0  1  1  0  0  1  1
1  1  1  1  1  0  1  0  0  0  1  1
1  1  1  1  1  0  0  1  0  0  1  1
1  1  1  1  1  1  1  1  0  0  1  1
1  1  1  1  0  0  1  1  0  0  1  1
1  1  1  1  1  0  1  1  0  0  1  0
1  1  1  1  1  0  1  1  0  0  0  1
1  1  1  1  1  0  1  1  0  1  1  1
1  1  1  1  1  0  1  1  1  0  1  1
1  0  1  0  1     1  1  0  1  1  1
1  0  0  1  1     1  1  0  1  1  1
1  1  1  1  1  1  1  1  0  1  1  1
0  0  1  1  1  1  1  1  0  1  1  1
1  0  1  1  1  1  1  0  0  1  1  1
```

```
1 0 1 1 1 1 0 1 0 1 1 1
1 0 1 1 1 0 1 1 0 1 1 1
1 0 1 1 0 1 1 1 0 1 1 1
1 0 1 1 1 1 1 1 0 1 1 0
1 0 1 1 1 1 1 1 0 1 0 1
1 0 1 1 1 1 1 1 0 0 1 1
1 0 1 1 1 1 1 1 1 1 1 1
0 0 0 0 0 1 1 1 1 1 1 1
0 1 1 0 0 1 1 1 1 1 1 1
1 0 1 0 0 1 1 1 1 1 1 1
0 0 1 0 0 1 1 0 1 1 1 1
0 0 1 0 0 1 0 1 1 1 1 1
0 0 1 0 0 0 1 1 1 1 1 1
0 0 1 0 1 1 1 1 1 1 1 1
0 0 1 0 0 1 1 1 1 1 1 0
0 0 1 0 0 1 1 1 1 1 0 1
0 0 1 0 0 1 1 1 1 0 1 1
0 0 1 0 0 1 1 1 0 1 1 1
0 1 0 1 0 1 1 1 1 1 1 1
1 0 0 1 0 1 1 1 1 1 1 1
0 0 0 1 0 1 1 0 1 1 1 1
0 0 0 1 0 1 0 1 1 1 1 1
0 0 0 1 0 0 1 1 1 1 1 1
0 0 0 1 1 1 1 1 1 1 1 1
0 0 0 1 0 1 1 1 1 1 1 0
0 0 0 1 0 1 1 1 1 1 0 1
0 0 0 1 0 1 1 1 1 0 1 1
0 0 0 1 0 1 1 1 0 1 1 1
1 1 1 1 0 1 1 1 1 1 1 1
0 1 1 1 0 1 1 0 1 1 1 1
0 1 1 1 0 1 0 1 1 1 1 1
0 1 1 1 0 0 1 1 1 1 1 1
0 1 1 1 1 1 1 1 1 1 1 1
0 1 1 1 0 1 1 1 1 1 1 0
0 1 1 1 0 1 1 1 1 1 0 1
0 1 1 1 0 1 1 1 1 0 1 1
0 1 1 1 0 1 1 1 0 1 1 1
1 0 1 1 0 1 1 0 1 1 1 1
1 0 1 1 0 1 0 1 1 1 1 1
1 0 1 1 0 0 1 1 1 1 1 1
1 0 1 1 1 1 1 1 1 1 1 1
1 0 1 1 0 1 1 1 1 1 1 0
1 0 1 1 0 1 1 1 1 1 0 1
1 0 1 1 0 1 1 1 1 0 1 1
1 0 1 1 0 1 1 1 0 1 1 1
0 0 1 1 0 1 0 0 1 1 1 1
0 0 1 1 0 0 1 0 1 1 1 1
0 0 1 1 1 1 1 0 1 1 1 1
0 0 1 1 0 1 1 0 1 1 1 0
0 0 1 1 0 1 1 0 1 1 0 1
0 0 1 1 0 1 1 0 1 0 1 1
0 0 1 1 0 1 1 0 0 1 1 1
0 0 1 1 0 0 0 1 1 1 1 1
0 0 1 1 1 1 0 1 1 1 1 1
0 0 1 1 0 1 0 1 1 1 1 0
```

```
0  0  1  1  0  1  0  1  1  1  0  1
0  0  1  1  0  1  0  1  1  0  1  1
0  0  1  1  0  1  0  1  0  1  1  1
0  0  1  1  1  0  1  1  1  1  1  1
0  0  1  1  0  0  1  1  1  1  1  0
0  0  1  1  0  0  1  1  1  1  0  1
0  0  1  1  0  0  1  1  1  0  1  1
0  0  1  1  0  0  1  1  0  1  1  1
0  0  1  1  1  1  1  1  1  1  1  0
0  0  1  1  1  1  1  1  1  1  0  1
0  0  1  1  1  1  1  1  1  0  1  1
0  0  1  1  1  1  1  1  0  1  1  1
0  0  1  1  0  1  1  1  1  1  0  0
0  0  1  1  0  1  1  1  1  0  1  0
0  0  1  1  0  1  1  1  0  1  1  0
0  0  1  1  0  1  1  1  1  0  0  1
0  0  1  1  0  1  1  1  0  1  0  1
0  0  1  1  0  1  1  1  0  0  1  1
```

```
CCCCCCCCCCCCCCCCCCCCCCCCCCCCCCCCCCCCCCCCCCCCCC
C  This program is intended for detecting all    C
C  the legal syndrome patterns for triple NEC    C
C  scheme. It applies to either two-bit or       C
C  three-bit differentially encoded ODQPSK-type  C
C  modulation schemes. The output of a correc-   C
C  tion pulse depends upon the match between theC
C  detected syndrome pattern and stored patternsC
C  A total of 119 unique syndrome patterns can   C
C  be detected in this program.                  C
CCCCCCCCCCCCCCCCCCCCCCCCCCCCCCCCCCCCCCCCCCCCCC
      SUBROUTINE PATTD3(IN1,IN2,IN3,IN4,IN5,IN6,IN7
    + ,IN8,IN9,IN10,IN11,IN12,OUT)
      LOGICAL*1 OUT,INPUT(12),LS(121,12),IN1,IN2,IN3,
    + IN4,IN5,IN6,IN7,IN8,IN9,IN10,IN11,IN12
      INTEGER COUNT,I,J,K,S(121,12)
C     INITIALIZE THE DATA AREA STORING SYNDROMES
      DATA  (S(1,J),J=1,12)   /0,0,1,1,0,1,1,1,1,1,1,1/
      DATA  (S(2,J),J=1,12)   /0,1,0,1,1,0,0,1,0,0,0,1/
      DATA  (S(3,J),J=1,12)   /1,1,1,1,1,0,1,1,0,0,1,1/
      DATA  (S(4,J),J=1,12)   /1,0,1,1,1,1,1,1,0,1,1,1/
      DATA  (S(5,J),J=1,12)   /0,0,1,0,0,1,1,1,1,1,1,1/
      DATA  (S(6,J),J=1,12)   /0,0,0,1,0,1,1,1,1,1,1,1/
      DATA  (S(7,J),J=1,12)   /0,1,1,1,0,1,1,1,1,1,1,1/
      DATA  (S(8,J),J=1,12)   /1,0,1,1,0,1,1,1,1,1,1,1/
      DATA  (S(9,J),J=1,12)   /0,0,1,1,0,1,1,0,1,1,1,1/
      DATA  (S(10,J),J=1,12)  /0,0,1,1,0,1,0,1,1,1,1,1/
      DATA  (S(11,J),J=1,12)  /0,0,1,1,0,0,1,1,1,1,1,1/
      DATA  (S(12,J),J=1,12)  /0,0,1,1,1,1,1,1,1,1,1,1/
      DATA  (S(13,J),J=1,12)  /0,0,1,1,0,1,1,1,1,1,1,0/
      DATA  (S(14,J),J=1,12)  /0,0,1,1,0,1,1,1,1,1,0,1/
      DATA  (S(15,J),J=1,12)  /0,0,1,1,0,1,1,1,1,0,1,1/
      DATA  (S(16,J),J=1,12)  /0,0,1,1,0,1,1,1,0,1,1,1/
      DATA  (S(17,J),J=1,12)  /1,0,0,1,0,1,0,1,1,1,0,1/
      DATA  (S(18,J),J=1,12)  /1,1,0,1,0,0,0,1,1,0,0,1/
      DATA  (S(19,J),J=1,12)  /0,1,0,0,1,0,0,1,0,0,0,1/
      DATA  (S(20,J),J=1,12)  /0,1,1,1,1,0,0,1,0,0,0,1/
      DATA  (S(21,J),J=1,12)  /0,0,0,1,1,0,0,1,0,0,0,1/
      DATA  (S(22,J),J=1,12)  /1,1,0,1,1,0,0,1,0,0,0,1/
      DATA  (S(23,J),J=1,12)  /0,1,0,1,1,0,0,0,0,0,0,1/
      DATA  (S(24,J),J=1,12)  /0,1,0,1,1,0,1,1,0,0,0,1/
      DATA  (S(25,J),J=1,12)  /0,1,0,1,1,1,0,1,0,0,0,1/
      DATA  (S(26,J),J=1,12)  /0,1,0,1,0,0,0,1,0,0,0,1/
      DATA  (S(27,J),J=1,12)  /0,1,0,1,1,0,0,1,0,0,0,0/
      DATA  (S(28,J),J=1,12)  /0,1,0,1,1,0,0,1,0,0,1,1/
      DATA  (S(29,J),J=1,12)  /0,1,0,1,1,0,0,1,0,1,0,1/
      DATA  (S(30,J),J=1,12)  /0,1,0,1,1,0,0,1,1,0,0,1/
      DATA  (S(31,J),J=1,12)  /0,1,1,1,0,0,1,1,1,0,1,1/
      DATA  (S(32,J),J=1,12)  /1,1,1,0,1,0,1,1,0,0,1,1/
      DATA  (S(33,J),J=1,12)  /1,1,0,1,1,0,1,1,0,0,1,1/
      DATA  (S(34,J),J=1,12)  /1,0,1,1,1,0,1,1,0,0,1,1/
      DATA  (S(35,J),J=1,12)  /0,1,1,1,1,0,1,1,0,0,1,1/
      DATA  (S(36,J),J=1,12)  /1,1,1,1,1,0,1,0,0,0,1,1/
      DATA  (S(37,J),J=1,12)  /1,1,1,1,1,0,0,1,0,0,1,1/
      DATA  (S(38,J),J=1,12)  /1,1,1,1,1,1,1,1,0,0,1,1/
```

136

```
DATA  (S(39,J),J=1,12)  /1,1,1,1,0,0,1,1,0,0,1,1/
DATA  (S(40,J),J=1,12)  /1,1,1,1,1,0,1,1,0,0,1,0/
DATA  (S(41,J),J=1,12)  /1,1,1,1,1,0,1,1,0,0,0,1/
DATA  (S(42,J),J=1,12)  /1,1,1,1,1,0,1,1,0,1,1,1/
DATA  (S(43,J),J=1,12)  /1,1,1,1,1,0,1,1,1,0,1,1/
DATA  (S(44,J),J=1,12)  /1,0,1,0,1,1,1,1,0,1,1,1/
DATA  (S(45,J),J=1,12)  /1,0,0,1,1,1,1,1,0,1,1,1/
DATA  (S(46,J),J=1,12)  /1,1,1,1,1,1,1,1,0,1,1,1/
DATA  (S(47,J),J=1,12)  /0,0,1,1,1,1,1,1,0,1,1,1/
DATA  (S(48,J),J=1,12)  /1,0,1,1,1,1,1,0,0,1,1,1/
DATA  (S(49,J),J=1,12)  /1,0,1,1,1,1,0,1,0,1,1,1/
DATA  (S(50,J),J=1,12)  /1,0,1,1,1,0,1,1,0,1,1,1/
DATA  (S(51,J),J=1,12)  /1,0,1,1,0,1,1,1,0,1,1,1/
DATA  (S(52,J),J=1,12)  /1,0,1,1,1,1,1,1,0,1,1,0/
DATA  (S(53,J),J=1,12)  /1,0,1,1,1,1,1,1,0,1,0,1/
DATA  (S(54,J),J=1,12)  /1,0,1,1,1,1,1,1,0,0,1,1/
DATA  (S(55,J),J=1,12)  /1,0,1,1,1,1,1,1,1,1,1,1/
DATA  (S(56,J),J=1,12)  /0,0,0,0,0,1,1,1,1,1,1,1/
DATA  (S(57,J),J=1,12)  /0,1,1,0,0,1,1,1,1,1,1,1/
DATA  (S(58,J),J=1,12)  /1,0,1,0,0,1,1,1,1,1,1,1/
DATA  (S(59,J),J=1,12)  /0,0,1,0,0,1,1,0,1,1,1,1/
DATA  (S(60,J),J=1,12)  /0,0,1,0,0,1,0,1,1,1,1,1/
DATA  (S(61,J),J=1,12)  /0,0,1,0,0,0,1,1,1,1,1,1/
DATA  (S(62,J),J=1,12)  /0,0,1,0,1,1,1,1,1,1,1,1/
DATA  (S(63,J),J=1,12)  /0,0,1,0,0,1,1,1,1,1,1,0/
DATA  (S(64,J),J=1,12)  /0,0,1,0,0,1,1,1,1,1,0,1/
DATA  (S(65,J),J=1,12)  /0,0,1,0,0,1,1,1,1,0,1,1/
DATA  (S(66,J),J=1,12)  /0,0,1,0,0,1,1,1,0,1,1,1/
DATA  (S(67,J),J=1,12)  /0,1,0,1,0,1,1,1,1,1,1,1/
DATA  (S(68,J),J=1,12)  /1,0,0,1,0,1,1,1,1,1,1,1/
DATA  (S(69,J),J=1,12)  /0,0,0,1,0,1,1,0,1,1,1,1/
DATA  (S(70,J),J=1,12)  /0,0,0,1,0,1,0,1,1,1,1,1/
DATA  (S(71,J),J=1,12)  /0,0,0,1,0,0,1,1,1,1,1,1/
DATA  (S(72,J),J=1,12)  /0,0,0,1,1,1,1,1,1,1,1,1/
DATA  (S(73,J),J=1,12)  /0,0,0,1,0,1,1,1,1,1,1,0/
DATA  (S(74,J),J=1,12)  /0,0,0,1,0,1,1,1,1,1,0,1/
DATA  (S(75,J),J=1,12)  /0,0,0,1,0,1,1,1,1,0,1,1/
DATA  (S(76,J),J=1,12)  /0,0,0,1,0,1,1,1,0,1,1,1/
DATA  (S(77,J),J=1,12)  /1,1,1,1,0,1,1,1,1,1,1,1/
DATA  (S(78,J),J=1,12)  /0,1,1,1,0,1,1,0,1,1,1,1/
DATA  (S(79,J),J=1,12)  /0,1,1,1,0,1,0,1,1,1,1,1/
DATA  (S(80,J),J=1,12)  /0,1,1,1,0,0,1,1,1,1,1,1/
DATA  (S(81,J),J=1,12)  /0,1,1,1,1,1,1,1,1,1,1,1/
DATA  (S(82,J),J=1,12)  /0,1,1,1,0,1,1,1,1,1,1,0/
DATA  (S(83,J),J=1,12)  /0,1,1,1,0,1,1,1,1,1,0,1/
DATA  (S(84,J),J=1,12)  /0,1,1,1,0,1,1,1,1,0,1,1/
DATA  (S(85,J),J=1,12)  /0,1,1,1,0,1,1,1,0,1,1,1/
DATA  (S(86,J),J=1,12)  /1,0,1,1,0,1,1,0,1,1,1,1/
DATA  (S(87,J),J=1,12)  /1,0,1,1,0,1,0,1,1,1,1,1/
DATA  (S(88,J),J=1,12)  /1,0,1,1,0,0,1,1,1,1,1,1/
DATA  (S(89,J),J=1,12)  /1,0,1,1,1,1,1,1,1,1,1,1/
DATA  (S(90,J),J=1,12)  /1,0,1,1,0,1,1,1,1,1,1,0/
DATA  (S(91,J),J=1,12)  /1,0,1,1,0,1,1,1,1,1,0,1/
DATA  (S(92,J),J=1,12)  /1,0,1,1,0,1,1,1,1,0,1,1/
DATA  (S(93,J),J=1,12)  /1,0,1,1,0,1,1,1,0,1,1,1/
```

```fortran
      DATA (S(94,J),J=1,12)  /0,0,1,1,0,1,0,0,1,1,1,1/
      DATA (S(95,J),J=1,12)  /0,0,1,1,0,0,1,0,1,1,1,1/
      DATA (S(96,J),J=1,12)  /0,0,1,1,1,1,1,0,1,1,1,1/
      DATA (S(97,J),J=1,12)  /0,0,1,1,0,1,1,0,1,1,1,0/
      DATA (S(98,J),J=1,12)  /0,0,1,1,0,1,1,0,1,1,0,1/
      DATA (S(99,J),J=1,12)  /0,0,1,1,0,1,1,0,1,0,1,1/
      DATA (S(100,J),J=1,12) /0,0,1,1,0,1,1,0,0,1,1,1/
      DATA (S(101,J),J=1,12) /0,0,1,1,0,0,0,1,1,1,1,1/
      DATA (S(102,J),J=1,12) /0,0,1,1,1,1,0,1,1,1,1,1/
      DATA (S(103,J),J=1,12) /0,0,1,1,0,1,0,1,1,1,1,0/
      DATA (S(104,J),J=1,12) /0,0,1,1,0,1,0,1,1,1,0,1/
      DATA (S(105,J),J=1,12) /0,0,1,1,0,1,0,1,1,0,1,1/
      DATA (S(106,J),J=1,12) /0,0,1,1,0,1,0,1,0,1,1,1/
      DATA (S(107,J),J=1,12) /0,0,1,1,1,0,1,1,1,1,1,1/
      DATA (S(108,J),J=1,12) /0,0,1,1,0,0,1,1,1,1,1,0/
      DATA (S(109,J),J=1,12) /0,0,1,1,0,0,1,1,1,1,0,1/
      DATA (S(110,J),J=1,12) /0,0,1,1,0,0,1,1,1,0,1,1/
      DATA (S(111,J),J=1,12) /0,0,1,1,0,0,1,1,0,1,1,1/
      DATA (S(112,J),J=1,12) /0,0,1,1,1,1,1,1,1,1,1,0/
      DATA (S(113,J),J=1,12) /0,0,1,1,1,1,1,1,1,1,0,1/
      DATA (S(114,J),J=1,12) /0,0,1,1,1,1,1,1,1,0,1,1/
      DATA (S(115,J),J=1,12) /0,0,1,1,1,1,1,0,1,1,1,1/
      DATA (S(116,J),J=1,12) /0,0,1,1,0,1,1,1,1,1,0,0/
      DATA (S(117,J),J=1,12) /0,0,1,1,0,1,1,1,1,0,1,0/
      DATA (S(118,J),J=1,12) /0,0,1,1,0,1,1,1,0,1,1,0/
      DATA (S(119,J),J=1,12) /0,0,1,1,0,1,1,1,1,0,0,1/
      DATA (S(120,J),J=1,12) /0,0,1,1,0,1,1,1,0,1,0,1/
      DATA (S(121,J),J=1,12) /0,0,1,1,0,1,1,1,0,0,1,1/
      OUT=.FALSE.
      COUNT=0
      INPUT(1)=IN1
      INPUT(2)=IN2
      INPUT(3)=IN3
      INPUT(4)=IN4
      INPUT(5)=IN5
      INPUT(6)=IN6
      INPUT(7)=IN7
      INPUT(8)=IN8
      INPUT(9)=IN9
      INPUT(10)=IN10
      INPUT(11)=IN11
      INPUT(12)=IN12
C     NUMERIC TO LOGIC CONVERSION
      DO 10 I=1,121
      DO 5 K=1,12
      IF (S(I,K).EQ.1) THEN
            LS(I,K)=.TRUE.
      ELSE
            LS(I,K)=.FALSE.
      ENDIF
5         CONTINUE
10    CONTINUE
C     DETECT SYNDROME PATTERNS
      DO 100 I=1,121
      DO 50 K=1,12
```

```
          IF (INPUT(K).EQ.LS(I,K)) THEN
                  COUNT=COUNT+1
          ENDIF
50            CONTINUE
          IF (COUNT.EQ.12) GO TO 200
          COUNT=0
100           CONTINUE
          GO TO 300
200           OUT=.TRUE.
300           RETURN
          END
```

Appendix C:

List of syndrome patterns for triple NEC

This appendix lists all the syndrome patterns needed for triple error correction. As can be seen, each syndrome matrix contains 12 syndromes, generated from 16 error symbols according to the equations (2-24). A total of 118 distinct syndrome patterns can be obtained from 2^{16} patterns, which are useful for triple error correction. As has been discussed in chapter 2, as long as the number of erroneous symbols present at the outputs of the differential detectors is no larger than three, correct error-correction operations can always be guaranteed.

$$\begin{bmatrix}0011\\0111\\1111\end{bmatrix} \quad \begin{bmatrix}0101\\1001\\0001\end{bmatrix} \quad \begin{bmatrix}1111\\1011\\0011\end{bmatrix} \quad \begin{bmatrix}1011\\1111\\0111\end{bmatrix} \quad \begin{bmatrix}0010\\0111\\1111\end{bmatrix} \quad \begin{bmatrix}0111\\1011\\0011\end{bmatrix}$$

$$\begin{bmatrix}0001\\0111\\1111\end{bmatrix} \quad \begin{bmatrix}0111\\0111\\1111\end{bmatrix} \quad \begin{bmatrix}1011\\0111\\1111\end{bmatrix} \quad \begin{bmatrix}0011\\0110\\1111\end{bmatrix} \quad \begin{bmatrix}0011\\0101\\1111\end{bmatrix} \quad \begin{bmatrix}1111\\1111\\0011\end{bmatrix}$$

$$\begin{bmatrix}0011\\0011\\1111\end{bmatrix} \quad \begin{bmatrix}0011\\1111\\1111\end{bmatrix} \quad \begin{bmatrix}0011\\0111\\1110\end{bmatrix} \quad \begin{bmatrix}0011\\0110\\1011\end{bmatrix} \quad \begin{bmatrix}0011\\0111\\0111\end{bmatrix} \quad \begin{bmatrix}1111\\0011\\0011\end{bmatrix}$$

$$\begin{bmatrix}0100\\1001\\0001\end{bmatrix} \quad \begin{bmatrix}1110\\1011\\0011\end{bmatrix} \quad \begin{bmatrix}1010\\1111\\0111\end{bmatrix} \quad \begin{bmatrix}0000\\0111\\1111\end{bmatrix} \quad \begin{bmatrix}0110\\0111\\1111\end{bmatrix} \quad \begin{bmatrix}1111\\1011\\0111\end{bmatrix}$$

$$\begin{bmatrix}1010\\0111\\1111\end{bmatrix} \quad \begin{bmatrix}0010\\0110\\1111\end{bmatrix} \quad \begin{bmatrix}0010\\0101\\1111\end{bmatrix} \quad \begin{bmatrix}0010\\0011\\1111\end{bmatrix} \quad \begin{bmatrix}0010\\1111\\1111\end{bmatrix} \quad \begin{bmatrix}1111\\1111\\0111\end{bmatrix}$$

$$\begin{bmatrix}0010\\0111\\1110\end{bmatrix} \quad \begin{bmatrix}0010\\0111\\1101\end{bmatrix} \quad \begin{bmatrix}0010\\0111\\1011\end{bmatrix} \quad \begin{bmatrix}0010\\0111\\0111\end{bmatrix} \quad \begin{bmatrix}0101\\1000\\0001\end{bmatrix} \quad \begin{bmatrix}1111\\0111\\1111\end{bmatrix}$$

$$\begin{bmatrix}1111\\1010\\0011\end{bmatrix} \quad \begin{bmatrix}1011\\1110\\0110\end{bmatrix} \quad \begin{bmatrix}0001\\0110\\1111\end{bmatrix} \quad \begin{bmatrix}0111\\0110\\1111\end{bmatrix} \quad \begin{bmatrix}1011\\0110\\1111\end{bmatrix} \quad \begin{bmatrix}0111\\0011\\1111\end{bmatrix}$$

$$\begin{bmatrix}0011\\0100\\1111\end{bmatrix} \quad \begin{bmatrix}0011\\0010\\1111\end{bmatrix} \quad \begin{bmatrix}0011\\1110\\1111\end{bmatrix} \quad \begin{bmatrix}0011\\0110\\1110\end{bmatrix} \quad \begin{bmatrix}0011\\0110\\1101\end{bmatrix} \quad \begin{bmatrix}0111\\1111\\1111\end{bmatrix}$$

$$\begin{bmatrix}0011\\0110\\0111\end{bmatrix} \quad \begin{bmatrix}0011\\0110\\1110\end{bmatrix} \quad \begin{bmatrix}0011\\0110\\1101\end{bmatrix} \quad \begin{bmatrix}1111\\1011\\0010\end{bmatrix} \quad \begin{bmatrix}0101\\1001\\0000\end{bmatrix} \quad \begin{bmatrix}0111\\0111\\1011\end{bmatrix}$$

$$\begin{bmatrix}0111\\0111\\0111\end{bmatrix} \quad \begin{bmatrix}1111\\1011\\1011\end{bmatrix} \quad \begin{bmatrix}1011\\1011\\0111\end{bmatrix} \quad \begin{bmatrix}1011\\0011\\1111\end{bmatrix} \quad \begin{bmatrix}0011\\1011\\1111\end{bmatrix} \quad \begin{bmatrix}0011\\0011\\1011\end{bmatrix}$$

$$\begin{bmatrix}1011\\1111\\0110\end{bmatrix}\quad\begin{bmatrix}0001\\0111\\1110\end{bmatrix}\quad\begin{bmatrix}0111\\0111\\1110\end{bmatrix}\quad\begin{bmatrix}1011\\0111\\1110\end{bmatrix}\quad\begin{bmatrix}0011\\0101\\1110\end{bmatrix}\quad\begin{bmatrix}0011\\0011\\0111\end{bmatrix}$$

$$\begin{bmatrix}0011\\0011\\1110\end{bmatrix}\quad\begin{bmatrix}0011\\1111\\1110\end{bmatrix}\quad\begin{bmatrix}0011\\0111\\1100\end{bmatrix}\quad\begin{bmatrix}0011\\0111\\1010\end{bmatrix}\quad\begin{bmatrix}0011\\0111\\0110\end{bmatrix}\quad\begin{bmatrix}1011\\1111\\0011\end{bmatrix}$$

$$\begin{bmatrix}1001\\0101\\1101\end{bmatrix}\quad\begin{bmatrix}1101\\0001\\1001\end{bmatrix}\quad\begin{bmatrix}0111\\1001\\0001\end{bmatrix}\quad\begin{bmatrix}0001\\1001\\0001\end{bmatrix}\quad\begin{bmatrix}1101\\1001\\0001\end{bmatrix}\quad\begin{bmatrix}1011\\0111\\1011\end{bmatrix}$$

$$\begin{bmatrix}0101\\1011\\0001\end{bmatrix}\quad\begin{bmatrix}0101\\1101\\0001\end{bmatrix}\quad\begin{bmatrix}0101\\0001\\0001\end{bmatrix}\quad\begin{bmatrix}0101\\1001\\0011\end{bmatrix}\quad\begin{bmatrix}0101\\1001\\0101\end{bmatrix}\quad\begin{bmatrix}0011\\1111\\1011\end{bmatrix}$$

$$\begin{bmatrix}0101\\1001\\1001\end{bmatrix}\quad\begin{bmatrix}1101\\1011\\0011\end{bmatrix}\quad\begin{bmatrix}1001\\1111\\0111\end{bmatrix}\quad\begin{bmatrix}0101\\0111\\1111\end{bmatrix}\quad\begin{bmatrix}1001\\0111\\1111\end{bmatrix}\quad\begin{bmatrix}0011\\0111\\0011\end{bmatrix}$$

$$\begin{bmatrix}0001\\0101\\1111\end{bmatrix}\quad\begin{bmatrix}0001\\0011\\1111\end{bmatrix}\quad\begin{bmatrix}0001\\1111\\1111\end{bmatrix}\quad\begin{bmatrix}0001\\0111\\1101\end{bmatrix}\quad\begin{bmatrix}0001\\0111\\1011\end{bmatrix}\quad\begin{bmatrix}0011\\1111\\0111\end{bmatrix}$$

$$\begin{bmatrix}0001\\0111\\0111\end{bmatrix}\quad\begin{bmatrix}1111\\1001\\0011\end{bmatrix}\quad\begin{bmatrix}1011\\1101\\0111\end{bmatrix}\quad\begin{bmatrix}0111\\0101\\1111\end{bmatrix}\quad\begin{bmatrix}1011\\0101\\1111\end{bmatrix}\quad\begin{bmatrix}1011\\0111\\0111\end{bmatrix}$$

$$\begin{bmatrix}0011\\0001\\1111\end{bmatrix}\quad\begin{bmatrix}0011\\1101\\1111\end{bmatrix}\quad\begin{bmatrix}0011\\0101\\1101\end{bmatrix}\quad\begin{bmatrix}0011\\0101\\1011\end{bmatrix}\quad\begin{bmatrix}0011\\0101\\0111\end{bmatrix}\quad\begin{bmatrix}1011\\1111\\1111\end{bmatrix}$$

$$\begin{bmatrix}1111\\1011\\0001\end{bmatrix}\quad\begin{bmatrix}1011\\1111\\0101\end{bmatrix}\quad\begin{bmatrix}0111\\0111\\1101\end{bmatrix}\quad\begin{bmatrix}1011\\0111\\1101\end{bmatrix}\quad\begin{bmatrix}0011\\0011\\1101\end{bmatrix}\quad\begin{bmatrix}0011\\1111\\1101\end{bmatrix}$$

$$\begin{bmatrix}0011\\0111\\1001\end{bmatrix}\quad\begin{bmatrix}0011\\0111\\0101\end{bmatrix}\quad\begin{bmatrix}0111\\0011\\1011\end{bmatrix}\quad\begin{bmatrix}1011\\1011\\0011\end{bmatrix}$$

APPENDIX D:

BOSS simulation programs

The following Fortran subroutines are used to define some BOSS primitive modules used in the simulation. During the simulation processes, these subroutines are called by BOSS as external procedures. Also, BOSS allows users to modify these programs to realize different signal processing functions.

```
CCCCCCCCCCCCCCCCCCCCCCCCCCCCCCCCCCCCCCCCCCCCCC
C  This subroutine realizes multiplexing    C
C  of four input signals into one output.   C
C  The operation is controlled by four      C
C  status signals according to a specific   C
C  Markov process. This program is used in  C
C  the simulation of ST-ODQ1 ;K system for  C
C  the user-defined primitive module calledC
C  MULTIPLEXER.                             C
CCCCCCCCCCCCCCCCCCCCCCCCCCCCCCCCCCCCCCCCCCCCCC
      subroutine switch(rin1,rin2,rin3,rin4,c1,c2,
    + c3,c4,rout,xx)
      logical*1 c1,c2,c3,c4
      if (c1.xor.c2.xor.c3.xor.c4.eq..false.) then
      rout=-1
      else
      goto 100
      endif
      return
100   if (c1.eq..true.) then
      rout=rin1
      xx=rout
      else
      if (c2.eq..true.) then
            rout=rin2
            xx=rout
      else
      if (c3.eq..true.) then
            rout=rin3
            xx=rout
            else
        if (c4.eq..true.) then
            rout=rin4
            xx=rout
            else
              rout=xx
                    endif
                    endif
            endif
      endif
      return
      end
```

```fortran
CCCCCCCCCCCCCCCCCCCCCCCCCCCCCCCCCCCCCCCCCCCCC
C This program realizes one bit differential C
C encoding of a input binary data stream. TheC
C only parameter needing to be specified is  C
C INO, the number of samples per input bit.   C
C This program is intended for the primitive C
C module )IFFERENTIAL ENCODER. Multi-diff.    C
C encoding operation may be achieved by a     C
C cascade of several DIFFERENTIAL ENCODER     C
C modules.                                    C
CCCCCCCCCCCCCCCCCCCCCCCCCCCCCCCCCCCCCCCCCCCCC
subroutine encode(input,output,ino,k,out)
integer k,ino
logical*1 input,output,out
dimension out(50)
k=k+1
output=input.xor.out(k)
out(k)=output
if(k.eq.ino) k=0
return
end
```